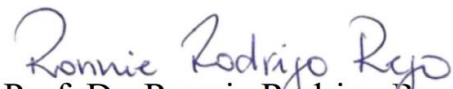


Dissertation presented to the Instituto Tecnológico de Aeronáutica, in partial fulfillment of the requirements for the degree of Master of Science in the Program of Aeronautics and Mechanical Engineering, Area of Materials, Manufacturing and Automation.

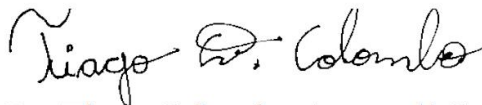
Angelo Alves Carvalho

**SURFACE INTEGRITY EVOLUTION OF Nb-Ti
MICROALLOYED STEELS ALONG THE GEAR
MANUFACTURING CHAIN**

Dissertation approved in its final version by the signatories below:



Prof. Dr. Ronnie Rodrigo Rego
Advisor



Prof. Dr. Tiago Cristofer Aguzzoli Colombo
Co-advisor

Prof. Dr. Prof. Pedro Teixeira Lacava
Pro-Rector of Graduate Courses

Campo Montenegro
São José dos Campos, SP - Brazil
2020

Cataloging-in-Publication Data
Documentation and Information Division

Carvalho, Angelo Alves
Surface integrity evolution of Nb-Ti microalloyed steels along the gear manufacturing chain /
Angelo Alves Carvalho.
São José dos Campos, 2020.
113f.

Dissertation of Master of Science – Program of Aeronautics and Mechanical Engineering, Area of
Materials, Manufacturing and Automation – Instituto Tecnológico de Aeronáutica, 2020. Advisor: Prof.
Dr. Ronnie Rodrigo Rego.

1. Gear. 2. Manufacturing chain. 3. Surface integrity. 4. Microalloyed steel 5. HSLA. I. Instituto
Tecnológico de Aeronáutica. II. Surface integrity evolution of Nb-Ti microalloyed steels along the gear
manufacturing chain.

BIBLIOGRAPHIC REFERENCE

CARVALHO, Angelo Alves. **Surface integrity evolution of Nb-Ti microalloyed steels along the gear manufacturing chain**. 2020. 113f. Dissertation of Master of Science in Materials, Manufacturing and Automation – Instituto Tecnológico de Aeronáutica, São José dos Campos.

CESSION OF RIGHTS

AUTOR NAME: Angelo Alves Carvalho

PUBLICATION TITLE: Surface integrity evolution of Nb-Ti microalloyed steels along the gear manufacturing chain

PUBLICATION KIND/YEAR: Dissertation / 2020

It is granted to Instituto Tecnológico de Aeronáutica permission to reproduce copies of this dissertation to only loan or sell copies for academic and scientific purposes. The author reserves other publication rights and no part of this dissertation can be reproduced without his authorization.

Angelo Alves Carvalho

DCTA - Departamento de Ciência e Tecnologia Aeroespacial, Praça Marechal-do-Ar Eduardo
Gomes, 50 - Vila das Acácias
12228-900 - São José dos Campos-SP, Brazil

**SURFACE INTEGRITY EVOLUTION OF Nb-Ti
MICROALLOYED STEELS ALONG THE GEAR
MANUFACTURING CHAIN**

Angelo Alves Carvalho

Thesis Committee Composition:

Prof. Dr.	Alfredo Rocha de Faria	Chairperson	-	ITA
Prof. Dr.	Ronnie Rodrigo Rego	Advisor	-	ITA
Prof. Dr.	Tiago Cristofer Aguzzoli Colombo	Co-advisor	-	FATEC
Prof. Dr.	Gilmar Patrocínio Thim	Internal member	-	ITA
Prof ^ª . Dr ^ª .	Izabel Fernanda Machado	External member	-	USP

ITA

Acknowledgements

Many people contributed for this Master Thesis in such different ways, and to whom I owe sincere thanks:

To all my family, especially to my parents, Regis and Josiane, who always supported my decisions and taught me the most important values in life. All I am is because of you both.

To Rebecca, for the comprehension, for not letting me be overcome by exhaustion, and for helping me to become a better person every day.

To Ronnie Rego, my advisor, who dedicated part of his time to guide me along the entire research. I am grateful for the opportunity, and for all the discussions, teachings, and suggestions, which increased the quality of the research.

To Tiago Colombo, co-advisor of the research, who accepted the challenge and provided countless insights, which contributed to the full understanding and exploration of the results observed along the research.

To André Oliveira, who accompanied the conduction of the entire research and played a key role in several moments. To Caio Gomes, who was always willing to help and it happened many times. And to the other members of GIE during the research, Ana Impere, Arthur Nogueira, Artur Cantisano, Bruno Oliveira, Denis Lima, Guilherme Guimarães, Guilherme Santos, Lucas Robatto, Luiz Fonseca, Nathianne Andrade, Rodrigo Metzger. Everyone has helped at some point and more than co-workers, they are truly friends.

To Gerdau, represented by Rafael Galdino, who supported the research providing the materials herein investigated, and to the industrial partners Max Gear, Maxirate and Engrecon. I am also grateful to Toninho, whose help has overcome some of the challenges the research has faced.

To ITA, CCM, LabMat, and CAPES for all the resources provided, which were essential for conducting the research.

To God for giving me health and strength to overcome difficulties and for placing all these people in my path, who have assisted me in my professional and personal development.

*“Life's most persistent and urgent question is:
'What are you doing for others?'"*
(Martin Luther King, Jr.)

Resumo

A crescente demanda por engrenagens que apresentem elevado desempenho promove o estudo da aplicação de novos materiais, como os aços microligados que aparecem como uma alternativa com potencial econômico frente a alguns dos aços utilizados atualmente em engrenagens. A cadeia de manufatura de engrenagens envolve uma sequência de processos de aportes térmico e/ou mecânico que alteram o estado de equilíbrio do material. A influência de cada um dos processos pode ser identificada mesmo ao fim da cadeia, o que torna necessário a compreensão de cada processo individualizado. Neste cenário, o estudo aqui apresentado tem como objetivo a caracterização da evolução da integridade de superfície de aços microligados com nióbio e titânio ao longo de uma cadeia convencional de manufatura de engrenagens. A adição dos microligantes em aços usualmente utilizados para engrenagens é avaliada tanto de forma holística considerando a cadeia de manufatura inteira quanto de forma individual para cada processo de manufatura. As investigações realizadas buscam compreender como os processos impactam a integridade de superfície dos aços microligados, em termos de tamanho de grãos, estado de tensão residual, topografia e nível de distorções. Os resultados aqui obtidos mostram que a adição dos elementos microligantes induz uma microestrutura com grãos refinados após os processos com aporte térmico. A adição combinada de nióbio e titânio indicou ainda um aumento da homogeneidade do tamanho de grão. As novas ligas se mostraram favoráveis em termos de estado de tensão residual e topografia, em que apresentam maiores níveis de tensão residual compressiva juntamente a uma superfície de menor rugosidade. Os resultados também indicam uma redução dos níveis de distorção associados a estrutura de grãos homogênea, como a obtida com a adição combinada de Nb e Ti. Por fim, uma potencial melhoria de processo é apontada, o aumento da temperatura de cementação pode levar à obtenção da camada cementada necessária com redução de custo e tempo de processo. Os resultados do presente estudo mostram que a cadeia de manufatura de engrenagens é sensível à adição dos elementos microligantes, de modo que as novas ligas apresentaram uma integridade de superfície modificada. Dentre os processos de manufatura, aqueles que apresentaram maior alteração em seus resultados foram o recozimento isotérmico, a cementação e a retificação. Os aços microligados representam, portanto, uma classe de materiais que pode ser empregada na cadeia de manufatura de engrenagens e oferece um estado otimizado de integridade de superfície.

Abstract

The increasing demand for high performance gears promotes the study of application of new materials, such as microalloyed steels that appear as an alternative with economic potential to some of the steels currently used in gears. Gear manufacturing chain involves a sequence of processes with thermal and/or mechanical loading that alters the equilibrium state of the material. The influence of each process can be identified even at the end of the chain, which requires an understanding of each individualized process. In this scenario, the study herein presented has the objective of characterizing the surface integrity evolution of niobium and titanium microalloyed steels along a conventional gear manufacturing chain. The addition of microalloying elements in steels usually applied for gears is evaluated both holistically considering the entire manufacturing chain and individually for each manufacturing process. Investigations are conducted to understand how processes impact the surface integrity of microalloyed steels in terms of grain size, residual stress state, topography, and distortion level. The results herein obtained show that the addition of microalloying elements induces a microstructure with refined grain structure after the processes with thermal loading. The combined addition of niobium and titanium also indicated an increase in grain size homogeneity. The benefits of the new alloys are observed in the residual stress state and in the topography, in which they present higher levels of compressive residual stress combined with a surface with reduced roughness. The results also indicate a reduction in the distortion levels associated with homogeneous grain structure, such as that obtained with the combined addition of Nb and Ti. Finally, a potential process improvement is raised, the increase of the carburizing temperature may lead to the achievement of the required carburized layer with cost and process time savings. The results of this study showed that the gear manufacturing chain is sensitive to the addition of microalloying elements, so that the new alloys showed modified surface integrity. Among the manufacturing processes, those which presented the highest modification in their results were isothermal annealing, carburizing, and grinding. Therefore, microalloyed steels represent a class of materials that can be employed in the gear manufacturing chain and offer an optimized surface integrity state.

List of Figures

Figure 1.1. A conventional gear manufacturing chain.	20
Figure 1.2. The summarized structure of this study.	22
Figure 2.1. The different gear types.	23
Figure 2.2. The main possible processes for teeth cutting (NIKOLAOS; ARISTOMENIS, 2012; KLOCKE; BRECHER; BRUMM, 2014; REGO, 2016).....	26
Figure 2.3. The main possible heat treatments for gear surface hardening (AGMA, 2008; DAVIS, 2005; GROSCH, 2014; REGO, 2016).	27
Figure 2.4. The main possible processes for finishing (HARADA; MORI; MAKI, 2003; KLOCKE; BRINKSMEIER; WEINERT, 2005; KARPUSCHEWSKI; KNOCH; HIPKE, 2008; REGO, 2016).	28
Figure 2.5. The integrated approach of manufacturing, dynamic behavior, and gear design. .	29
Figure 2.6. Topography alterations due to manufacturing processes (REGO, 2011; BERGSETH; SJÖBERG; BJÖRKLUND, 2012).	31
Figure 2.7. Relationship between mechanical, thermal, and structural phenomena of the residual stress origins (INOUE, 2014; REGO, 2016).	33
Figure 2.8. The main gear failure modes and fatigue mechanism, regarding to the rolling contact fatigue (ALBAN, 2002; REGO, 2016).	34
Figure 2.9. The characteristics of contact fatigue and bending failures (LECHNER; NAUNHEIMER, 1999; MCPHERSON; RAO, 2000; DING; RIEGER, 2003; DAVIS, 2005; BELSAK; FLASKER, 2006).	36
Figure 2.10. The gear sizing conventional procedure (ISO, 2007).	38
Figure 2.11. The main effects of the precipitate particles due to microalloying elements (LIU; JONAS, 1989; DEARDO, 2003; BAKER, 2019).	41

Figure 2.12. The main benefits of microalloying elements (WISE; MATLOCK, 2000).....	43
Figure 2.13. The results of microalloyed steels in fatigue tests and grain size controlling (TOBIE; HIPPENSTIEL; MOHRBACHER, 2017).	45
Figure 2.14. The studies in conventional gear steel with microalloying element addition regarding to abnormal grain growth and fatigue lifetime (ALOGAB <i>et al.</i> , 2007; THOMPSON; MATLOCK; SPEER, 2007; MA <i>et al.</i> , 2008)	47
Figure 2.15. The ratio Ti/N effects in microalloyed steels (MEDINA <i>et al.</i> , 1999).	47
Figure 2.16. Results of the keywords research.	49
Figure 3.1. The basis for the hypothesis, the objective of the study and how to approach it...	50
Figure 4.1. Chemical composition of specimens and gear manufacturing chain investigated.	52
Figure 4.2. The experimental scope of the study.....	54
Figure 4.3. Maximum power and torque of vehicles sold in 2018 in Brazil (FENABRAVE, 2019).....	55
Figure 4.4. The gear-dedicated test rigs and curve of contact/bending fatigue.....	56
Figure 4.5. <i>ITA Geometry</i> main parameters.	57
Figure 4.6. The hot forging process.....	58
Figure 4.7. The isothermal annealing process.	59
Figure 4.8. The hobbing process.	60
Figure 4.9. The carburizing process.	61
Figure 4.10. The grinding process.	62
Figure 4.11. The microstructure investigation procedure.....	63
Figure 4.12. The topography and distortion assessment procedure.	65
Figure 4.13. The <i>Peak Shift</i> method and applied XRD parameters.....	67
Figure 4.14. The method applied for depth generation.	67
Figure 4.15. The hardness mapping procedure.	69

Figure 5.1. Grain size evolution along the manufacturing processes.....	72
Figure 5.2. Grain size after the carburizing (CELADA-CASERO; SIETSMA; SANTOFIMIA, 2019).....	73
Figure 5.3. Hardness mapping along teeth (a) and hardness profile of carburized layer (b) at the end of the manufacturing chain.	74
Figure 5.4. Comparison of the hardness profile along the carburized layer at different carburizing temperatures (T_c).	76
Figure 5.5. Topography analysis of the microalloyed steels (WHITEHOUSE, 1978; AGMA, 2014).....	77
Figure 5.6. Gear distortion level of the microalloyed steels (KLOCKE; BRECHER; BRUMM, 2014; AGMA, 2002).	78
Figure 5.7. Residual stress profile along depth.	79
Figure 5.8. Assessment of residual stress heterogeneity on surface.....	81
Figure 5.9. Grain size after rolling.	84
Figure 5.10. Grain size after forging.	85
Figure 5.11. Grain size after annealing.....	86
Figure 5.12. Grain size after hobbing.	88
Figure 5.13. Topography analysis after hobbing.	89
Figure 5.14. Topography (a) and distortion level (b) after carburizing.....	91
Figure 5.15. RS depth profile (a) and RS surface heterogeneity (b) induced by the carburizing process.	92
Figure 5.16. The impacts of abnormal grain growth (AGG), as presented by the +Nb, to the homogeneity in properties.	93
Figure 5.17. Topography (a) and distortion level (b) after grinding.	95

Figure 5.18. RS depth profile (a) and RS surface heterogeneity (b) induced by the grinding process.	96
Figure 5.19. The improvements of the microalloyed steels and the contribution of the grinding process.	98

List of Acronyms

AGG	Abnormal grain growth
AGMA	American Gear Manufacturers Association
AGS	Austenitic grain size
ASTM	American Society for Testing and Materials
BC	Before Christ
CBMM	<i>Companhia Brasileira de Metalurgia e Mineração</i>
CCM	<i>Centro de Competência em Manufatura</i>
CMM	Coordinate Measuring Machine
DIN	<i>Deutsches Institut für Normung</i>
Dist.	Distortion
FEM	Finite Element Method
HSLA	High-strength low alloy
ICE	Internal combustion engine
ISO	International Organization for Standardization
ITA	<i>Instituto Tecnológico de Aeronáutica</i>
LabMat	<i>Laboratório de Materiais</i>
MA	Microalloyed
NVH	Noise Vibration Harshness
OEM	Original Equipment Manufacturer
RS	Residual stress
RS _{het.}	Residual stress heterogeneity
RS _{prof.}	Residual stress profile
SAE	Society of Automobile Engineers

SURF	Surface
Top.	Topography
XRD	X-ray diffraction

Acronyms to describe the specimens

REF	Reference steel
+Nb	Nb-microalloyed steel
+NbTi	NbTi-microalloyed steel

List of Symbols

a	Center distance
a_e	Radial depth of cut
b	Face width
C_a	Tip relief
cBN	Cubic boron nitride
C_f	Root relief
C_α	Profile crowning
C_β	Lead crowning
d	Reference diameter
d_p	Pitch diameter
f_a	Axial feed
Fe	Iron
$f_{H\alpha}$	Profile slope deviation
$f_{H\beta}$	Helix slope deviation
F_p	Cumulative pitch deviation
f_{pt}	Single pitch deviation
$f_{pt,max}$	Maximum single pitch deviation
F_t	Nominal transverse tangential load
F_x	Cutting force, in the direction of the radial depth of cut
F_y	Cutting force, in the feed direction
hp	Horsepower
HV	Vickers hardness
HV _{0.2}	Vickers hardness at load $F = 1.962 \text{ N}$
K_A	Application factor
$K_{F\alpha}$	Transverse load factor (root stress)
$K_{F\beta}$	Face load factor (root stress)
kgf	kilogram-force
$K_{H\alpha}$	Transverse load factor (contact stress)
$K_{H\beta}$	Face load factor (contact stress)
K_v	Dynamic factor

m_n	Normal module
P_{\max}	Maximum power
P_N	Nominal power
p_t	Pitch
R_a	Arithmetic mean roughness
R_k	Core roughness
R_{pk}	Reduced peak height
R_q	Root mean square roughness
R_{vk}	Reduced valley depth
R_z	Mean peak to valley roughness
S_F	Safety factor for bending fatigue failure
$S_{F,\min}$	Minimum safety factor for bending fatigue failure
S_H	Safety factor for contact fatigue failure
$S_{H,\min}$	Minimum safety factor for contact fatigue failure
T_{\max}	Maximum torque
T_N	Torque
T_{nc}	Non-recrystallization temperature
u	Gear ratio
wt	Weight
Y_B	Rim thickness factor
Y_{DT}	Deep tooth factor
Y_F	Tooth form factor
Y_{NT}	Life factor (bending stress)
$Y_{R,relT}$	Relative surface factor
Y_S	Stress correction factor (1)
Y_{ST}	Stress correction factor (2)
Y_X	Size factor (tooth root)
Y_β	Helix angle factor (root stress)
$Y_{\delta,relT}$	Relative notch sensitivity factor
z	Number of teeth
Z	Depth
$Z_{B/D}$	Single pair tooth contact factor
Z_E	Elasticity factor
Z_H	Zone factor

Z_L	Lubricant factor
Z_{\max}	Depth of maximum compressive residual stress
Z_{NT}	Life factor (contact stress)
Z_R	Roughness factor
Z_{Ir}	Zirconium
Z_{stock}	Depth of the stock
Z_V	Velocity factor
Z_W	Work hardening factor
Z_X	Size factor (contact stress)
Z_β	Helix angle factor (contact stress)
Z_ε	Contact ratio factor
α	Ferritic phase
α_n	Normal pressure angle
β	Helix angle
γ	Austenitic phase
ε_c	Critical deformation
2θ	Diffacted beam angle
$\sigma_{F,\text{lim}}$	Allowable bending stress
$\sigma_{H,\text{lim}}$	Allowable contact stress
σ_{RS}	Residual stress value
$\overline{\sigma_{RS}}$	Average residual stress
$\sigma_{RS,\text{max}}$	Maximum residual stress value
$\sigma_{RS,\text{min}}$	Minimum residual stress value
$\sigma_{RS,\text{std}}$	Standard deviation of residual stress values
ϕ	XRD azimuthal direction
ψ	Grain lattice orientation

Contents

1	INTRODUCTION.....	19
2	LITERATURE REVIEW.....	23
2.1	Gear manufacturing chain	23
2.2	Connection among manufacturing, dynamic behavior, and gear design.....	28
2.2.1	Manufacturing-induced surface integrity	29
2.2.2	Dynamic behavior	33
2.2.3	Gear design.....	36
2.3	Microalloyed steels	39
2.3.1	The effects of niobium (Nb) as microalloying element	43
2.3.2	The effects of titanium (Ti) as microalloying element.....	44
2.4	State of the art of microalloyed steels in gear applications	45
3	OBJECTIVE AND APPROACH	50
4	MATERIALS AND METHODS	52
4.1	Overall experimental scope	52
4.2	Specimens' design	54
4.3	Specimens' manufacturing	57
4.3.1	Hot forging	57
4.3.2	Isothermal annealing	58
4.3.3	Soft machining	59
4.3.4	Carburizing	60
4.3.5	Grinding.....	61
4.4	Specimens' tests	62
4.4.1	Microstructure investigation.....	62
4.4.2	Topography and dimensional analysis	63
4.4.3	Residual stress state assessment	65
4.4.4	Hardness mapping	68
4.5	Summary	69
5	RESULTS AND DISCUSSIONS	71
5.1	Behavior of microalloyed steels at the end of the manufacturing chain	71
5.1.1	Microstructure investigation and hardness mapping	71

5.1.2	Dimensional analysis and residual stress state	76
5.1.3	Summary	82
5.2	Influence of Nb-Ti addition on each manufacturing process	83
5.2.1	Billet processing	83
5.2.2	Teeth cutting	87
5.2.3	Carburizing	89
5.2.4	Grinding	94
5.2.5	Summary	98
6	CONCLUSIONS AND OUTLOOK	100
	REFERENCES	103
	APPENDIX A – TERMINOLOGY	112
A.1	Gear nomenclature for macro and microgeometry	112
	APPENDIX B – MATERIAL SPECIFICATIONS	113
B.1	Conventional gear steels	113

1 Introduction

Within the uncertain context of the impacts of electric vehicles establishment, the global growth in gear production will remain robust at an annual rate of 5.6%, at least until 2024. The production of new engines and transmission systems with an increasing number of gears is also expected, both stimulated by increased energy efficiency requirements (SCHULHAUSER *et al.*, 2016).

Considering electric vehicles, the transmission systems are required to provide higher torques and rotations during the operation, as it allows the achievement of higher energy efficiency (REICHERT *et al.*, 2016; MILETI *et al.*, 2020). Therefore, the mechanical components that constitute the transmission systems undergo incremental demands in aspects of durability and mechanical strength (ZHAO *et al.*, 2016). These demands also expand to all vehicle systems, being especially observed in gears of transmission system. As a form of increasing load capacity, one of the approaches widely used during gear design is the increase of the dimensions to reduce the actuating stress level (LECHNER; NAUNHEIMER, 1999).

However, the use of this approach conflicts with other demands such as energy efficiency in transmission systems, a factor that has become increasingly critical in the world economic scenario. Thus, other mechanisms for optimization of durability and mechanical strength have been the focus of studies in recent years, being approached both through modifications in manufacturing processes and the use of new materials and chemical compositions (MA *et al.*, 2008).

The growth of gear production reflects directly on the Brazilian scenario, which absorbs the tendency within the particularity of the "high added-value solutions" market (cost reduction). In this context, material may represent up to 30% of the production cost of a gear (DAVIS, 2005). From this contribution arises the constant concern of the national industry about the possibility to replace costly alloy elements usually added to improve durability and mechanical strength of transmission system components, such as nickel and chrome.

Within this aspect, the use of microalloying elements such as niobium (Nb) and titanium (Ti) in the chemical composition of steels for gears manufacturing appear as potential alternatives to conventional gear steels, which present up to 3% nickel, while microalloying content is less than 1%. In addition, Brazil is the country with the largest niobium reserves in

the world, with more than 98% (PEREIRA JR, 2014). This represents a competitive advantage regarding these potential new alloys and an economic motivation for this study.

Nonetheless, not only the metallurgical aspects of the chemical composition are responsible for the final integrity of a mechanical component. The transformations that the working materials are prone to may also affect their physical characteristics and so the mechanical behavior. For gears, a conventional manufacturing chain consists of many individual stages, including teeth cutting, heat treatment for material hardening, and finishing stages. Each of these individual stages causes, to some extent, modifications in the working material characteristics (HUSSON *et al.*, 2012).

Figure 1.1 presents a conventional gear manufacturing chain. The manufacturing processes involved in the production of automotive gears may include elevated thermal and mechanical loadings, which in turn may produce remarkable metallurgical modifications within the working material. In fact, each individual manufacturing process can contribute significantly to the properties variations that affect the gear surface integrity (REGO, 2016). Such variations may also be enhanced when different elements are added in the chemical composition. Therefore, the effect of the manufacturing chain should not be neglected when considering the use of alternative materials.

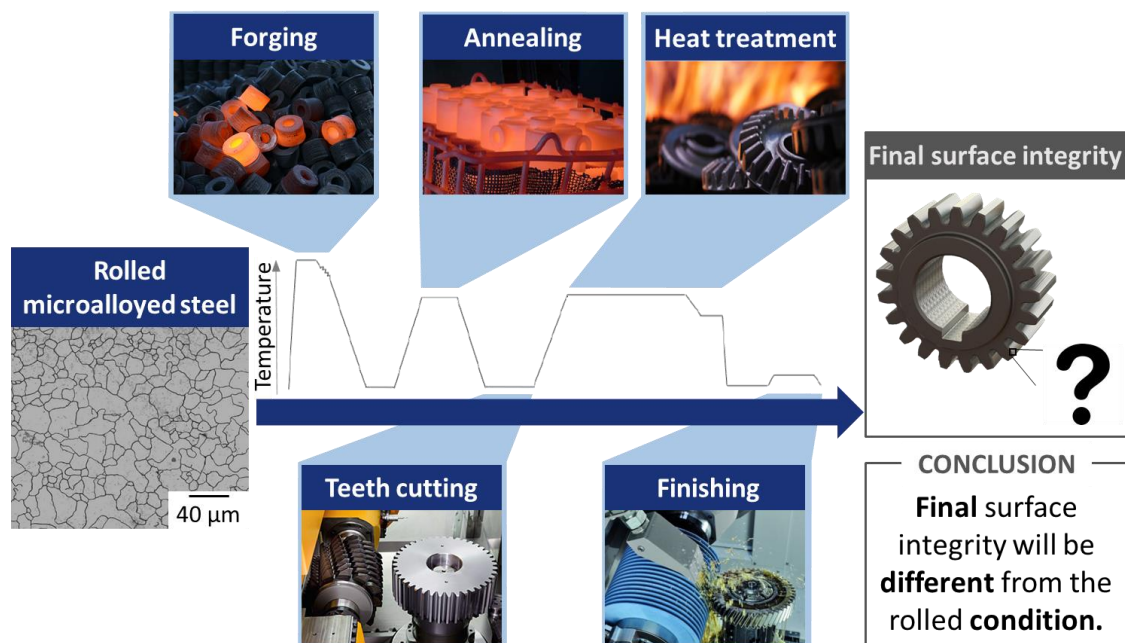


Figure 1.1. A conventional gear manufacturing chain.

The contribution of this study consists in covering different microalloyed steels along the gear manufacturing chain, with the objective of characterizing the surface integrity evolution along the manufacturing processes. It is expected that the findings provide a better understanding of the main factors affected by the manufacturing processes for each microalloyed steel.

The development of this approach was conducted at the Competence Center in Manufacturing (*Centro de Competência em Manufatura*, CCM-ITA). Part of the experimental scope was carried out at the Materials Laboratory (*Laboratório de Materiais*, LabMat-ITA). The importance of the study can also be verified by the investigations developed in a collaborative frame with Gerdau S.A..

The initial chapter of this study is the Literature review, which is intended to provide the background knowledge needed to guide the following chapters. It is divided into four sections, related to the gear manufacturing chain, interaction among the gear stages, microalloyed steels and an overview of the state-of-the-art related to microalloyed steels in gear and transmission systems.

After the Literature review, the objective of the study is announced, and aims to bridge the gap observed in the overview of the state-of-the-art. To organize the study conduction in accordance with the hypothesis, two research questions are stated and expected to be answered during the following chapters.

Experimental procedures are detailed in the Materials and method chapter. It is divided into four sections. The first one is a summary of the experimental scope along the manufacturing processes. The second one is dedicated to detail the gear design used in this study: the *ITA Geometry*. The parameters of each manufacturing process to which microalloyed steels were submitted are presented in the third section. The last section presents how each experiment was carried out and highlights its importance to the objective achievement.

Results and discussion are the subject of the following chapter, which is divided into two sections, addressed to each of the two research questions. The first section covers the surface integrity state at the end of the manufacturing chain while the second section considers each manufacturing process individually and the in-between surface integrity. Not only the results of experimental scope are displayed but also discussions are held over the findings.

The last chapter recalls the objective of the study and verifies the suitability of the findings in answering the research questions. The chapter is complemented by suggestions of forecast studies, which may contribute to bridge additional gaps not covered in the planned scope. The structure of this study is summarized in Figure 1.2.

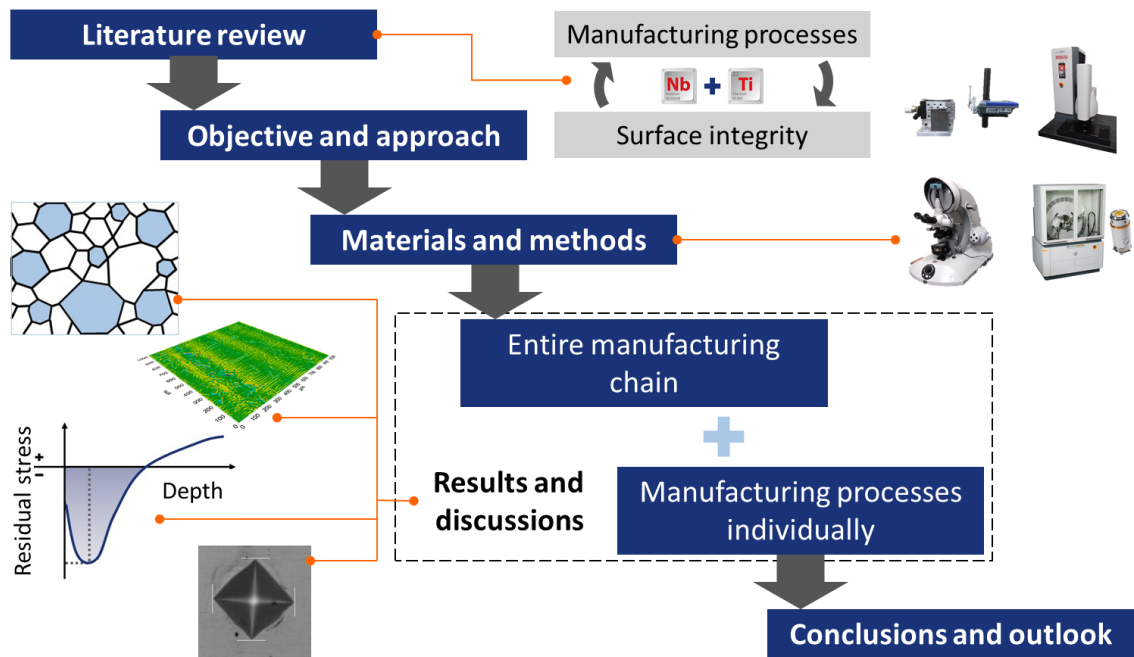


Figure 1.2. The summarized structure of this study.

2 Literature review

2.1 Gear manufacturing chain

The first gear design developments, still in primitive versions, were registered approximately in the 4th century BC (PRICE, 1959). Along the history, other alternative versions were developed, preserving the same concept, as the one developed by Leonardo da Vinci, in the 15th century (LIEB, 1921). Several studies were made since then, until achieving what it is understood today as gear, improving its performance, and expanding its applications.

Gearing is the most widely used form of transmission when significant power transmission over a short distance at constant velocity ratio is required (WARNER, 2017). As shown in Figure 2.1, gears can be divided according to the kind of transmission, such as: between two parallel rotation axis, cylindrical gears are used; between non-parallel rotation axis, bevel gears or worm gears are used; for power transmission between rotation and translation axis, rack and pinion gearing is used. Still within each type there are variants according to other transmission requirements (EITEL, 2003; GONZALEZ, 2015).

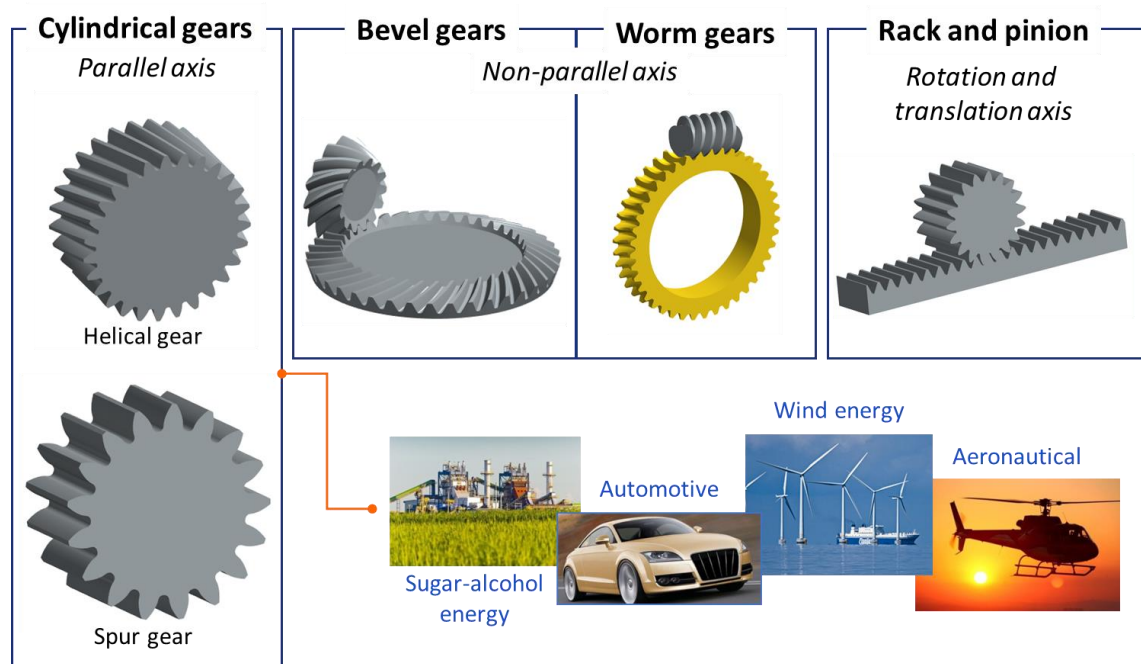


Figure 2.1. The different gear types.

Among the different gear types, the most used is the cylindrical gear in a wide variety of applications. In terms of size, they can range from 1 mm in diameter, applied on watches, for example, to marine gears, up to 8,000 mm. In terms of functional requirements, it can vary from sugar-alcohol energy applications, in which there are no NVH (Noise Vibration Harshness) concerns, to aeronautical where the tolerances are the tightest. Among the applications, the most relevant is the automotive sector, which represent about 73% of all gears manufactured annually (SCHULHAUSER *et al.*, 2016).

Within the cylindrical gear type, there are two main variants: spur gear and helical gear. The spur gear is the simplest gear design, with straight teeth, which means that they are parallel to the axial axis of the gear. Helical gears, on the other hand, have an angle between the gear face and the axial axis of the gear, named helix angle (β). This configuration allows them to be smoother and quieter during operation compared to spur gears and, therefore, they are the most used in the automotive sector (GONZALEZ, 2015).

The gear ratio (u) for a simple transmission between cylindrical gears, named parallel transmission, ranges from 1 to 6 (1:1 to 6:1). Nevertheless, a higher gear ratio is required for many applications, so it is common to use transmission systems that are composed of more than one parallel transmission in sequence (GONZALEZ, 2015). As the focus of the investigation in this study, the cylindrical gears will be from this point on simply called gears.

In addition to the gear ratio, and helix angle, the gear design takes into consideration several other parameters presented in appendix “A.1 Gear nomenclature for macro and microgeometry”. After defining the macrogeometry parameters, microgeometry parameters can also be established at the sizing stage, which is intended to optimize the contact pattern during operation.

As can be noticed, the gears provide a wide variety in terms of application and geometry parameters. For the manufacturing the same is observed, it is possible to obtain gears manufactured by several different manufacturing chains. A gear manufacturing chain considered conventional starts with the working material in a rolled round shape. From the rolled condition, a pre-form usually called billet is obtained by hot forging. Following the forging stage, a machining stage is conducted, in which the teeth cutting occurs. The gear is then submitted to a heat treatment to increase its mechanical strength and, finally, undergoes a finishing stage (KLOCKE; BRECHER; BRUMM, 2014).

Each stage described above can still be conducted by different processes or intermediate processes such as annealing stages and shot peening. Among the alternative gear manufacturing chains, the most relevant is powder metallurgy chain, and, recently, some studies have been

carried out considering additive manufacturing for gear manufacturing (ROBATTO, 2017; TEZEL; TOPAL; KOVAN, 2020).

The forging process is usually carried out at high temperatures, causing the working material to be submitted to a thermomechanical process, which means high thermal and mechanical loading simultaneously. With this, the billet may present heterogeneity in its microstructure and in its mechanical properties (SILVEIRA *et al.*, 2020). To mitigate microstructure heterogeneity, an annealing stage is usually performed between the forging and machining stages. At this stage, the working material is reheated to relieve its tensions and air cooled, recovering its ductility. At the end of the process, the billet will present a more homogeneous microstructure, reducing the negative effects of forging flow (CLARKE, 2014).

Within the machining stage, there are some additional processes, such as side facing, external diameter turning, internal drilling, and broaching. It is also in this stage that the teeth cutting occurs, which can be performed in two different forms: profile and generating process. In the profile teeth cutting, the teeth are formed individually, the billet is kept static until one tooth is completed and then the process starts on the next tooth. In the generating teeth cutting, all teeth are formed simultaneously using a tool that simulates one or more teeth and relative movement between the billet and the tool (DAVIS, 2005).

The teeth cutting can be executed by milling, a profile process in which the tool has the tooth shape and after completing the cut of one tooth, the billet is repositioned for the next tooth cutting. Despite the low cost of milling, the process is time-consuming and has limited accuracy. In contrast, the shaping process is considered the most versatile of all tooth cutting processes, although it is also time-consuming. It is a generating process in which the tool is a toothed disk and rotates synchronously with the billet. The teeth cutting occurs by stroke axial movements of tool, parallel to the billet (DAVIS, 2005).

Among the teeth cutting processes, the most applied is the hobbing process, which presents advantages in terms of tool cost, and cutting speed and accuracy. Hobbing is a generating process, used for spur gears, helical gears, worm and worm gears. The process consists of a tool named hob, a fluted worm with form-relieved teeth, which rotates together with the billet (movements 1 and 2), so with each tool revolution a tooth is cut. The axial feed (movement 3) of the tool results in the complete cutting of the teeth (DAVIS, 2005). Figure 2.2 presents the main possible processes for teeth cutting.

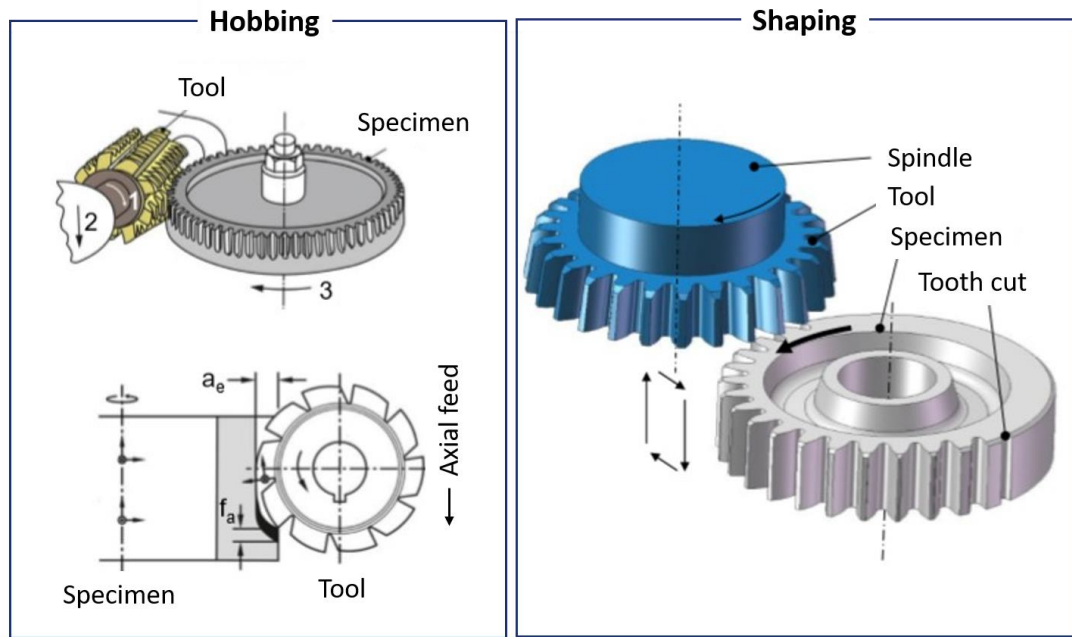


Figure 2.2. The main possible processes for teeth cutting (NIKOLAOS; ARISTOMENIS, 2012; KLOCKE; BRECHER; BRUMM, 2014; REGO, 2016).

To achieve the mechanical properties required for its operation, a heat treatment stage is usually included in the gear manufacturing chain, composed of quenching and tempering. Quenching is usually conducted using three possible methods: through hardening, case hardening and induction hardening (RAKHIT, 2000; DAVIS, 2005).

The through hardening process is used when high surface hardness is not required and medium carbon steels (0.3-0.6 wt%) are generally used. The process does not have only a hardened surface layer well-defined, but a hardness gradient along the depth since the surface cooling is more severe, increasing its hardness in relation to the core (RAKHIT, 2000; DAVIS, 2005).

The carburizing, nitriding and carbonitriding processes result in a hardened surface layer and a tough core and are called case hardening. For this process type, steels containing up to 0.3 wt% carbon are used. The most usual process among these is carburizing. It consists in keeping the steel in the austenitic phase in contact with an atmosphere rich in carbon, either by gas (more than 90% of the cases), liquid or solid and, consequently, the carbon content of the surface increases due to the diffusion mechanism. After hardening, the carbon-rich surface layer presents a martensitic/bainitic microstructure with a hardness much higher than the core. When a deep surface layer is not required (usually less than 0.4 mm), the process used is carbonitriding, where ammonia is included in the carburizing atmosphere for nitrogen diffusion

in the surface layer and allows the reduction of the process temperature. In some cases, nitriding is used, which allows to reduce the process temperature even more and, since fast cooling is not necessary, the dimensional variations are smaller (RAKHIT, 2000; DAVIS, 2005).

In some applications, a hardened surface layer is required, but no change in chemical composition is allowed. In these cases, the process used is induction hardening, in which the teeth are rapidly heated by electrical induction and quenched immediately. Steels with carbon content ranging from 0.4 to 0.6 wt% are used (RAKHIT, 2000). The heat treatment processes are shown in Figure 2.3.

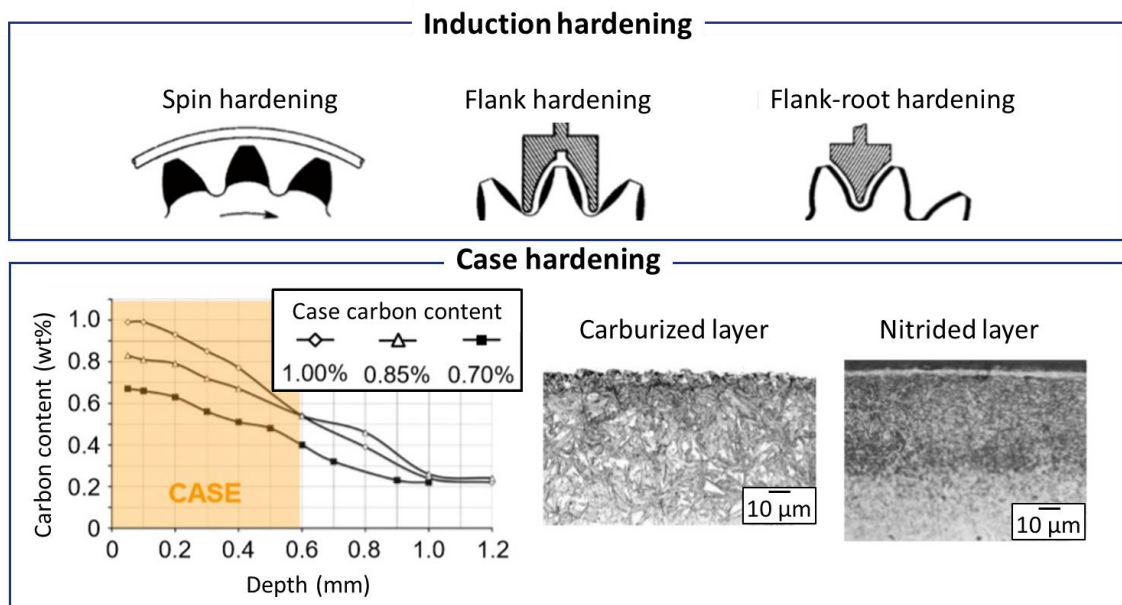


Figure 2.3. The main possible heat treatments for gear surface hardening (AGMA, 2008; DAVIS, 2005; GROSCH, 2014; REGO, 2016).

After heat treatment, gears are commonly submitted to a finishing stage. The process aims to reduce distortions and, consequently, obtain an increase in the mechanical strength and reduction of NVH emission in operation by surface roughness improvement. Moreover, it is at this stage that the microgeometry modifications are performed. The processes are carried out by abrasive tools, usually Al_2O_3 (aluminum oxide) or cBN (cubic boron nitride), removing a stock intentionally remained during the teeth cutting. This finishing process can also be classified either as generating or as profile grinding (KARPUSCHEWSKI; KNOCH; HIPKE, 2008).

The most usual finishing process is grinding and can be conducted either by profile or by generating. In profile grinding, the abrasive disk passes through the space between two teeth finishing both flanks of that gap. Then the process proceeds to the next gap. In generating grinding, the tool is similar to the hob, grinding all teeth simultaneously. The honing process appears as an alternative for grinding. In it, the ring-shaped tool with an integrated internal gearing is used for external gear finishing (DAVIS, 2005; KARPUSCHEWSKI; KNOCHE; HIPKE, 2008).

Another usual process in the gear manufacturing chain is shot peening. Different from other finishing processes, its goal is to induce compressive residual stresses on the surface by plastic deformation. Small round hard particles are controlled against the surface, consequently leading to mechanical strength improvement (KIRK, 1999; REGO, 2011). The main finishing processes are presented in Figure 2.4.

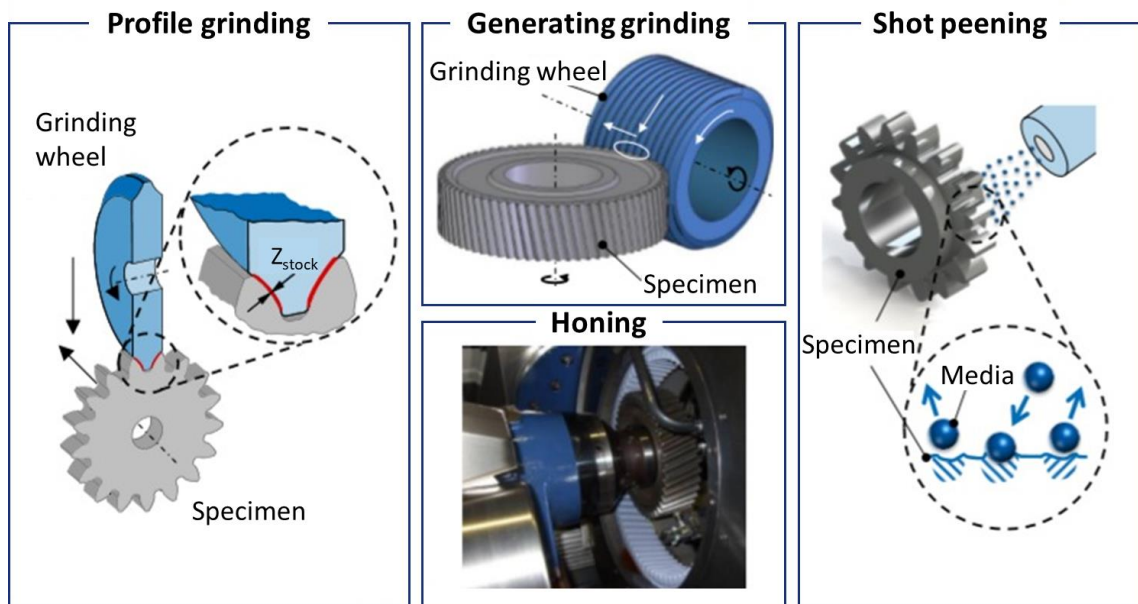


Figure 2.4. The main possible processes for finishing (HARADA; MORI; MAKI, 2003; KLOCKE; BRINKSMEIER; WEINERT, 2005; KARPUSCHEWSKI; KNOCHE; HIPKE, 2008; REGO, 2016).

2.2 Connection among manufacturing, dynamic behavior, and gear design

The integration of manufacturing, dynamic behavior and gear design stages is increasingly required to ensure the appropriate performance. The manufacturing processes have a direct influence on the dynamic behavior of the gears. The thermal and mechanical loadings

of the manufacturing processes are major sources of surface integrity disturbance, which have been shown to significantly affect the fatigue lifetime (REGO, 2016).

Dynamic behavior can be influenced by many factors, from external conditions to assembly errors and the suitable attributes differ for each application and requirements. NVH emission can be limiting for automotive gears, for example, but not for the mining industry. However, the dynamic behavior may be predicted at the gear sizing stage by numerical and analytical simulations (XU *et al.* 2007; FRANULOVIC *et al.*, 2011; OUYANG *et al.*, 2017).

Gear design considers well established standards for determining the dynamic behavior of gears, such as AGMA 2001-D04 and ISO 6336 (AGMA, 2004; ISO, 2007). These standards also include individual parameters for each application, such as loading uniformity. Moreover, they also cover the gear manufacturing chain, its errors and tolerance. Therefore, the three steps are connected to each other, as shown in Figure 2.5.

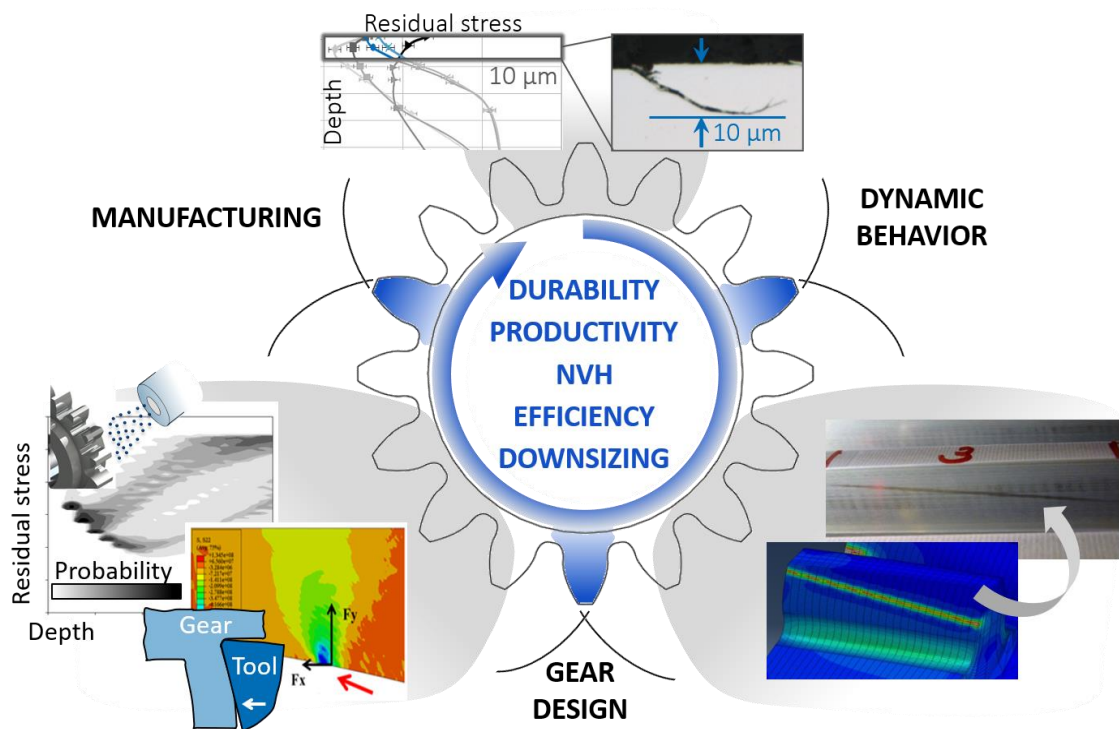


Figure 2.5. The integrated approach of manufacturing, dynamic behavior, and gear design.

2.2.1 Manufacturing-induced surface integrity

The selection of the processes which constitute a manufacturing chain has historically been based on cost and time. However, over recent years, the effect of the manufacturing-induced surface on the dynamic behavior of the component has become crucial to the definition

of the processes. Such surface aspects which influence the functional performance are described by surface integrity. Although it has several comprehensions, since it involves different subjects, surface integrity can be divided into two parts: the external aspects of topography, texture and finish surface; and the internal sub-surface aspects of metallurgy, hardness and residual stress (GRIFFITHS, 2001).

The first processes of the gear manufacturing chain, which means rolling, forging, and annealing, may be considered its impacts mostly on the microstructure. This is because their effects can be maintained until the end of the manufacturing chain, as in the case of the formation of a banded microstructure (NAVAS *et al.*, 2011). The microstructure is again significantly altered during the heat treatment process, whether through hardening, case hardening or induction hardening. The objective of the process is to obtain a martensitic microstructure by quenching. In the martensite the carbon remains in solid solution and is a much harder phase than the ferrite/perlite, promoting a substantial improvement of mechanical strength (BHADESHIA; HONEYCOMBE, 2017).

There is also a necessity to be concerned with the teeth topography, as well as the distortions generated by the processes. Both characteristics strongly influence the dynamic behavior as well as may alter the conditions of the following process. The surface roughness may indicate contact fatigue prematurely, since it may elevate the contact stresses and the valleys are crack nucleators (BERGSETH; SJÖBERG; BJÖRKLUND, 2012; LIU *et al.*, 2019). The gear fatigue lifetime is also influenced by the distortion level, which can promote inadequate meshing (GUTERRES; RUSNALDY; WIDODO, 2017). Such features also increase NVH emission, which is avoided in electric vehicles transmission systems (BRAUER, 2017).

As shown in Figure 2.6, topography is a record of the loadings of the manufacturing processes and has been better understood over the last few years (KLOCKE; BRINKSMEIER; WEINERT, 2005). The topography influences the real contact condition and, in addition to influencing contact stresses, it is a crucial factor for wear, friction, lubrication properties and NVH emission (BERGSETH; SJÖBERG; BJÖRKLUND, 2012). How the topography is analyzed is also an explored issue since it can be performed in several manners. The amplitude parameters are not enough to fully describe the surface topography, which can be achieved by the functional parameters (KLOCKE; BRINKSMEIER; WEINERT, 2005; BERGSETH; SJÖBERG; BJÖRKLUND, 2012).

Topography resultant from
different manufacturing
processes

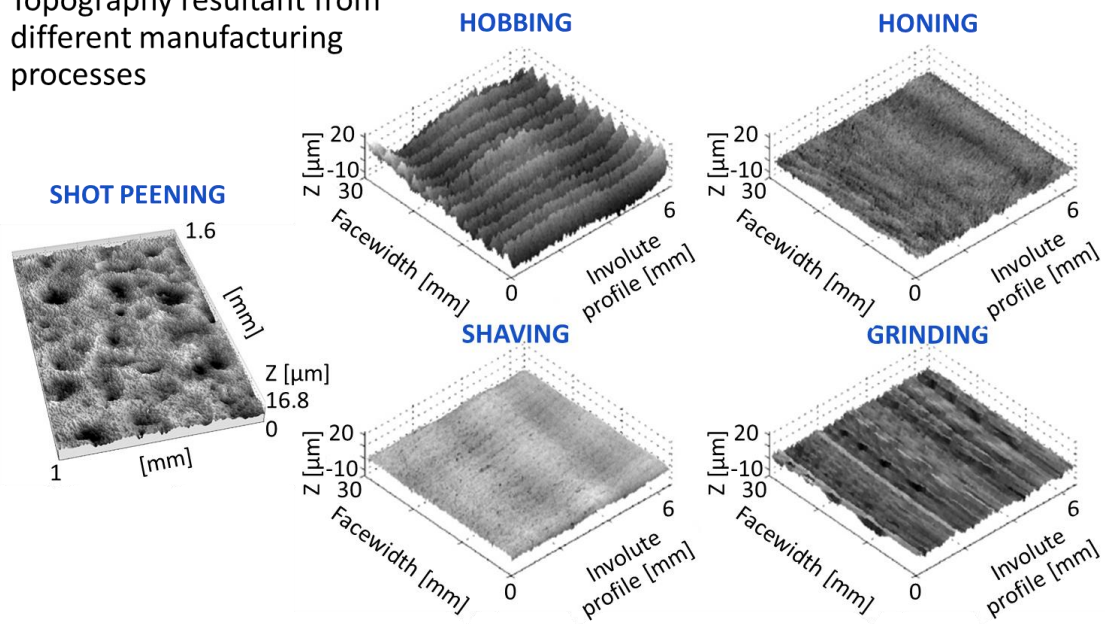


Figure 2.6. Topography alterations due to manufacturing processes (REGO, 2011; BERGSETH; SJÖBERG; BJÖRKLUND, 2012).

The main process that induces high levels of both surface roughness and distortion is the heat treatment, particularly quenching, and the finishing process is intended to reduce these parameters (AGMA, 2008; KLOCKE, 2009). Dimensional variations are inevitable at this stage and vary with the hardening process. The distortion level is influenced by each of the previous processes and is caused by the relief of both thermal and mechanical loading as well as phase transformations (AGMA, 2008; HUSSON *et al.* 2012).

Finally, the knowledge of the residual stress state is also of interest along the gear manufacturing chain. This is due to the extremely important role that the residual stress state plays with respect to the fatigue strength of materials (LU, 2002). Since fatigue is the main gear failure mode, this property is at the interface between manufacturing chain and dynamic behavior (DAVIS, 2005).

The residual stress state can be beneficial or detrimental to the gear fatigue lifetime due to the superposing principle. The real stress profile applied to the gear during its operation is the sum of the acting stresses and the residual stresses (LU, 2002). As a result, the residual stress state can increase or reduce the real stresses, depending on its signal. Since both nucleation and propagation of fatigue cracks are always under tensile actuating stresses, a compressive residual stress state is desirable, as they act to offset part of the actuating stresses, increasing the gear lifetime (ANDERSON, 2005; HAUKE, 1997).

They originate from elastic accommodations in a structure as a result of inhomogeneous plastic strains (LÖHE; LANG; VÖHRINGER, 2002; BOUCHARD; WHITERS, 2006). The induction of residual stresses can occur by thermal, mechanical, or structural phenomena. Usually, a combination of them is involved on manufacturing processes, as they are strongly correlated (LU, 2002).

Residual stresses from mechanical origins require that the material undergoes plastic deformation, which in microstructure level will result in inhomogeneous plastic strains. Under external loading, different fractions of the working material are prone to different strain levels. After the loading removal, as a tentative of the material to accommodate the plastic deformation, residual stresses are generated (WANG; GONG, 2002).

Thermal induction of residual stresses occurs mainly due to temperature gradient in the component originated due to the heat exchange during manufacturing processes. The different rates of heating and cooling along the part generate expansions and contractions in different regions. In a similar frame to the case of mechanically originated residual stresses, the internal stresses that arise due to thermal heterogeneity subsequently turn to residual stresses (BHADESHIA, 2002).

Depending on the heat generated in these processes, the temperatures involved can reach a level that promotes microstructural alterations. Phase transformation may occur, also being a source of residual stresses induction, due to differences on the microstructural properties of each phase (LU, 2002). Temperature variations may activate phase transformations, which can generate reconstructive or displacive shape changes. Reconstructive transformations are structural changes achieved by a flow of matter, without significant strains. This represents a sudden change on the lattice parameters and consequently on physical properties as density. More than volume changes can occur. Displacive transformations, such as the martensitic, convert physical changes in deformation of the structure, being a combination of shear on the invariant plan and dilatation normal to that plan (BHADESHIA, 2002). The different origins of residual stress are presented in Figure 2.7.

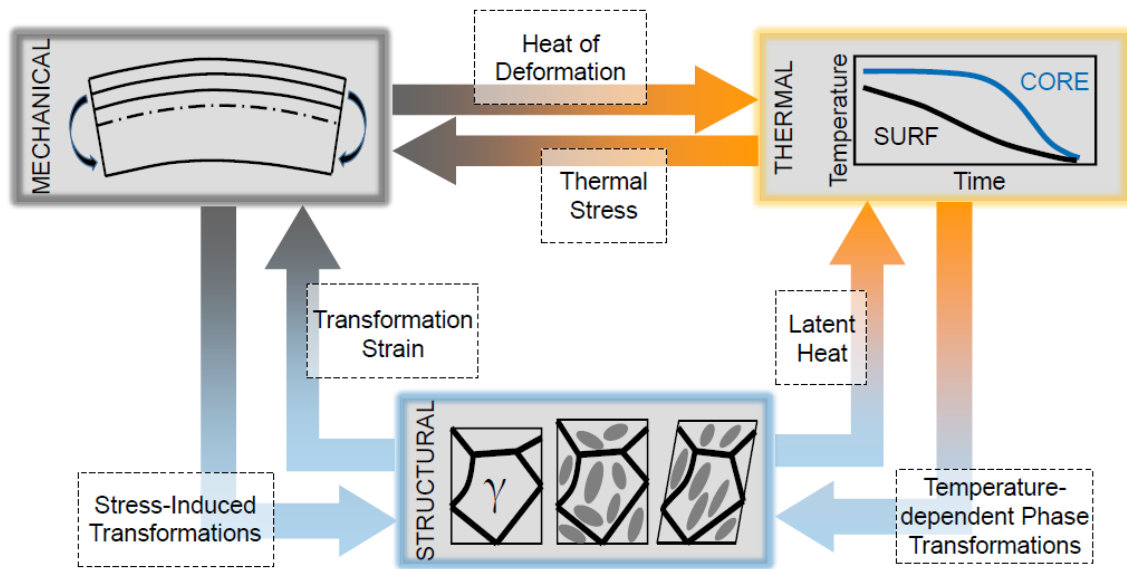


Figure 2.7. Relationship between mechanical, thermal, and structural phenomena of the residual stress origins (INOUE, 2014; REGO, 2016).

2.2.2 Dynamic behavior

The requirements of a gear can include several factors, regarding its dynamic behavior, such as NVH emission and efficiency. Depending on the application, one requirement may be more demanding than the other. However, regardless of the application, the gear is expected to operate for as long as possible without any repairs being necessary. Thus, the main requirement of any gear is its fatigue lifetime (LECHNER; NAUNHEIMER, 1999).

There are many gear failure modes, and, in most cases, there is no indication until the failure has totally occurred, compromising the gear operation. However, each failure mode has its own characteristics and mechanisms, so a detailed study on the failed gears often gives enough information to indicate the failure cause and enable actions to mitigate the next failures. This can be achieved either by design changes, new manufacturing processes or even mechanisms to reduce operating severity (ALBAN, 1985).

The classification of the gear failure modes varies among the authors. American Gear Manufacturers Association (AGMA) (2014) has identified 42 different gear failure modes, which were divided into seven main categories: wear, scuffing, plastic deformation, cracking, fracture, contact fatigue and bending fatigue. Alban (2002) proposes the division of gear failure modes into four main categories, fatigue, impact, wear, and stress rupture, and each of these categories still has specific types of failure. Despite all classifications, fractured surfaces may

not have a unique failure mode because the failure can start in a mode and then change to another.

Fatigue failures are the most common gear failure mode. They occur under cyclic stresses, even below the ultimate tensile stress. There are three characteristic stages of this type of failure: crack nucleation, propagation under successive loading cycles and final rupture. Fatigue failures are highly dependent on the number of loading cycles at the stress level applied and are greatly amplified by notches, grooves, surface discontinuities and subsurface imperfections (DAVIS, 2005).

Generally, the material and metallurgical characteristics are within the gear specifications. The typically failures origins are imperfections at the surface or non-metallic inclusions near the surface, occurring at the loaded side of the tooth. The cracks then propagate around the origin until reaching a critical size for the operation condition, at which the rupture occurs, either by ligament collapse in contact fatigue or by overload in bending fatigue (DING; RIEGER, 2003; DAVIS, 2005; WULPI, 2013). Figure 2.8 summarizes the gear failure modes, with emphasis to the fatigue mechanism.

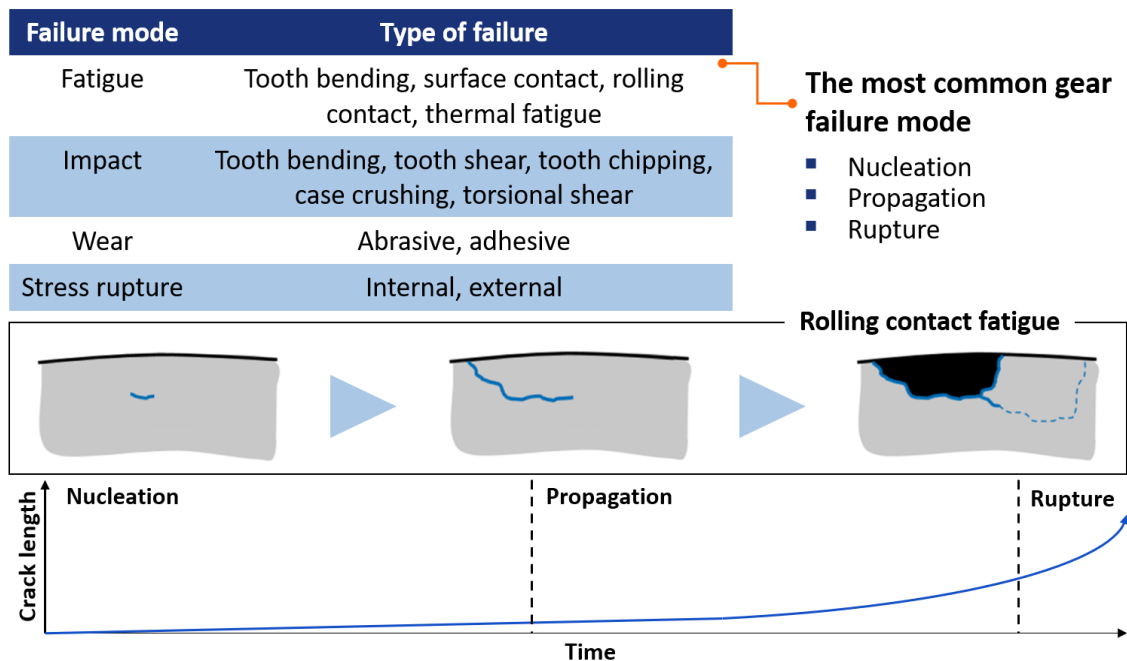


Figure 2.8. The main gear failure modes and fatigue mechanism, regarding to the rolling contact fatigue (ALBAN, 2002; REGO, 2016).

Among the gear fatigue failures, the most relevant modes are the contact fatigue in the tooth flank and the bending fatigue in the tooth root. The contact fatigue failures can be defined

as the failure caused by alternating contact stresses under rolling and sliding condition. The friction in the tooth surface alter the magnitude and the distribution of the stresses in and below the contact area. After cracks have initiated, they propagate at a shallow angle to the surface. Besides the material fracture, some microstructural alterations may result from the contact fatigue failure, such as martensitic transformation from the retained austenite and residual stresses (DAVIS, 2005).

There are some types of contact fatigue, but their terminology is controversial among the authors. The types can also be classified based on the location of the fracture origin (ALBAN, 2002; DING; RIEGER, 2003; DAVIS, 2005; WULPI, 2013; REGO, 2016).

- *Surface-origin pitting*: It is characteristic of combined rolling and sliding, thus the damage occurring on the dedendum (region below the pitch diameter). The maximum shear stress in this type is brought to the surface because of the friction at the interface. The cracks propagate to the core in a direction of between 20° and 40° with the surface. Usually, the damage caused by this mechanism does not overcome a depth of 20 µm.
- *Subsurface-origin pitting*: It is the result of fatigue below the surface in the region of highest shear stress. The origin is commonly a non-metallic inclusion or discontinuity in the structure. The crack initially propagates parallel to the surface, driven by the shear propagation mode, experiences a change of direction, and moves towards the surface under the opening propagation mode. The damage caused by this mechanism is typically between 20 and 100 µm but can overcome 200 µm.
- *Subcase fatigue*: The fatigue initiates near the case/core interface due to the shear stresses. The basic cause is inadequate metal strength in the subcase region. Large cavities are formed in a short time.

Bending fatigue is the most common fatigue failure mode in gears. The classical bending fatigue failure is that which occurs in the region designed to receive the maximum bending stress, at the root radius surface, in the gear applications. Usually the crack nucleation occurs in the central region of the face width, it propagates to the tooth core towards the root radius on the non-loaded side, until the fracture occurs, and the tooth is removed completely (DAVIS, 2005). Bending fatigue is usually related to higher loading levels when compared to contact fatigue.

Since contact and bending fatigue are the main gear failure modes, they should also be considered at the gear teeth design. Not only the geometry, but also the material and surface integrity are fundamental to avoid such failure modes. The main standards consider such features to predict the load capacity of gears (AGMA, 2004; ISO, 2007). Both contact and bending fatigue are demonstrated in Figure 2.9.

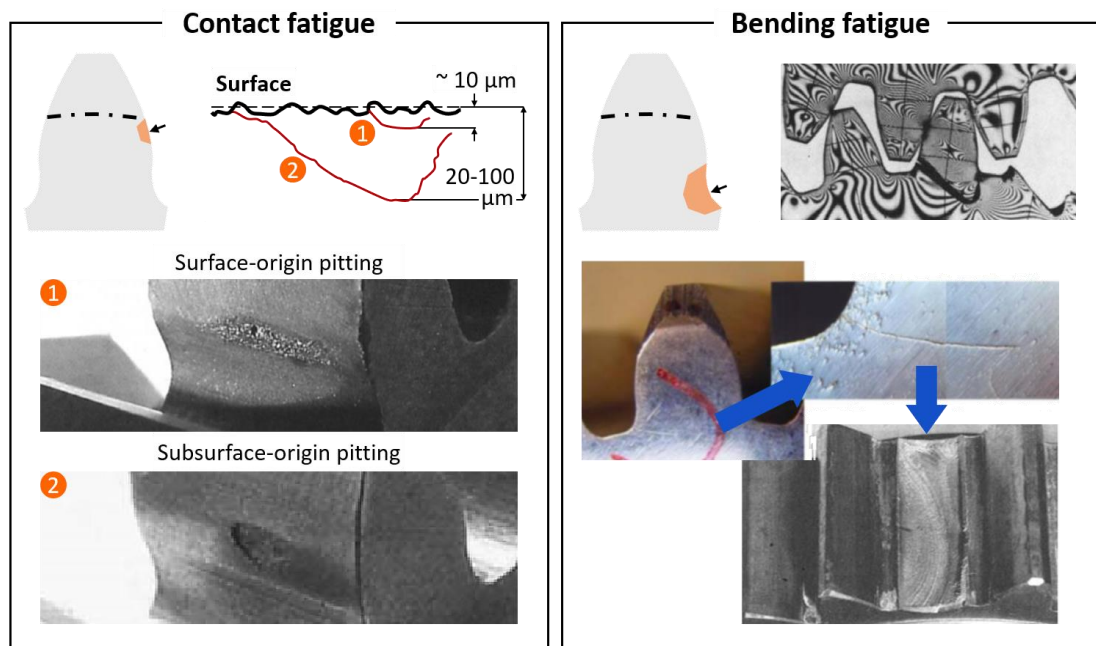


Figure 2.9. The characteristics of contact fatigue and bending failures (LECHNER; NAUNHEIMER, 1999; MCPHERSON; RAO, 2000; DING; RIEGER, 2003; DAVIS, 2005; BELSAK; FLASKER, 2006).

2.2.3 Gear design

The gear design method has experienced several improvement phases along the years, also following the geometry optimizations (LITVIN, 1997). The calculation considers the operating stresses, material, geometry, manufacturing, and various experimental correction factors (ISO, 2007). Some standards offer the proper procedure for gear design in addition to the values of the correction factors.

The calculation for gear sizing is complex and non-linear due to the experimental character of many factors (ISO, 2007). Therefore, it is difficult to define an equation for each parameter to be optimized and iteration operations are often necessary. The conventional

procedure starts with a collection of initial requirements and assumptions and, consequently, some parameters that cannot be altered. Then, the remaining flexible parameters are proposed. Thus, the correction factors can be defined, and the safety factors calculated. If the obtained safety factors are not suitable, the flexible parameters should be modified.

Regarding to calculation of contact fatigue failure, contact stress is the basic principle used for the calculation of contact stress. It is a significant indicator of the stresses at the gear flank generated during operation. However, there are some other influences for the contact fatigue occurrence, such as friction coefficient, direction, and magnitude of sliding and lubricant. Such considerations are not yet included in the loading calculation currently, but they are included in the correction factors (ISO, 2007).

For the calculation of bending fatigue failure, a simple beam submitted to a bending stress is considered and some of the correction factors consider the actual gear tooth geometry. Other aspects are added as correction factors, such as the loading direction, if it is unidirectional or if there is also reverse loading (ISO, 2007).

Some aspects of the dynamic behavior are also considered in the gear design, mainly by the application factor (K_A) and dynamic factor (K_V), according to ISO 6336-1 standard (ISO, 2007). The application factor considers the loading variation, in terms of both input and output torque, due to external influences. The dynamic factor, in contrast, considers loading increments due to internal dynamic effects.

The influence of manufacturing on gear sizing occurs primarily through four correction factors: transverse load factor for contact stress ($K_{H\alpha}$), face load factor for contact stress ($K_{H\beta}$), transverse load factor for bending stress ($K_{F\alpha}$) and face load factor for bending stress ($K_{F\beta}$). They consider an irregular load distribution over the face width ($K_{H\beta}$ and $K_{F\beta}$) and the involute profile ($K_{H\alpha}$ and $K_{F\alpha}$) due to meshing misalignment, which may be caused by manufacturing inaccuracies. The influence of roughness in the process of both contact and bending fatigue failure is also considered (ISO, 2007a; ISO, 2007b; ISO, 2007c). Figure 2.10 shows the conventional gear sizing procedure.

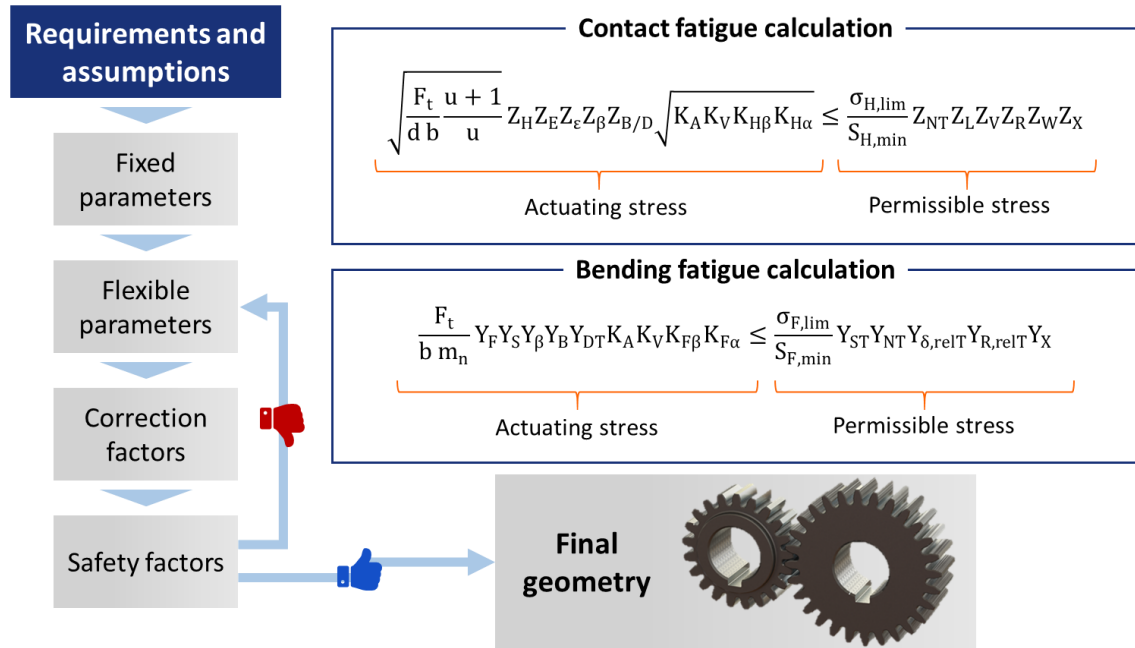


Figure 2.10. The gear sizing conventional procedure (ISO, 2007).

As one of the main parameters considered in gear design, the material's fatigue strength is critical. The definition of the material goes beyond fatigue strength however, and involves several aspects in addition to gear sizing, such as the gear manufacturing chain and application.

Manufacturing requirements include machinability, forgeability and heat treatment response. The operating requirements are related to the ability of the gear to perform under the loading conditions for which it was designed and therefore include all mechanical property requirements. The different regions of the gear tooth require different operating requirements. In the root region, good surface hardness is required to improve bending fatigue lifetime, while in the flank a combination of high hardness and good subsurface resistance is required to resist contact stresses and wear (DAVIS, 2005). There is also the necessity for the core to be tough so that it can resist the deflections imposed by meshing. Thus, the choice of the material is associated with required performance and manufacturing cost considerations.

Several alloys concepts, thermomechanical and thermochemical processes have been developed to achieve this combination of required properties, such as the heat treatment, in particular the carburizing (TOBIE; HIPPENSTIEL; MOHRBACHER, 2017). Some examples of commonly carburized gear steels are SAE 1018, 4320, 5120, 8620, and 9310 as well as other grades such as DIN 20MnCr5, DIN 16MnCr5, ZF-7B, 20MoCr4, and V2525 (DAVIS, 2005). Alloy concepts significantly vary in different regions due to historical definitions, practical experiences, and local preferences for certain alloying elements. Steels with similar content

may even be named differently by standards, such as SAE 5120 and DIN 20MnCr5 or DIN 18CrNiMo7-6 and SAE 4340 (TOBIE; HIPPENSTIEL; MOHRBACHER, 2017). A list of the conventional gear steels is presented in appendix “B.1 Conventional gear steels”.

Another property not yet fully considered in the gear design, despite the proved influence on the fatigue lifetime is the residual stress state induced by manufacturing processes. The shot peening process, for example, induces compressive residual stresses, which decrease the actuating stresses during operation and may result in an increase of up to 80% in fatigue lifetime, but ISO 6336-5 recommends to be more conservative and considers an improvement of 5 or 10% (ISO, 2007; LAMBERT; AYLOTT; SHAW, 2018).

2.3 Microalloyed steels

Microalloyed steels (MA steels), also called high-strength low alloy (HSLA) steels, are an important category of materials, estimated to represent approximately 12% of the total world steel production (BAKER, 2016). They were initially developed at the 1960s by oil and gas extraction sector, as a result of researches into new steels with higher strength, in addition to improved toughness and good weldability, in comparison with low carbon steels, to produce large diameter pipelines (GLADMAN, 1997). However, their applications were soon expanded to construction and transportation sectors, with uses in heavy-duty highways, construction and farm machinery, storage tanks, automobile components, bridges, offshore structures, and transmission towers (DAVIS, 2001).

The term “microalloyed steels” was originally used for alloys containing small additions of niobium and vanadium. Small amounts of aluminum were already used to obtain an improved combination of mechanical strength and toughness, but such alloys were not considered microalloyed steels. The same occurs for alloys with small boron contents, added for hardenability enhancement. However, any alloy containing elements in small amounts intentionally added to modify the alloy properties can be considered as microalloyed steels (GLADMAN, 1997). They can be divided into six categories (which are not necessarily distinct groups), based on their microstructures and alloying elements (DAVIS, 2001):

- *Weathering steels*: Contain small amounts of alloying elements, such as copper and phosphorous for improved atmospheric corrosion resistance and solid solution hardening.

- *Microalloyed ferrite-perlite steels*: Contain small (less than 0.1 wt%) additions of carbide or carbonitride-forming elements, such as niobium, vanadium and/or titanium for precipitation hardening, grain refinement, and possibly transformation temperature control.
- *As rolled perlitic steels*: May include carbon-manganese steels but may also have small additions of other alloying elements to improve mechanical strength, toughness, formability, and weldability.
- *Acicular ferrite (low carbon bainite) steels*: low carbon (less than 0.05% C) steels with a good combination of high mechanical strength, weldability, formability, and good toughness.
- *Dual phase MA steels*: Present a microstructure of martensite dispersed in a ferritic matrix and provide a good combination of ductility and high tensile strength.
- *Inclusion-shaped-controlled steels*: Provide improved ductility and through-thickness toughness by the small additions of elements such as calcium, zirconium, titanium, or rare elements, so that the shape of sulfide inclusions is changed from elongated stringers to small, dispersed, almost spherical globules.

Despite the variety of microalloying elements, microalloyed steels are generally employed to steels that have elements added in small amounts to promote grain refinement and precipitation hardening by stable carbides, nitrides and carbonitrides (GLADMAN, 1997). Thus, a conventional microalloyed steel has low carbon content, typically 0.05-0.25 wt% C, to provide adequate formability and weldability, up to 2.0 wt% manganese and small additions of vanadium, niobium, and titanium (all usually max. 0.1 wt%) in various combinations (DAVIS, 2001). Some other elements, such as chromium, nickel, aluminum, molybdenum, copper, nitrogen, boron, and zirconium, might also be present. Small additions of sulfur and tellurium may be added to improve steel's machinability (BAKER, 2016).

The two main effects of microalloying elements are due to their precipitates. These particles hinder the grain coarsening by the pinning effect and the dispersion of fine particles provides an improvement in the alloy mechanical strength by the precipitation hardening mechanism (GLADMAN, 1997). Therefore, the benefits of microalloyed steels are usually connected to thermal and thermomechanical loading processes.

In the thermomechanical processes, in addition to the high temperature inducing a grain coarsening, as the working material is hot deformed, a large number of defects are generated in

the microstructure. These defects increase the thermodynamic potential for austenite recrystallization. As soon as a critical deformation is reached (ϵ_c), nucleation of new grains free of deformation occurs, along preferential sites, such as grain boundaries (SELLARS; WHITEMAN, 1979; PADILHA; SICILIANO JR, 2005). This phenomenon generates a severe softening in the alloy mechanical properties.

Several studies demonstrate that the addition of microalloying elements also retards the austenite recrystallization and niobium was the one that showed the best result, followed by titanium and vanadium (DEARDO, 2003; VERVYNCKT *et al.*, 2011; LAN *et al.*, 2011). Thus, microalloyed steels also show an increase in non-recrystallization temperature (T_{nc}), allowing the reduction of process time without compromising mechanical properties.

The precipitation of carbides, nitrides and carbonitrides, the main particles that influence mechanical and metallurgical properties in microalloyed steels, may occur at three different stages of the manufacturing chain (LIU; JONAS, 1989; BAKER, 2019). They are presented in Figure 2.11 and described below.

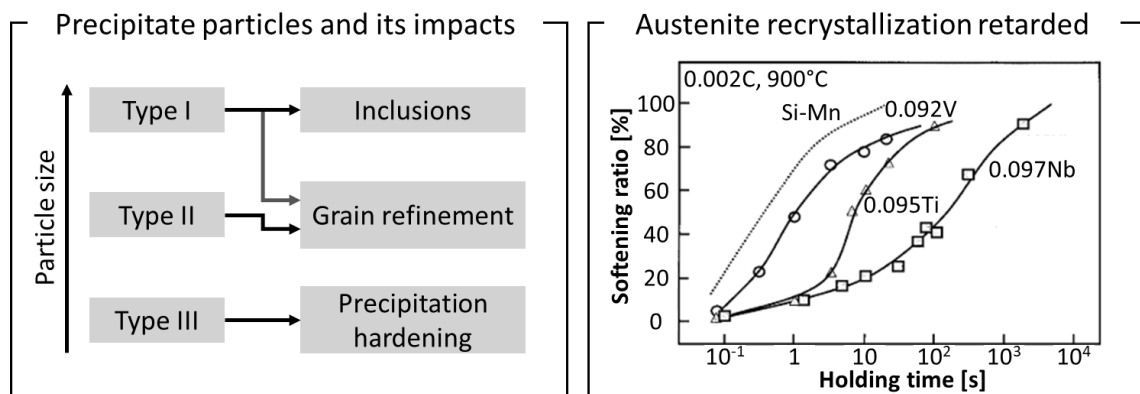


Figure 2.11. The main effects of the precipitate particles due to microalloying elements (LIU; JONAS, 1989; DEARDO, 2003; BAKER, 2019).

Type I precipitate particles, often described as inclusions, are formed in the liquid phase and during or after solidification for the duration of casting, on the liquid/solid interface or in delta ferrite. They are very stable and generally too large to influence austenite recrystallization, but the smallest ones may retard coarsening of austenite grains during reheating (LIU; JONAS, 1989; BAKER, 2019).

Type II precipitate particles are formed in austenite after solution treatment and during hot deformation, as the temperature decreases. The precipitates are strain induced, which means

that they are nucleated on dislocations, and can retard the austenite recrystallization. Grain refinement of microalloyed steels is mainly due to this type of particles (LIU; JONAS, 1989; BAKER, 2019).

Type III precipitate particles are formed during or after austenite to ferrite phase transformation, nucleating on the austenite/ferrite interface and in ferrite. A fine precipitate dispersion, which may include interface precipitation, is usually observed, and results in a precipitation hardening (LIU; JONAS, 1989; BAKER, 2019).

Poorhaydari, Patchett and Ivey (2006) showed that grain refinement is responsible for the highest contribution to the enhanced mechanical strength of microalloyed steels, representing about 70%. This results in improved toughness and high mechanical strength, properties that are commonly antagonist. Such simultaneous effect is not observed if the increase in mechanical strength is obtained without grain refinement. Thus, this is the only metallurgical method to increase both mechanical strength and toughness at the same time, being an attractive technique (TAKAHASHI; IINO, 1996).

Due to the superior mechanical properties of microalloyed steels when compared to conventional low carbon steels, they provide a more efficient design, with improved performance, even under difficult environmental conditions (BAKER, 2016). Furthermore, their application allows reductions in component weight and manufacturing costs, because of their favorable strength-to-weight ratio in comparison with conventional low carbon steels (DAVIS, 2001).

Both the refined grain structure and its homogeneity in the microalloyed steels also influence the residual stress state and the distortions level resultant from manufacturing processes. In carburizing, the martensitic transformation temperature is influenced by the austenitic grain size (YANG; BADHESHIA, 2009). When there is a heterogeneity in grain size, the transformation can start locally in the coarser grains. The volumetric changes of the following transformations cannot be accommodated by the already martensitic regions, leading to an increase in both distortion level and residual stresses (TRUTE; BLECK; KLINKENBERG, 2007; TOBIE; HIPPENSTIEL; MOHRBACHER, 2017). In addition, a coarse grain structure is associated with tensile surface residual stresses during grinding, which is not desirable (GOTOH *et al.* 2010).

The grain size is also fundamental to the fatigue lifetime of a material, following the Hall Petch relation (BHADESHIA; HONEYCOMBE, 2017). As shown in Figure 2.12, the most sensitive metallurgical characteristic to the fatigue lifetime of a material is the case grain

size. The core grain size appears in third after the surface residual stress (WISE; MATLOCK, 2000). Consequently, microalloyed steels become very promising in gear applications.

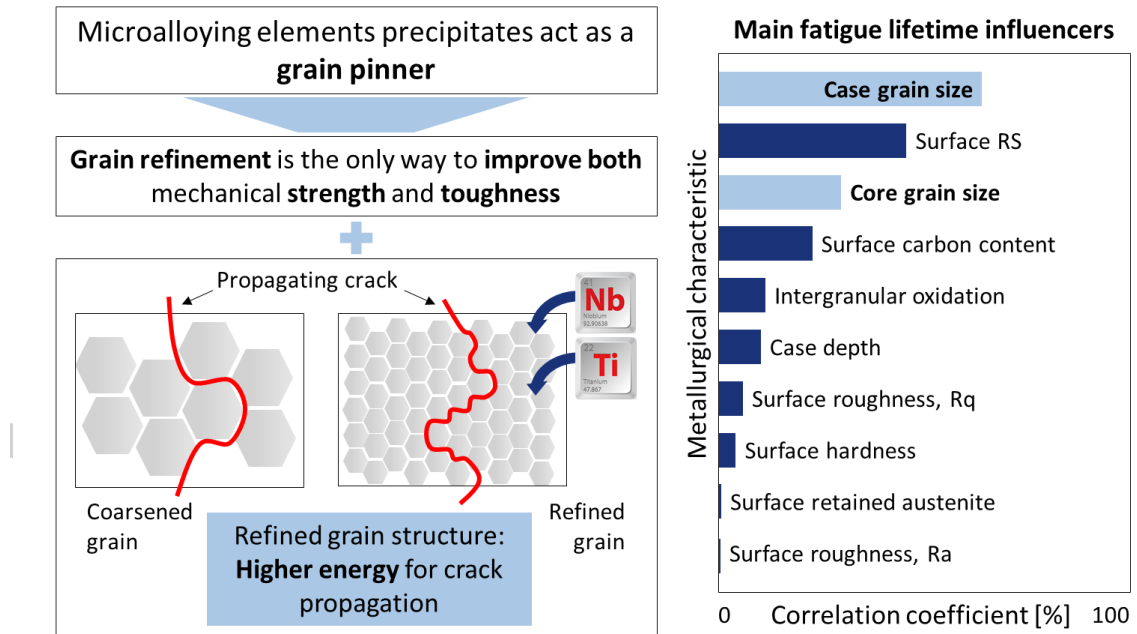


Figure 2.12. The main benefits of microalloying elements (WISE; MATLOCK, 2000).

2.3.1 The effects of niobium (Nb) as microalloying element

The commercial production of niobium from its world's largest reserve located in Brazil has started in 1965 by *Companhia Brasileira de Metalurgia e Mineração* (CBMM) and resulted in a dramatic reduction of niobium's price. After that year, niobium was for the first time available in abundance as microalloying element. Before that, only vanadium and titanium were available on a commercial scale (DEARDO, 2003). Nowadays, Brazil's production of niobium is estimated to represent 93% of the total world production of niobium (PEREIRA JR, 2014). Thus, its utilization as microalloying element is an important economic advantage.

The importance of niobium as microalloying element in steels has encouraged numerous studies over the last years. This interest is based on niobium's strong tendency to form carbonitrides in steels, but relatively little tendency to form sulfides, oxides, or solid solutions of this compounds (DEARDO, 2003). Such carbonitrides are formed in the austenitic field and generally result in a fine dispersion, which leads to mechanical strength enhancement by precipitation hardening, which also depends on the size and amount of precipitate niobium-based compounds (OLEA, 2002; DAVIS, 2001). Although vanadium behaves similarly to

niobium in terms of tendency to form carbonitrides and may also be used as a microalloying element, niobium is more effective as grain refiner (DAVIS, 2001).

Niobium improves the mechanical properties of the microalloyed steels by two manners. The first is by precipitation hardening itself. However, its main contribution in the mechanical properties is the precipitation above the transformation temperature and the retarding in austenite recrystallization, promoting a refined grain structure. The grain refinement produces an increase in mechanical strength and toughness. Concentrations usually range from 0.02 to 0.1 wt% (OLEA, 2002).

2.3.2 The effects of titanium (Ti) as microalloying element

The benefits of Ti addition in steels have long been noticed, at various applications. As long ago as 1914, titanium additions of 0.02 wt% were known to reduce the segregation of carbon, sulfur and phosphorous in rail steels, according to Comstock (1915). By 1921, titanium was being used as an alloying element in steels (MORRISON, 2000). Pickering (1997) noted that among the elements normally considered as microalloying, that is Nb, Ti, V, Zr and possibly Al, titanium presents a particular versatile due to its strong affinity for C, N, S and O, while the other microalloying elements just show affinity with some of these.

Titanium carbide (TiC) and titanium nitride (TiN) are the most found titanium precipitates in microalloyed steels (BAKER, 2019). The important role played by these precipitates in microalloyed steels is related to its high thermal and chemical stability, then titanium carbonitride particles are precipitated at very small Ti addition and remain stable at the temperatures typically adopted for rolling and heat treatment processes (JÖNSSON, 1998). These precipitates act by retarding the austenite recrystallization and grain growth during such processes that involve high thermal loadings, thus benefiting the mechanical properties of the material.

Similar to niobium, the titanium employment as microalloying element may induce precipitation hardening and grain refinement, depending on the percentage used. In compositions higher than 0.05 wt%, Ti carbides provide a precipitation hardening effect. However, Ti is used commercially to hinder austenitic grain growth, increasing not only mechanical strength, but also toughness. Normally, titanium is present in concentrations from 0.01 to 0.02 wt% (OLEA, 2002). Some other precipitates may be added in microalloyed steels to obtain other properties improvements. Boron additions to Ti-microalloyed steels forming

TiB₂ (titanium diboride) have beneficial effects on the weld metal toughness (ZHOUNGYAO *et al.*, 1992).

2.4 State of the art of microalloyed steels in gear applications

Tobie, Hippenstiel and Mohrbacher (2017) conducted the only study found that investigates the use of microalloyed steels in gears with fatigue tests on gear-dedicated test rigs. They compared two Nb-microalloyed steels, a DIN 20MnCr5+Nb with additional molybdenum and nickel content, and a DIN 20CrMo5+Nb in both bending and contact fatigue. Among other additional assessments to the fatigue tests, they also investigated grain size controlling in a DIN 18CrNiMo7-6 steel and the same steel with Nb-Ti addition.

The results obtained from fatigue tests for the microalloyed steels proved that they can achieve a higher fatigue strength than other conventional gear steels, as shown in Figure 2.13. However, the study did not include fatigue tests of conventional gear steels in the same conditions as reference, but rather used data from the literature. The investigations of the effect of the microalloying elements on grain size control also showed positive results for the microalloyed steels, as it resulted in a more refined and homogeneous grain structure.

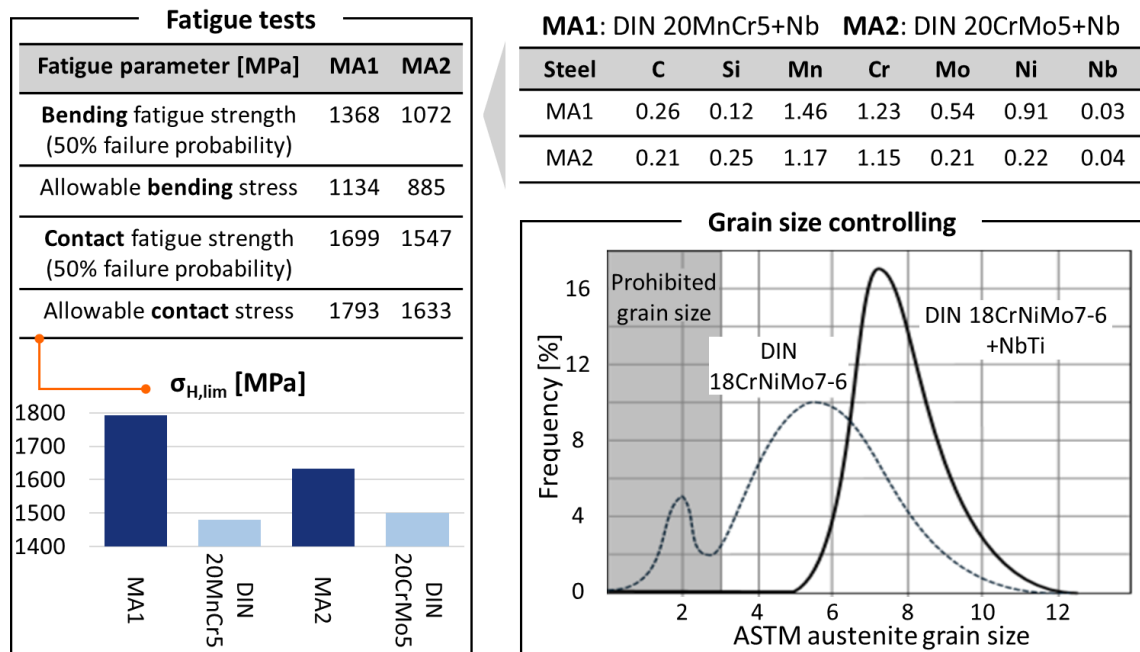


Figure 2.13. The results of microalloyed steels in fatigue tests and grain size controlling (TOBIE; HIPPENSTIEL; MOHRBACHER, 2017).

Alogab *et al.* (2007) studied the influence of niobium content, 0.00, 0.02, 0.06 and 0.10 wt%, in a SAE 8620 steel with Ti addition during the pseudocarburing process. The solubility of Nb and Ti precipitates was studied as well as the size of both grains and precipitates for different pseudocarburing temperatures. The results showed a grain refinement with an increase in Nb content. The higher Nb content also allowed the process temperature to be raised without abnormal grain growth. This is of great industrial interest since it reduces the process time and consequently increases productivity.

Thompson, Matlock, and Speer (2007) also studied SAE 8620 steel with Ti addition, varying the Nb content, being 0.02, 0.06 and 0.10 wt%. In addition to the investigation of the grain size during pseudocarburing, the heating rate and the bending fatigue strength were also evaluated. The higher Nb content resulted in a more refined grain structure. A higher heating rate also favored the grain refinement. An increase in fatigue strength followed the increase in Nb content and its consequent refined grain structure.

In contrast, Ma *et al.* (2008) indicated an optimal Nb content value. A steel with no Ti content was compared with 0.00, 0.04 and 0.08 wt% Nb addition, and the one that showed the best results in terms of grain refinement was the one containing 0.04 wt% Nb. The one with no Nb content resulted in the largest grain size. In this study, rotating bending fatigue tests were also performed: the results followed the expected from the grain size, the addition of Nb increased by 18% (0.04 wt% Nb) and 13% (0.08 wt% Nb) the fatigue strength after carburizing. The Figure 2.14 summarizes the studies in conventional gear steel with microalloying element addition.

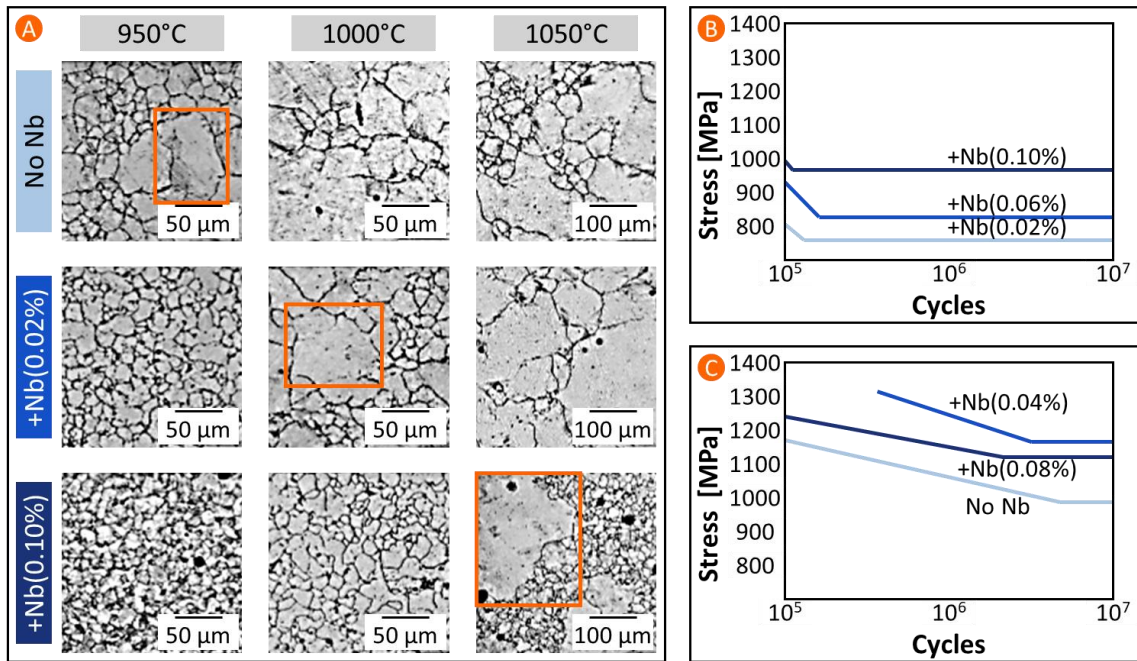


Figure 2.14. The studies in conventional gear steel with microalloying element addition regarding to abnormal grain growth and fatigue lifetime (ALOGAB *et al.*, 2007; THOMPSON; MATLOCK; SPEER, 2007; MA *et al.*, 2008)

Although the microalloying element addition provides a refined grain structure, it should be well controlled to ensure a fine precipitate dispersion. Large precipitates have the opposite effect, favoring the nucleation of fatigue cracks. This is studied, in particular, by Medina *et al.* (1999), which highlights the importance not only of Ti content but also of Ti/N ratio (Figure 2.15). Their results concluded that the best ratio for the grain refinement is approximately 2. In this ratio, the smallest precipitate sizes were also observed.

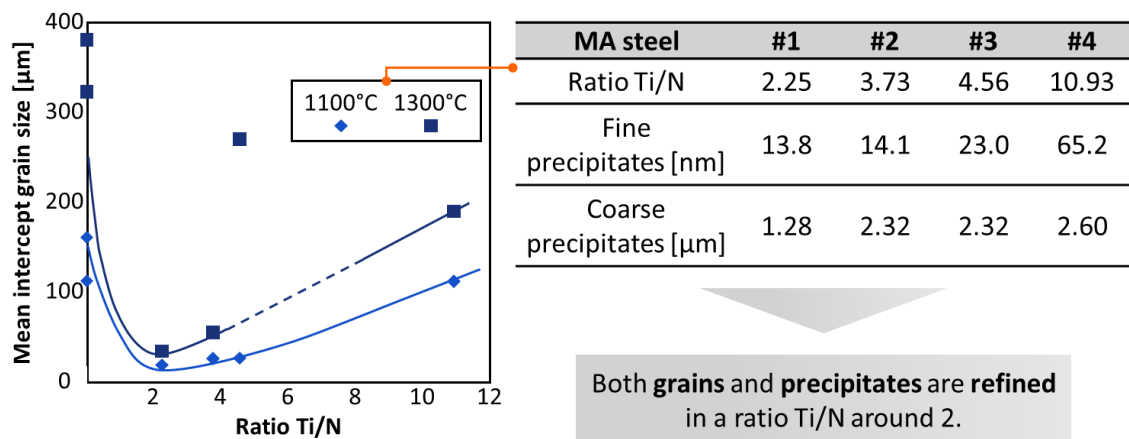


Figure 2.15. The ratio Ti/N effects in microalloyed steels (MEDINA *et al.*, 1999).

Knowledge on gear manufacturing chain with applications of the microalloyed steels has been intensified lately, due to its benefits. Among them, microalloyed steels present a refined grain structure, which turns into both fatigue strength and toughness improvement. However, studies and researches in this direction are still at the beginning. A keywords research was conducted on *Scopus*, in order not only to collect studies with similar content, but also to observe how related studies are arranged in terms of correlated keywords. Five groups of keywords were chosen:

1. “gear” or “gears”
2. “microalloy*” or “micro-alloy*” or “HSLA”
3. “Nb” or “niobium”
4. “Ti” or “titanium”
5. “surface integrity” or “grain size” or “refined grain”

As presented in Figure 2.16, the studies on microalloyed steels have a strong correlation with Nb, Ti and surface integrity. It has also shown that there is still a lack of microalloyed steels studies focused on gears. The studies that mention all keyword groups represent only a small fraction (11 studies), highlighting the scientific motivation for a subject that explores all these concepts. The low comprehension concerning the behavior of microalloyed steels along the gear manufacturing chain does not reflect the benefits that these new alloys may offer, as demonstrated in this section. The contribution of this study aims to bridge this gap. It is expected to understand how the addition of microalloying elements influences the surface integrity evolution along the gear manufacturing chain. Furthermore, the findings can give information on the dynamic behavior considering the new alloys and potential process improvements which may lead to optimized outcomes.

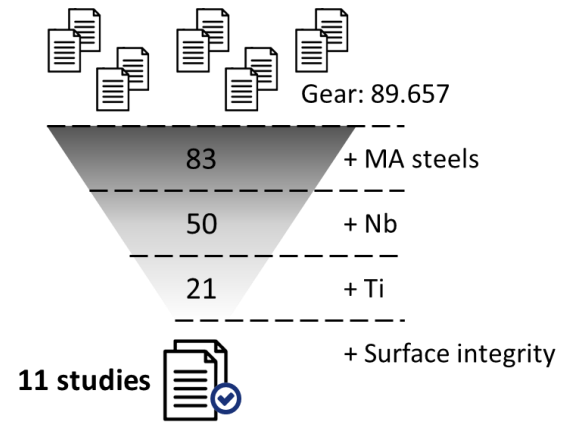
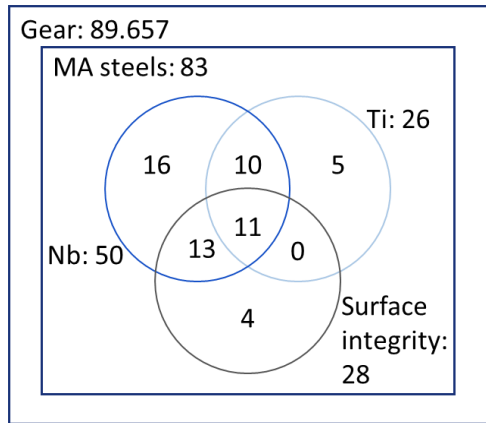


Figure 2.16. Results of the keywords research.

3 Objective and approach

The objective of this study is the characterization of the surface integrity evolution of NbTi-microalloyed steels along a conventional gear manufacturing chain. The concept of integrity in this study covers microstructural characteristics, topography and distortion aspects, and residual stress state. The investigation occurs initially on the microstructure level: grain size is analyzed together with its heterogeneity and it is complemented by a hardness mapping. Topography and distortion level are also assessed, and residual stress measurements close the experimental procedure. These assessments are compared as possible to completely understand the observed features. Figure 3.1 summarizes hypothesis, objective, and approach of this study.

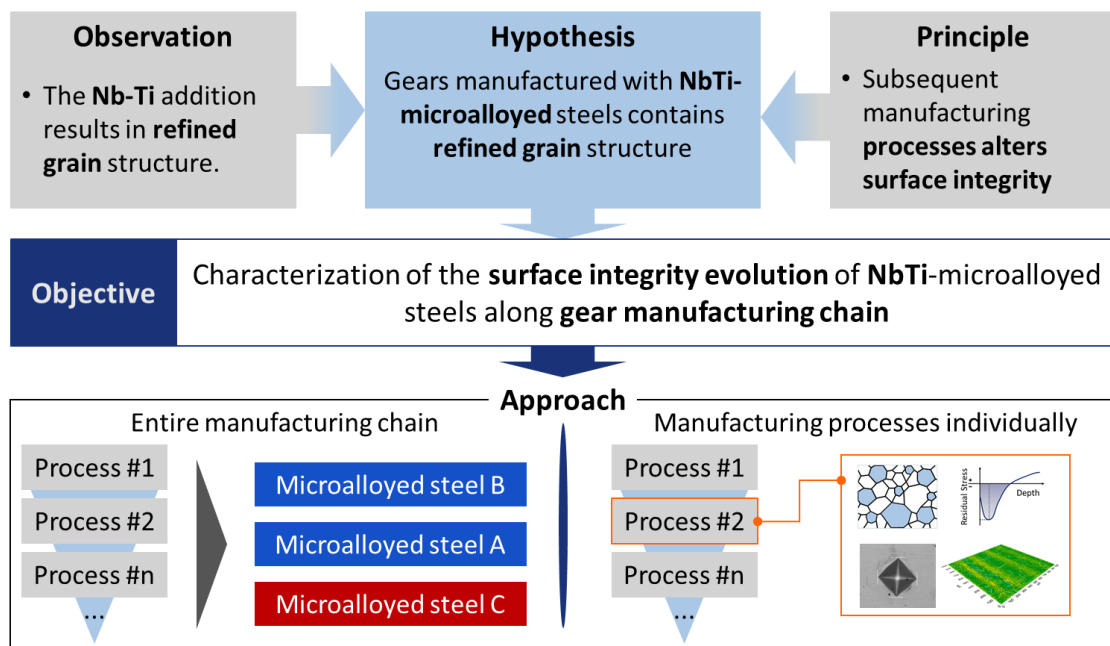


Figure 3.1. The basis for the hypothesis, the objective of the study and how to approach it.

In this scenario, two questions are established to conduct the research and organize the results:

- **1st research question:** How does NbTi-addition influence the final surface integrity state in a gear manufacturing chain?
- **2nd research question:** How sensitive is each gear manufacturing process to microalloyed steels?

The final surface integrity state of each NbTi-microalloyed steels after the entire manufacturing chain may differ from the initial conditions. Each process within the gear manufacturing chain imposes thermal and/or mechanical loading, which disturbs the equilibrium state of the material and may provide different outcomes (REGO, 2016). Therefore, the first evaluation, aimed to answer the 1st research question, considers the behavior of NbTi-microalloyed steels at the end of the gear manufacturing chain.

Each manufacturing process has its parameters well known when it is considered conventional gear steels. Since NbTi-microalloyed steels present particular properties, it is expected that some of the manufacturing processes tend to present different results. However, with the same parameters, NbTi-microalloyed steels may present different results in one or more processes along the manufacturing chain. As an example, NbTi-microalloyed steels are expected to present a more refined and homogeneous grain structure during heat treatment, leading to a lower distortion level, according to Epp and Hirsch (2012). Related to the 2nd research question, the second evaluation considers each manufacturing process individually.

It is expected that the novel results of this study allow to comprehend the microalloyed steels benefits in the particularities of the gear manufacturing chain. As an organic consequence, it will be possible to draw to which extent these alloys can be used in gear and transmission systems applications.

4 Materials and methods

4.1 Overall experimental scope

Within the possibilities offered by the microalloyed steels and the inherent complexity of the gear manufacturing chain, several analyses could be carried out from different perspectives. The herein presented study considers a conventional gear steel as reference, a DIN 16MnCr5 (equivalent to SAE 5115), and two different combinations of microalloying addition in this same steel. The first one contains only Nb as microalloying element in its composition, and the second one contains not only Nb but also Ti. Respectively, they are called from now on as REF, +Nb and +NbTi.

These three alloys are submitted to the same gear manufacturing chain. All processes and their respective parameters have been carefully defined and fixed to ensure that any changes observed are caused by the different properties of the materials. In addition, specimens of the three alloys, properly identified, were processed simultaneously, assuring that there were no changes due to different batches.

Before the teeth cutting, the alloys were hot rolled, hot forged and annealed, composing the billet processing. Then, the teeth cutting were performed by the hobbing process, followed by carburizing, and grinding processes. This gear manufacturing chain was selected to evaluate the behavior of microalloyed steels during conventional manufacturing processes. Figure 4.1 shows the chemical composition of the specimens and the gear manufacturing chain studied.

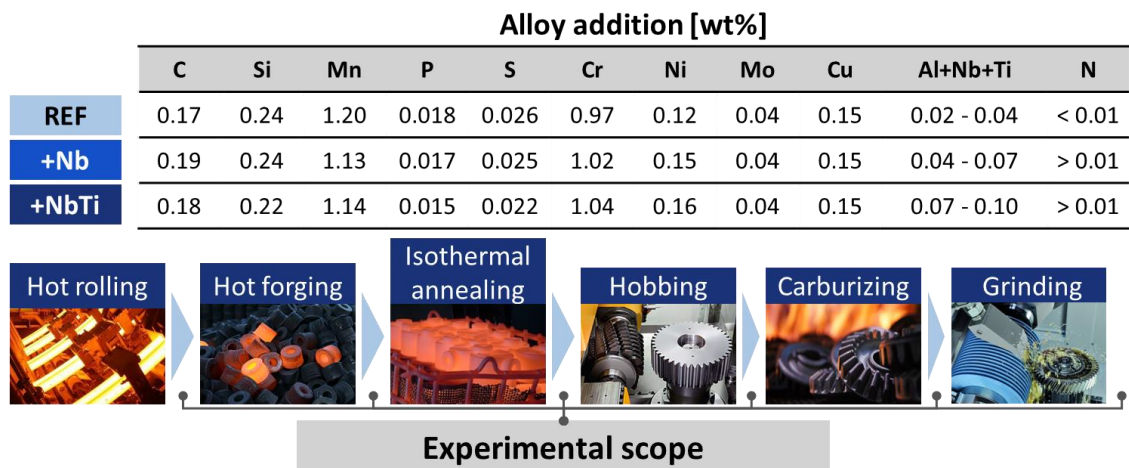


Figure 4.1. Chemical composition of specimens and gear manufacturing chain investigated.

All manufacturing processes were performed by industrial partners and monitored *in loco*. This allowed some occasional considerations to be collected and incorporated into the analyses, if necessary. The specimens' test was all conducted at CCM-ITA and LabMat-ITA. As a gear design, *ITA Geometry* was conceived, which has similar dimensions to those used in the automotive sector.

The definition of the parameters of each test was oriented to the features to be observed, also considering the assurance of correlation along the manufacturing processes. The choice of manufacturing processes and conventional parameters, in addition to the application of the same batches for all specimens, allows the number of test repetitions to be reduced. Additional tests, carried out by the industrial partners, ensure the uniformity of the results of the manufacturing processes, however they are not part of the scope herein presented.

The alloys microstructure may be affected by each of the manufacturing processes. Thus, it is examined with micrographies, by means of optical microscopy, with emphasis on the grain size. It may also complement the explanations of the differences observed in the other tests.

Since manufacturing processes impose high thermal and mechanical loadings, the alloys may be exposed to varied residual stress states along the chain. As demonstrated by Rego (2016), the residual stress state induced by each step of the manufacturing chain cannot be neglected for the fatigue lifetime. Thus, the study of evolution of the residual stress state of each of alloy is fundamental.

Part of the residual stresses are relieved in the form of both surface roughness and distortions, which are detrimental to the fatigue lifetime. Therefore, it is necessary to obtain topography and distortion measurements along the teeth for the different alloys. From that, it will also be possible to observe the dimensional stability of each alloy among the manufacturing processes.

In addition, hardness maps are provided to observe to which extent the hardness of the teeth is altered by the addition of microalloying elements. This is a critical property for gear applications, which can result in improved or reduced fatigue lifetime.

The experimental scope of this study is summarized in Figure 4.2. The investigation of the study herein presented covers the gear manufacturing chain. However, based on correlations already established in the literature, it is also possible to estimate some aspects of the dynamic behavior of the new alloys, considering its final surface integrity.

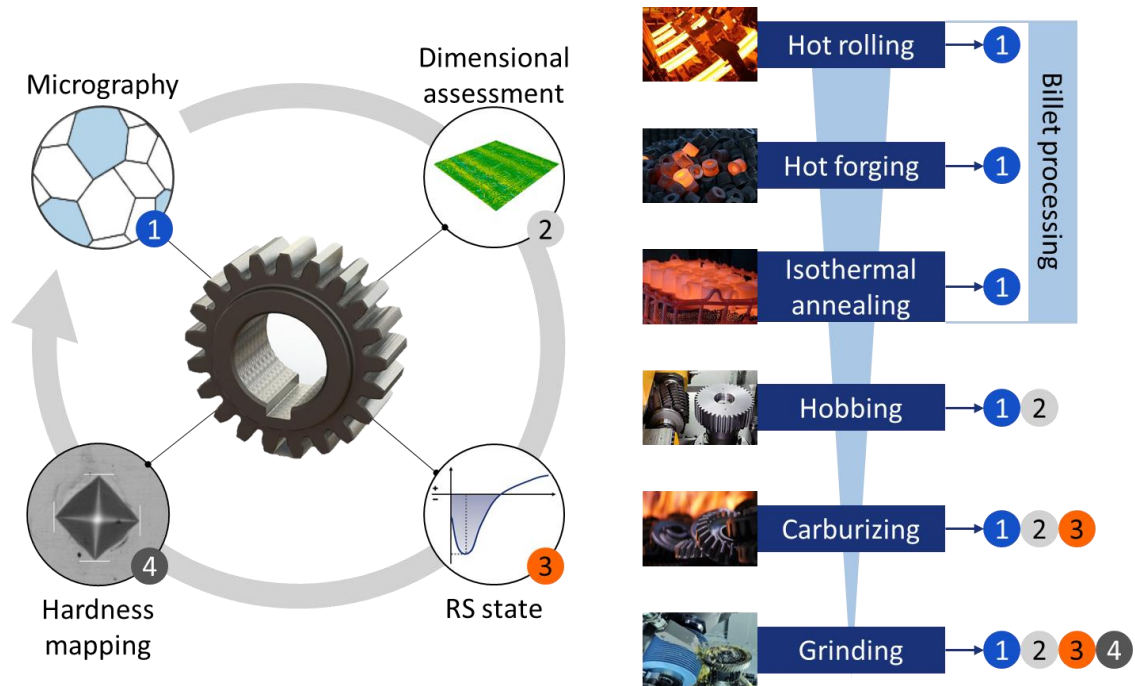


Figure 4.2. The experimental scope of the study.

4.2 Specimens' design

The automotive sector itself has a wide variation in terms of operating conditions. In this study, it is considered the segment of passenger vehicles, in which gears are characterized by normal module (m_n) from 1.5 to 3.0 mm. Among the gears that constitute automotive transmission systems, the ones that are submitted to the greatest number of cycles are the fifth gear, which present a gear ratio (u) around 1.25 (4:1). Therefore, it was developed the *ITA Geometry* for this study, aiming that its design represents the main characteristics of automotive gears. The *ITA Geometry* conception was conducted in accordance with the parameters of macrogeometry and microgeometry of automotive gears, to simulate the loadings in tests and be able to expand the results for automotive gears.

In its development, a mapping of the loading conditions of the vehicles in the Brazilian scenario was carried out. Both maximum power (P_{max}) and maximum torque (T_{max}) were collected for the 5 best-selling vehicles of each of the 6 main OEM companies in 2018, which represent almost 70% percent of all vehicles sold in the same year (FENABRAVE, 2019). The results of this investigation showed that the most frequent range of maximum power is between 100 and 120 hp, while maximum torque is between 150 and 175 N.m, as shown in Figure 4.3. The power considered for *ITA Geometry* was 110 hp and, considering that the future scenario

indicates increased loading conditions, an applied torque of 240 N.m in pinion was defined (FAID, 2015).

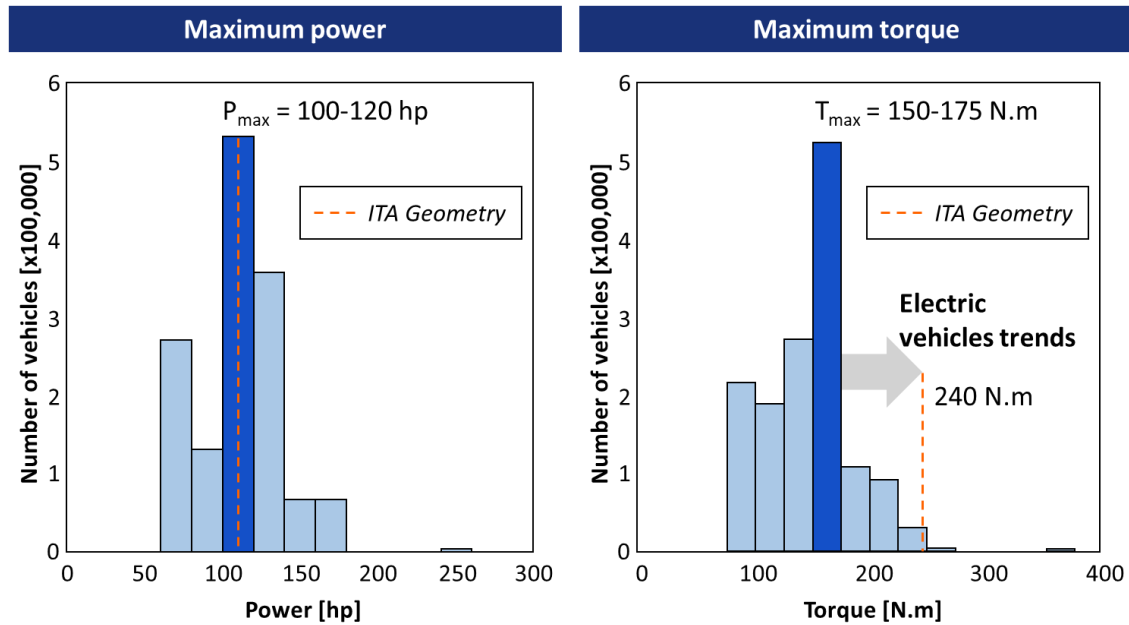


Figure 4.3. Maximum power and torque of vehicles sold in 2018 in Brazil (FENABRAVE, 2019).

The development of *ITA Geometry* also considered the structure that the CCM-ITA provides for dynamic behavior testing of transmission system components, in particular gear contact fatigue. This structure has a back-to-back test rig, capable of testing two center distances simultaneously, instrumented with sensors and actuators of torque, rotation speed, and lubricant temperature, all installed to operate independently. Among the possible center distances (a), the one that represents the automotive sector most expressively is 71 mm. Although automotive gears are, in general, helical gears, *ITA Geometry* has no helix angle (β). Thus, its application in a pulsator test rig, to be developed in CCM-ITA, is facilitated. In such test rig, teeth are tested individually with a fixed loading point, allowing the study of bending fatigue (DAVIS, 2005). A number of cycles of $5 \cdot 10^6$ to fatigue failure was defined for the calculation, considering safety factor for contact and bending fatigue failure (S_H and S_F) 1.0 and 1.4, respectively, in accordance with the standards ISO 6336-2 and ISO 6336-3 (ISO, 2007a; ISO, 2007b). Figure 4.4 shows both test rigs and the curve of contact/bending fatigue.

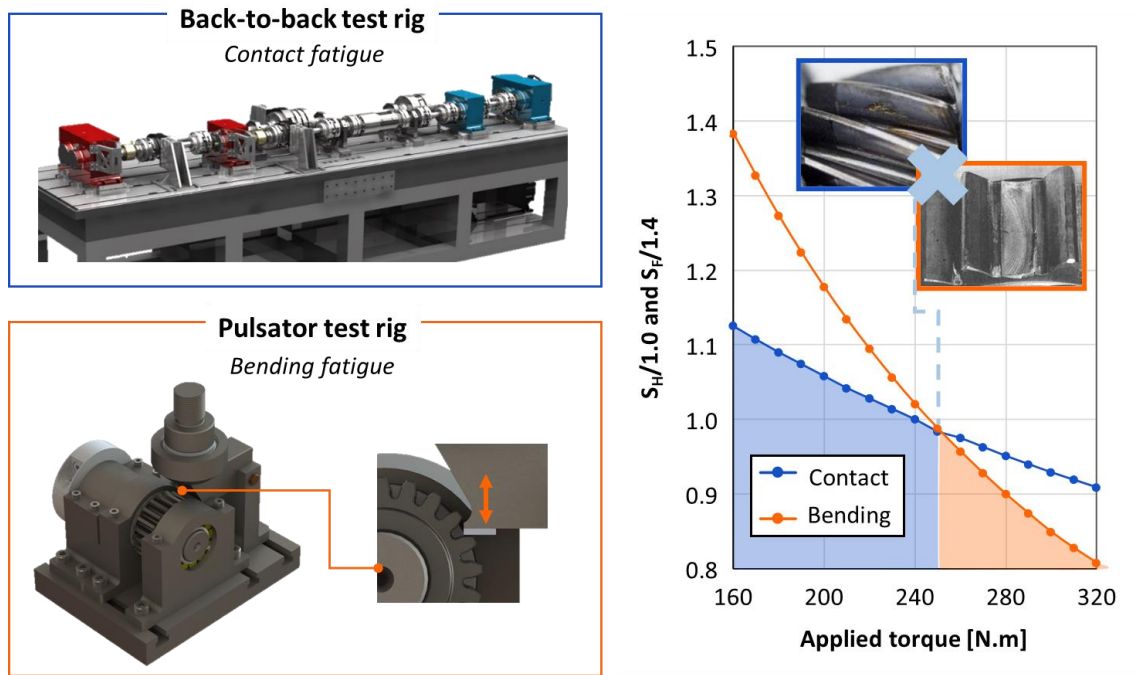


Figure 4.4. The gear-dedicated test rigs and curve of contact/bending fatigue.

Therefore, the range of normal module and gear ratio, as well as loading conditions, center distance and helix angle were defined. In a second plan, the *ITA Geometry* also has to be designed considering its manufacturing, to use conventional tools. Hence, the normal module and pressure angle were carefully selected considering the tools available from industrial partners. A normal module of 2.85 mm and a normal pressure angle (α_n) of 17.5° was defined. As a result of the calculation, a pair of 21 and 28 teeth was obtained, which is equivalent to a gear ratio of 1.33 and a pinion of pitch diameter (d_p) of 59.85 mm and face width (b) of 22 mm. For microgeometry, a lead crowning (C_β) of 8 μm was established.

The development of *ITA Geometry* allows a correlation of the results herein obtained for automotive gears both of vehicles with internal combustion engines (ICE) and also accompanies the trends of electric vehicles (FAID, 2015). It also allows the manufacturing using conventional tools and potential fatigue tests. *ITA Geometry* main parameters are presented in Figure 4.5.

The ITA Geometry

Parameters	Values
Nominal power (P_N)	110 hp
Nominal torque (T_N)	240 N.m
Normal module (m_n)	2.85 mm
Number of teeth (z)	21
Pitch diameter (d_p)	59.85 mm
Normal pressure angle (α_n)	17.5°
Helix angle (β)	0°
Face width (b)	22 mm
Lead crowning (C_β)	8 μ m
Gear ratio (u)	1.33
Center distance (a)	71 mm

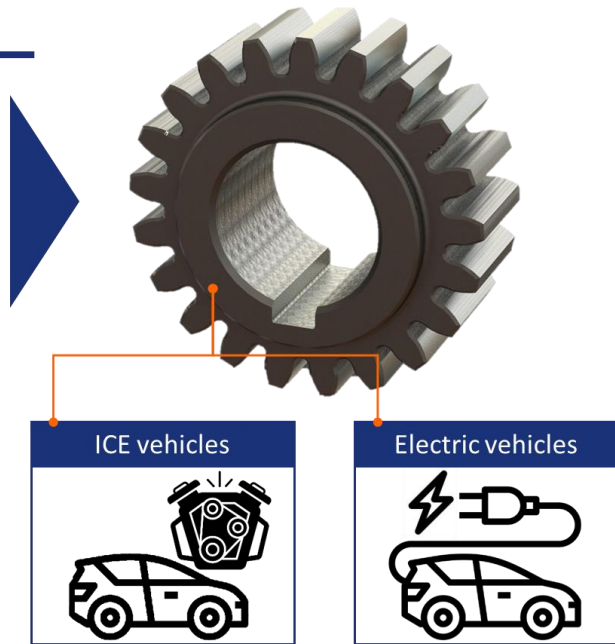


Figure 4.5. ITA Geometry main parameters.

4.3 Specimens' manufacturing

4.3.1 Hot forging

The investigations of this study start in the rolled condition, just before the forging process. Sections collected from the hot rolled bars of each alloy were donated by *Gerdau S.A.*. These sections, with 90 mm length and 41.28 mm diameter, were heated to 1220 °C and then hot forged to billets of 30 mm length, which means a reduction of 3:1. The initial length of rolled bar sections were defined considering the minimum reduction of 3:1 and final effective diameter of 66 mm. After the forging process, the specimens were box cooled to room temperature. The process was conducted in the facilities of *Max Gear Ltda.* and is summarized in Figure 4.6.

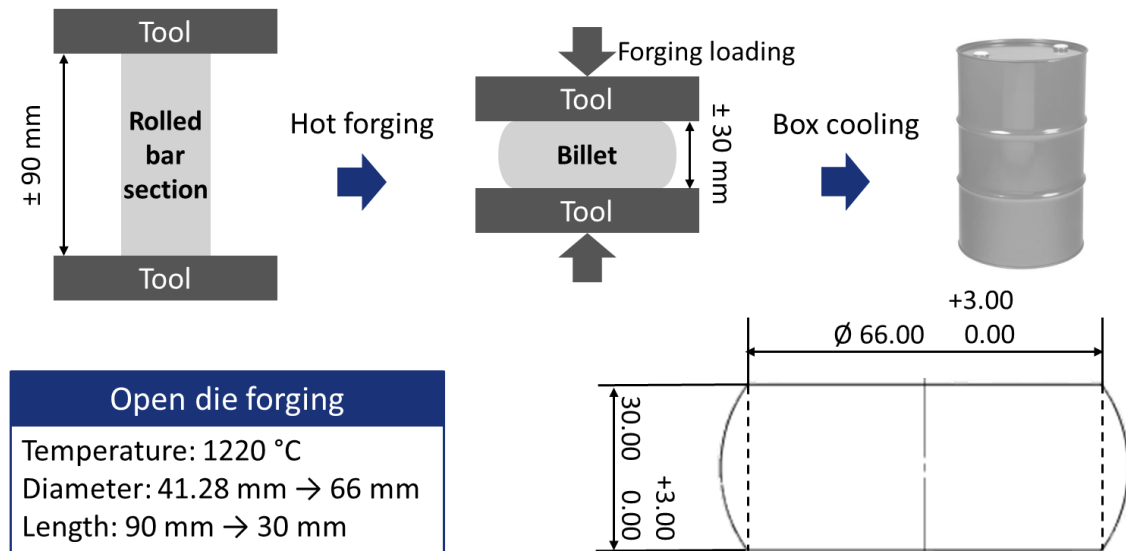


Figure 4.6. The hot forging process.

4.3.2 Isothermal annealing

One of the intermediate process in the gear manufacturing chain is annealing. It aims not only to homogenize the working material, but also to increase ductility and consequent reduce hardness to facilitate soft machining stage. One of the most widely used methods in the gear industry is isothermal annealing: after soaking at an austenitizing temperature, an intermediate temperature is used for low cooling rate followed by air cooling, reducing the total process time. It was conducted in the facilities of *Maxitrate Ltda.*.

All specimens were set in the same furnace, already heated to 940 °C. After heating the specimens, they remained in this furnace for 3 hours. Then, they were transferred to another furnace previously heated to 670 °C. After the temperature stabilization, the specimens were again kept for 3 hours and then air cooled. All specimens were disposed on four plates and randomly distributed to eliminate any undesired effect of temperature variation throughout the furnace. With the low cooling rate, a homogeneous perlitic microstructure is desired. Finally, as one of the objectives of the process, it is also expected that the alloys' hardness is reduced to facilitate the soft machining stage. The isothermal annealing process is summarized in Figure 4.7.

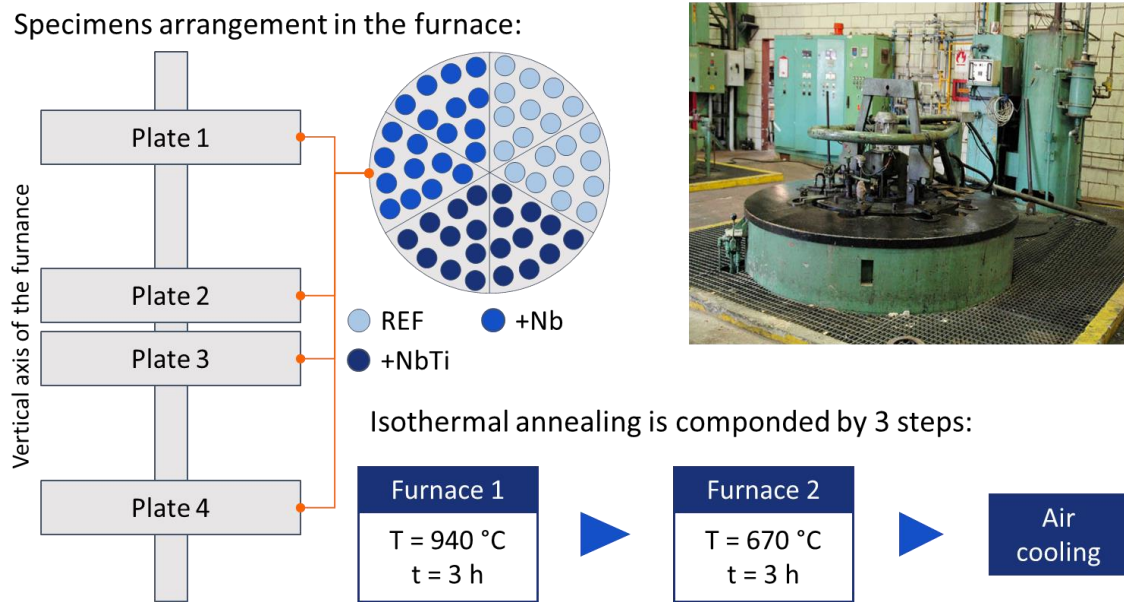


Figure 4.7. The isothermal annealing process.

4.3.3 Soft machining

Soft machining comprises all the operations that transform the forged billet into a gear form. It is compounded by side facing, external diameter turning, internal drilling, hobbing and broaching. Since the hobbing process, in which the teeth cutting occurs, is the only soft machining operation performed on the active regions of the teeth, this is the one of main interest in the content herein studied and, consequently, better explored. All operations of soft machining was conducted in the facilities of *Engrecon S.A.*.

The hobbing process promotes all gear teeth cutting simultaneously, differing, for example, from profile process, in which each tooth is machined individually and sequentially. Thus, the hobbing process is more industrially attractive, especially for small module gears. This is the reason for being selected in the gear manufacturing chain herein considered.

Since a grinding process is planned after carburizing, the geometry after hobbing is not the final one. It is necessary for a material layer to be maintained for subsequent removal during grinding. The defined amount of stock is 80 μm , in accordance with the range recommended by Davis (2005), considering the other parameters of *ITA Geometry*. This process is intended to be primarily mechanical, which means that the working material must not be heated to an excessive temperature. Therefore, the expected microstructure after this process should be similar to that found after isothermal annealing. The hobbing process is summarized in Figure 4.8.

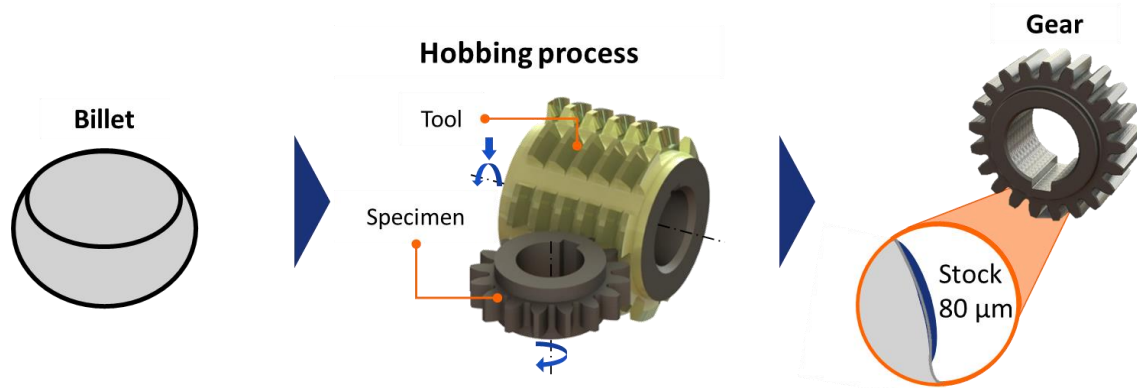


Figure 4.8. The hobbing process.

4.3.4 Carburizing

The carburizing process is intended to provide hardening to the working material, especially in the surface regions, which will prevent the fatigue crack nucleation. Carburizing is one of the most applied case hardening processes and consists of heating the working material in an atmosphere rich in carbon followed by quenching. The carbon will diffuse into the interior of the surface layers and quenching will induce the formation of martensite. Then there is a tempering stage to relieve part of the stresses generated by severe cooling. The process performed in this study was conducted in the facilities of *Engrecon S.A.*.

The gas carburizing process occurred in a batch furnace, with specimens of all alloys simultaneously. First, they were heated to 920 °C to an atmosphere with a concentration of 1.0% of carbon and maintained for 4 hours. The temperature was reduced to 830 °C and 0.8% carbon for 1 hours and finally the specimens were oil quenched at 140 °C for 15 minutes. Following quenching, the samples were tempered at a temperature of 180 °C for 2 hours. As in the isothermal annealing process, all specimens were randomly distributed on two levels to eliminate any undesired effect of temperature variation throughout the furnace. The carburized layer is expected to be between 0.6 and 0.8 mm for all specimens, according to Rakhit (2000). The carburizing process is summarized in Figure 4.9.

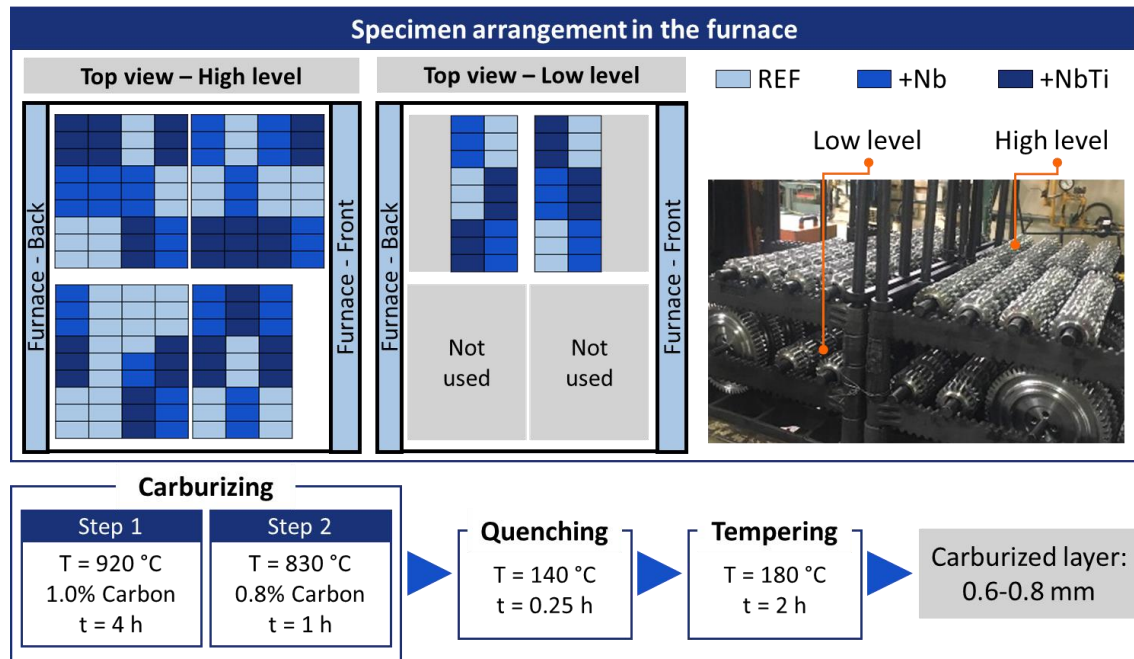


Figure 4.9. The carburizing process.

4.3.5 Grinding

Grinding was the selected finishing process to be applied to the teeth after carburizing. As in the teeth cutting, it is possible to grind either each tooth individually, by profile grinding, or all teeth simultaneously, by generating grinding. The performed process was the generating grinding, which is more widely applied, due to its higher productivity (KLOCKE; BRECHER; BRUMM, 2014). It was also conducted in the facilities of *Engrecon S.A.*

The grinding tool is made of abrasive material, which removes stock by abrasion until the tooth obtains its final form. It is important that the conditions are not so severe, avoiding excessive temperature increase and any unexpected thermal loading on the working material. In the case of this study, only the tooth flank is ground, keeping the tooth root intact.

Grinding is the last process in the gear manufacturing chain, which means that after this process the geometry must be within the expected tolerances and the teeth quality must reach the desired values, here being DIN 7 quality. In addition, analysis after the process is especially important since the surface integrity is in its final state to which it will be subjected to the operating conditions. The grinding process is summarized in Figure 4.10.

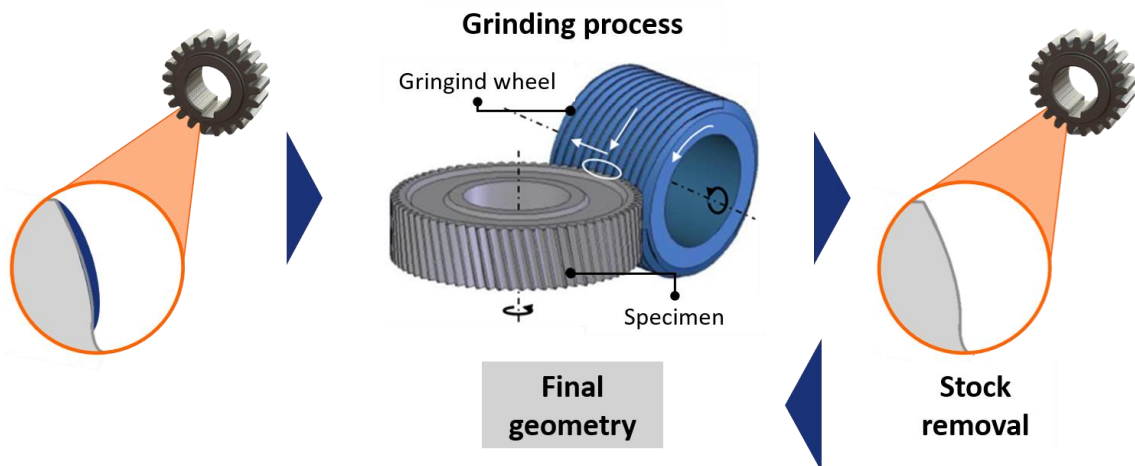


Figure 4.10. The grinding process.

4.4 Specimens' tests

4.4.1 Microstructure investigation

The first category of tests is the materials investigation at microstructural level. Microstructure investigation is intended to assess the grain size of the alloys after each manufacturing process. It also aims to understand the microstructural evolution along the entire chain and to support the discussions of the findings obtained in subsequent test categories. For this purpose, specimens were analyzed by optical microscopy after each manufacturing process. The observed sections at each stage vary according to what was intended to be examined. Even with different observed sections, the comparison among manufacturing processes was ensured.

The preparation for all sections was similar. The sections of interest were revealed by disc cutter with lubrication to avoid excessive surface heating. Then, they were ground, polished and etched with a 2% Nital solution (2% HNO_3 + 98% alcohol). The sections were assessed with a *Carl Zeiss Ultraphot III* microscope at LabMat-ITA. The images were treated using the MIPAR Image Analysis Software and the grain size was evaluated by the equivalent diameter, according to the standard ASTM E112-13 (ASTM, 2013).

For the rolled sections, two sections, radial to the bar axis, were collected: one near the surface and another in the half of the radius. Already close to the gear design, the billet shape of forged and annealed condition allows the observation to be near the region of the teeth. The sections were collected at a distance from the center of the billets equal to half of the pitch diameter (pitch diameter of *ITA Geometry* is 59.85 mm), parallel to the diameter and axial axis

of the billet. After the soft machining stage, the teeth cutting occurs. Then, the sections for the hobbing, carburizing and grinding steps are identical. A tooth is cut in the half of its face width, which means 11 mm from one of the surfaces (face width of *ITA Geometry* is 22 mm). The section is then radial to the gear axis. This section contains details of the entire tooth profile in the middle of the flank, where the highest loadings occur. It is possible to observe the regions of the pitch diameter to the tooth root, locations of the main fatigue failure modes, respectively contact and bending fatigue. The microstructure investigation procedure is summarized in Figure 4.11.

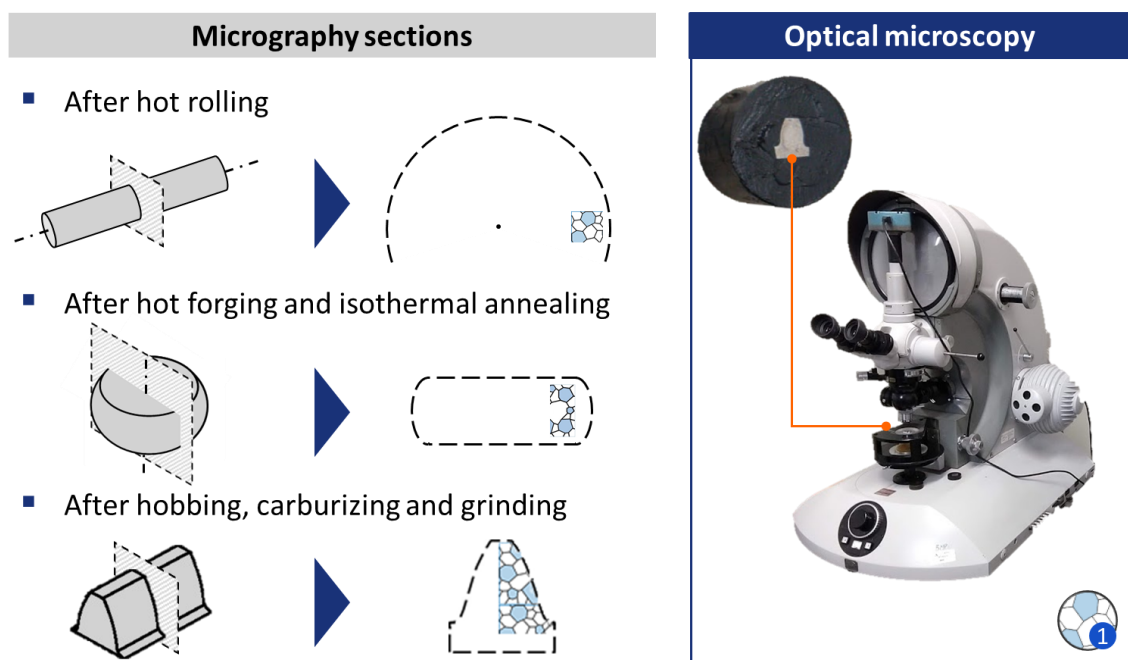


Figure 4.11. The microstructure investigation procedure.

4.4.2 Topography and dimensional analysis

The residual stress relief occurs with dislocations movement and consequent geometric distortions (EPP; HIRSCH, 2012). The topography assessment is intended to observe and understand the extension of residual stress state relieved along the gear tooth.

The assessments were performed in all processes after teeth cutting. The carburizing and grinding were selected due to its contribution to geometric variations. Additionally, a previous condition was also studied, after hobbing, to observe the initial topography right after teeth cutting.

The *Surtronic S-100 Series* Surface Roughness Tester was the contact profilometer used to measure topographic profiles. The direction of stylus displacement was aligned with the gear flank. The analyzed region was from the tip to the root, being considered the whole gear flank. At least 100 parallel profiles were measured along the entire face width with approximately 25 μm of distance between each one.

A micrometric precision platform was used for the tooth positioning to ensure the parallelism between the profiles. Gauge blocks were used considering the tooth sides, which were faced at machining stage, as references for the positioning. Any influence of different cutting angles on specimens were excluded by the Gaussian filter during data postprocessing, according to ISO 13565-2 (ISO, 1996). The raw data experimentally obtained was treated in the software *TalyMap Gold version 7.4*, to individualize the roughness and waviness profiles. The Gaussian filter was used considering a cut-off value of 2.5 mm.

From the profiles obtained, the most common parameters R_a , R_q and R_z are identified. However, they are not sufficient to represent the functionality of the surface, which can be obtained by the also calculated parameters R_k , R_{pk} and R_{vk} . In addition, Abbott-Firestone curves were plotted, which represents the cumulative probability of the surface profile height. It is expected that the carburized condition presents the most irregular surface, due to the thermal loading of the process, while after the grinding the surface is expected to be the least irregular.

The distortion on gears is an effect that refers the teeth to the gear hub and in-between them. Therefore, a complete measurement under the same coordinate system was required for this dimensional analysis. A *Klingelnberg P40* gear measuring center, which has the concept of a Coordinate Measuring Machine (CMM) but also equipped with a rotary table, was used for the measurements. The involute and lead profiles from four teeth were measured, both in the right and left flanks. The pitch error are calculated based on a measurement involving all the teeth. All the measurements and the results' assessments followed the standard DIN 3961 (DIN, 1978). Figure 4.12 summarizes the topography and distortion assessment procedure.

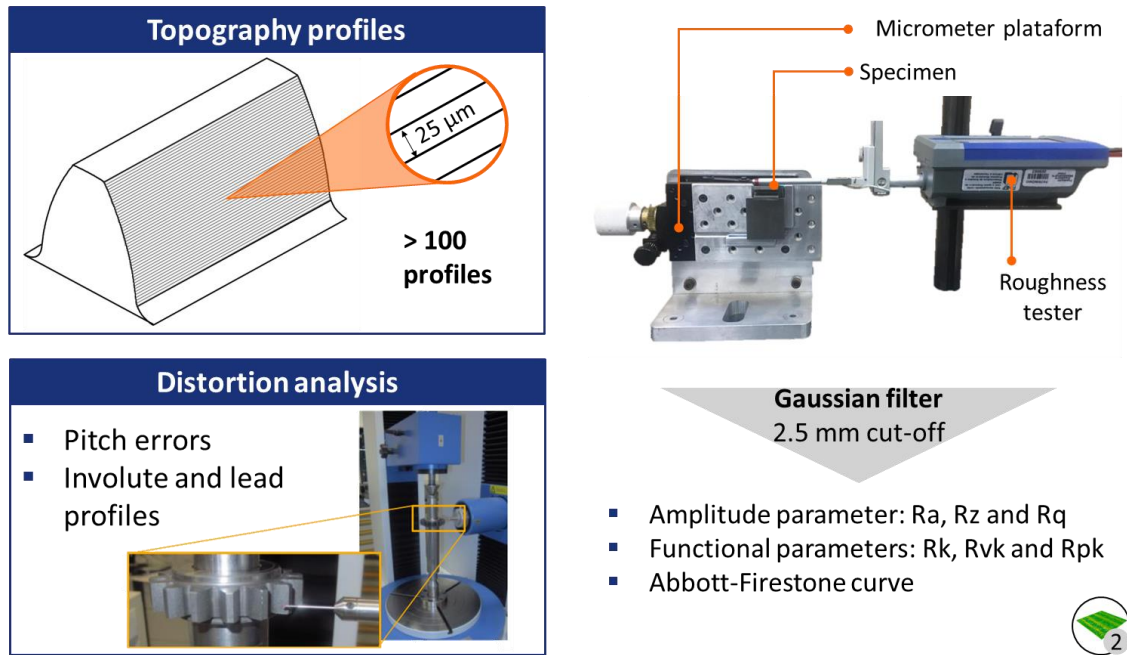


Figure 4.12. The topography and distortion assessment procedure.

4.4.3 Residual stress state assessment

For a complete evaluation of the relationship between residual stress and mechanical properties, it is necessary to obtain a residual stress profile, which means obtaining the residual stress values for different depths. It is known for instance that surface residual stress states are critical in failure processes, while dimensional stability is mainly a function of residual stress in deep regions.

According to Réti (2002), the residual stress state is strongly altered by the carburizing process since this is the process with the highest thermal loading and microstructural modification. Therefore, measurements of the residual stress state were performed after this process, as well as at the end of the gear manufacturing chain, which is after grinding. The method used for determining the residual stress state was the X-ray diffraction (XRD), one of the most common methods, using a *PANalytical Empyrean* diffractometer at LabMat-ITA.

Since the wavelength range of X-rays is similar to the interplanar atomic spacing of crystalline structures, they are used to identify phases and study crystalline structure by the diffraction caused by the atoms in the incident radiation beams. Such methods that use X-rays, such as XRD, are supported by Bragg's law, which relates interplanar atomic spacing to the diffraction angle of the radiation beams (2θ) (CULLITY, 1956).

The detection of the radiation beams after incidence allows an intensity curve to be plotted according to the variation of the diffraction angle, called diffractogram. Different beam incidence angles (ψ) are induced, so that it is possible to obtain information about grains of different orientations and therefore several diffractograms are generated, one for each beam incidence angle. The residual stress state can be evaluated from the strains using the *Peak Shift* method, since it will alter the interplanar atomic spacing and, consequently, the peak intensity (CULLITY, 1956). The peak intensity variation for each diffractogram is, then, used to define the residual stress state.

The selected angle for the analyses was the one related to the planes (211) of α -Fe around $2\theta = 156^\circ$ (CULLITY, 1956). Usually, it is intended to investigate a peak with the value of 2θ as high as possible, since the uncertainty in determining this angle is reduced as higher is its value (NOYAN; COHEN, 1987). This is the main reason for choosing Cr radiation for these measurements. The low energy of the incident radiation beam shifts the peaks to the right in the diffractometer, so that the Bragg's law is satisfied, increasing the accuracy of the method. Although the microstructure evaluated is mostly martensitic, since the measurements are conducted after the carburizing process, there will be a retained austenite content. However, according to the results obtained by Rego (2016), this content will not induce significant changes in the residual stress measurements and the analysis may be focused on the α -Fe angle.

Therefore, 2θ was varied from 152° to 160° , for the diffractometer of the specimens with stepsize of 0.15° and exposure time of 18 seconds. The procedure was repeated for 7 different ψ values, from 0° to 60° , at intervals of 10° . All measurements were repeated after rotation of the specimen by 90° at the ϕ -angle (measured surface plane). The surface measurement were conducted by using squared spot sizes of a 3x3 mm located at the region correspondent to the pitch diameter and in the center of the face width. Complementary measurements were carried out in four spots with sizes of 1x1 mm positioned inside the previous 3x3 mm spots, to assess the surface heterogeneity. Figure 4.13 shows the *Peak Shift* method and the parameters used in the XRD tests.

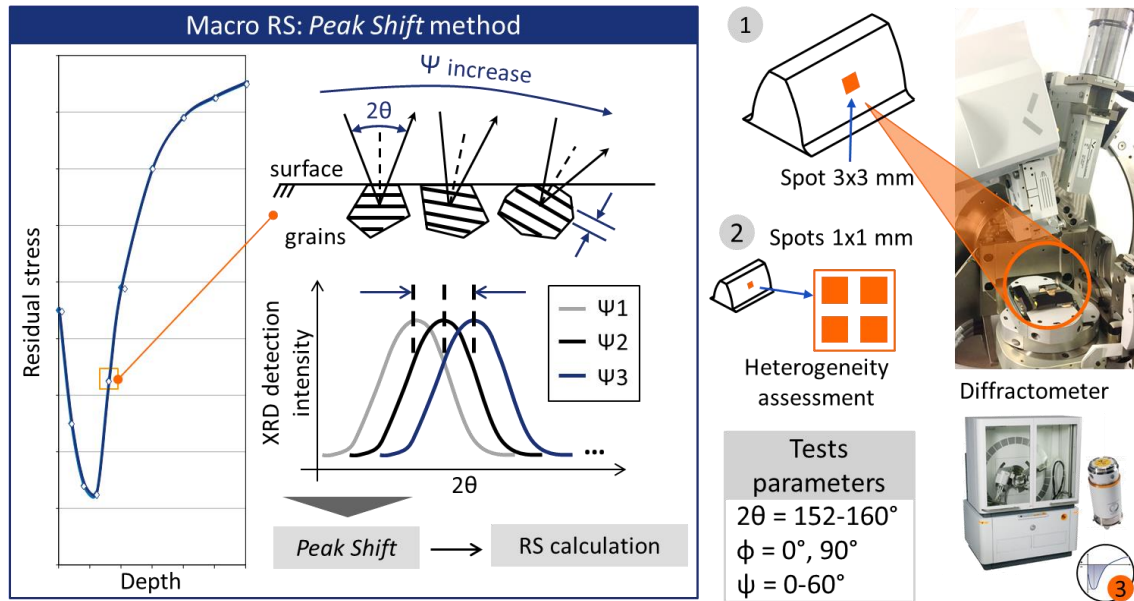


Figure 4.13. The *Peak Shift* method and applied XRD parameters.

The depth values selected were: 20, 30, 50, 100, 200 and 300 μm . These depths values were defined to describe not only the depth where the maximum residual stress is found, but also its intensity, as well as the aspect of the stabilization region at greater depths.

For the generation of the different depth values, the performed method was a chemical etching, which does not induce significant changes in the residual stress state, and is shown in Figure 4.14. The solution used contained 15% nitric acid (HNO_3) and 1% urea ($\text{CH}_4\text{N}_2\text{O}$) in distilled water. Only the region to be measured was removed, while the rest was protected to avoid contact with the solution. Depth measurements were performed by a dial indicator.

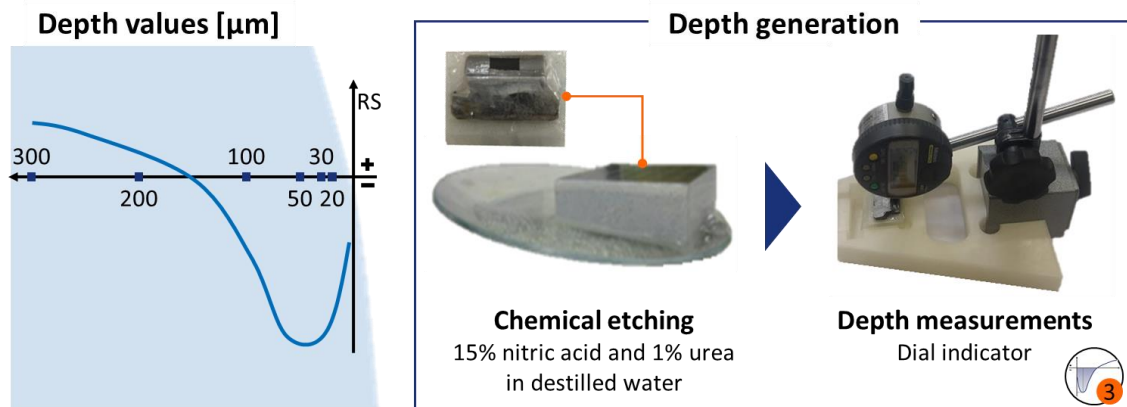


Figure 4.14. The method applied for depth generation.

4.4.4 Hardness mapping

According to ISO 6336-5 (ISO, 2007), the gear fatigue lifetime is correlated to its mechanical strength. The greater its mechanical strength, the greater the loading required for crack nucleation. Therefore, the mechanical strength of the tooth can be assessed through a hardness mapping and can be expanded for tensile and shear strength, properties associated with the loading modes of bending and contact fatigue, respectively.

The grain size is correlated to the mechanical strength, in accordance with the Hall Petch relation (BHADESHIA; HONEYCOMBE, 2017). Thus, it is expected that a possible effect of the microalloying elements and the manufacturing chain on the grain size may be observed on the hardness maps. Since micrographies of the carburized layer are difficult to reveal grain boundaries, the hardness maps can complement the grain size assessment in a comparative approach. The hardness mapping procedure was performed on the specimens obtained after grinding, as it allows a direct correlation to the fatigue strength, since it is the last manufacturing process.

The test was performed using the *Vickers* method, in accordance with ISO 6507-1 (ISO, 2018), which consists of indentations with a diamond tip and preset applied force according to the expected hardness of the material. The higher the mechanical strength, the lower the plastic deformation caused by the indenter and consequently the mark left after the loading removal. Therefore, based on the dimensions of the indentation mark, it is possible to quantify the hardness (ISO, 2018). The equipment used was the *Emco-Test DuraScan 50* hardness testing machine at LabMat-ITA.

The indentation loading used for the hardness measurements was 0.2 kgf. The samples for hardness indentations were prepared following conventional metallographic procedures. The indentations were distributed along half of the tooth cross section, with a stepsize of 0.1 mm, covering from the root to the tip of the tooth.

The hardness maps allow the understanding of the carburized layer depth along the entire gear tooth. The homogenization of the carburized layer is also important since a region of lower hardness would facilitate the nucleation of cracks. In addition, the maps contribute to the assessments of grain size and it is an adequate indicator of fatigue strength, as mentioned previously (DUDLEY, 1996; BHADESHIA; HONEYCOMBE, 2017). The hardness mapping procedure is summarized in Figure 4.15.

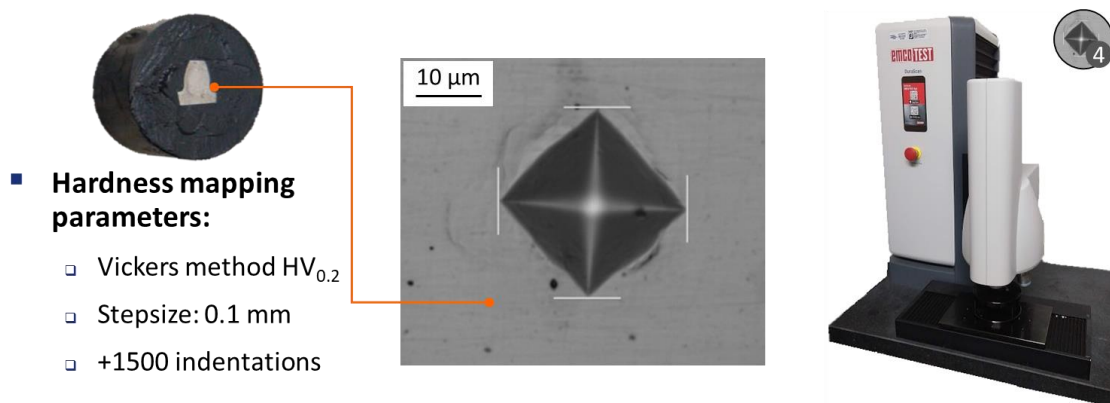


Figure 4.15. The hardness mapping procedure.

4.5 Summary

Three different alloys were selected for investigation: a reference material, DIN 16MnCr5 (equivalent to SAE 5115), which is a conventional gear steel and the same steel microalloyed with Nb in the first case and with Nb and Ti in the second case (REF, +Nb and +NbTi, respectively). All were submitted to the same manufacturing processes and parameters, to ensure that any difference observed in the tests is due only to the microalloying elements. The gear design is also the same for all, the *ITA Geometry*, which represents the same characteristics of gears in the automotive sector.

The specimens are submitted to all processes that constitute a conventional gear manufacturing chain. The first process is hot rolling, in which the ingot is transformed into a rolled bar, then cut into sections and hot forged to produce billets. They are submitted to an isothermal annealing process, which softens the working material for the subsequent soft machining stage, when the teeth cutting occurs by the hobbing process. Finally, the gears are submitted to carburizing, in which a hardened surface layer is produced followed by the grinding, intended to reduce distortions along the tooth caused mainly by carburizing. For each of the processes, the specimens were conducted in the same batch and monitored *in loco*.

Tests were conducted after each of the manufacturing processes to compare the behavior of the alloys. In order to representatively evaluate the surface integrity evolution, four categories of tests were performed: after each process, optical microscopy was performed to observe the grain size and detect any possible anomalies in terms of microstructure; X-ray diffraction tests were executed after the carburizing and grinding processes, obtaining information about the residual stress state of the specimens; after the same manufacturing

processes and after teeth cutting the topography and distortion level of the specimens were evaluated; and after the grinding, hardness maps were collected along the entire cross section of the tooth. The tests were performed at both CCM-ITA and LabMat-ITA.

As a result, it is expected to observe the behavior of microalloyed steels along the gear manufacturing chain in terms of the surface integrity evolution. The tests can show individual results of each manufacturing process and are arranged so that it can be compared to each other integrating a holistic analysis of the entire manufacturing chain.

5 Results and discussions

The results of this study are structured in two sections, dedicated to each of the research questions established in the chapter “Objective and approach”. Therefore, answers are expected by the end of each section and they are integrated in the final chapter “Conclusions and outlook”.

5.1 Behavior of microalloyed steels at the end of the manufacturing chain

The first section is dedicated to a holistic view of how the new alloys performed in the gear manufacturing chain, considering its final surface integrity state. Elements of microstructure, hardness maps, topography and distortion, and residual stress state are presented, and they are intended to understand the behavior of microalloyed steels in the gear manufacturing chain.

5.1.1 Microstructure investigation and hardness mapping

The alloys microstructure was investigated mostly in terms of grain size. As expected, they proved to be different along the entire manufacturing chain, both in terms of average grain size and homogeneity.

The phase composition was similar for all alloys: mostly ferritic/perlitic from the rolled to teeth cutting and martensitic/bainitic after carburizing. Figure 5.1 shows the evolution of the grain size while the it remained ferritic/perlitic and a microstructure after the hobbing process, which means just after the teeth cutting.

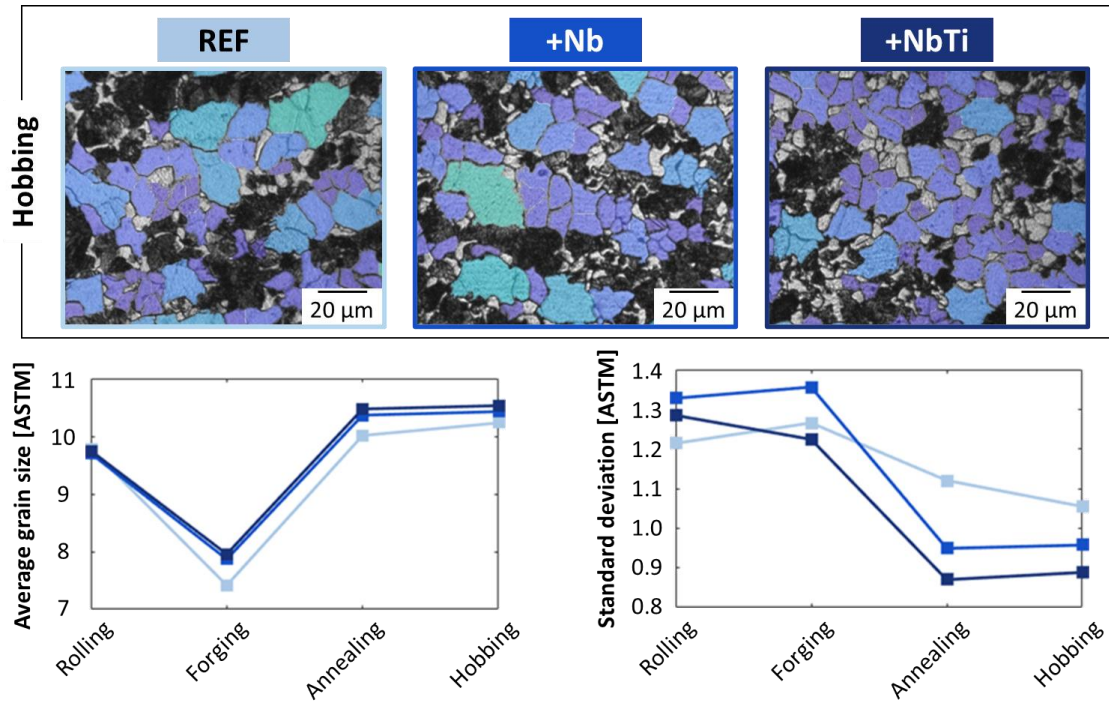


Figure 5.1. Grain size evolution along the manufacturing processes.

Besides the rolled condition, in which the average grain size was similar for all alloys, the +NbTi was the one that presented the most refined grain structure along the manufacturing processes, followed by the +Nb. This result shows that the microalloying elements acted as expected, hindering the grain coarsening in the processes of high thermal loading.

This is in agreement with several studies, such as El-Bitar *et al.* (2012) and Ogawa *et al.* (2016), which also verified the grain refinement in forging and annealing processes, respectively, when using microalloyed steels. On the other hand, the rolled condition, which showed no significant difference in grain size, differs from the results of Vervynckt *et al.* (2011), which identified a 50% reduction in the austenitic grain size after hot rolling with the increase in Nb and Ti content. Consequently, a ferritic/perlitic grain refinement should have also been noted in this process (SMALLMAN; NGAN, 2014).

Figure 5.1 also provides an assessment of the homogeneity of the grain size along the same processes. In addition to being the most refined, the +NbTi microstructure also stands out for being the most homogeneous. This result was also observed by Tobie, Hippenstiel and Mohrbacher (2017) and may lead to higher homogeneity level in several other parameters (TRUTE; BLECK; KLINKENBERG, 2007).

After carburizing, it was not possible to quantify the grain size in the martensitic/bainitic phase. However, the alloys could be compared in terms of the martensite needle length, which

does not exceed a grain boundary (SMALLMAN; NGAN, 2014). Qualitatively, the smaller needles observed in microalloyed steels suggest a remained refined grain structure, as shown in Figure 5.2. Similarly, An *et al.* (2019) also observed a refined grain structure using microalloyed steels during carburizing but considering the austenitic grain size.

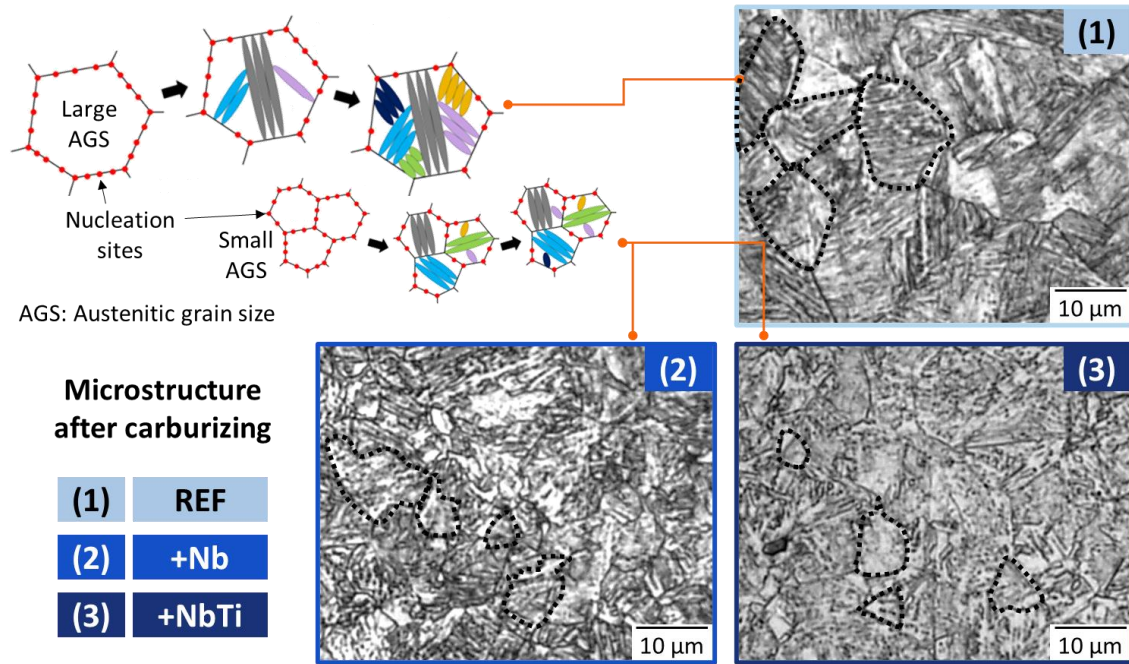


Figure 5.2. Grain size after the carburizing (CELADA-CASERO; SIETSMA; SANTOFIMIA, 2019).

At the end of the manufacturing chain, the gears were also evaluated in terms of hardness. Hardness maps were collected for each alloy in a tooth cross section in the center of the face width and are presented in Figure 5.3. These measurements complement the understanding of how the microalloying elements act in the gear manufacturing chain after carburizing, in which the quantification of the grain size was not possible. The values obtained along the entire tooth are also discriminated in the most critical regions regarding gear fatigue lifetime, which are the regions near the pitch diameter and the tooth root (DAVIS, 2005). The hardness profiles along the carburized layer, expected to have a depth between 0.6 and 0.8 mm, are then compared in these critical regions among the alloys.

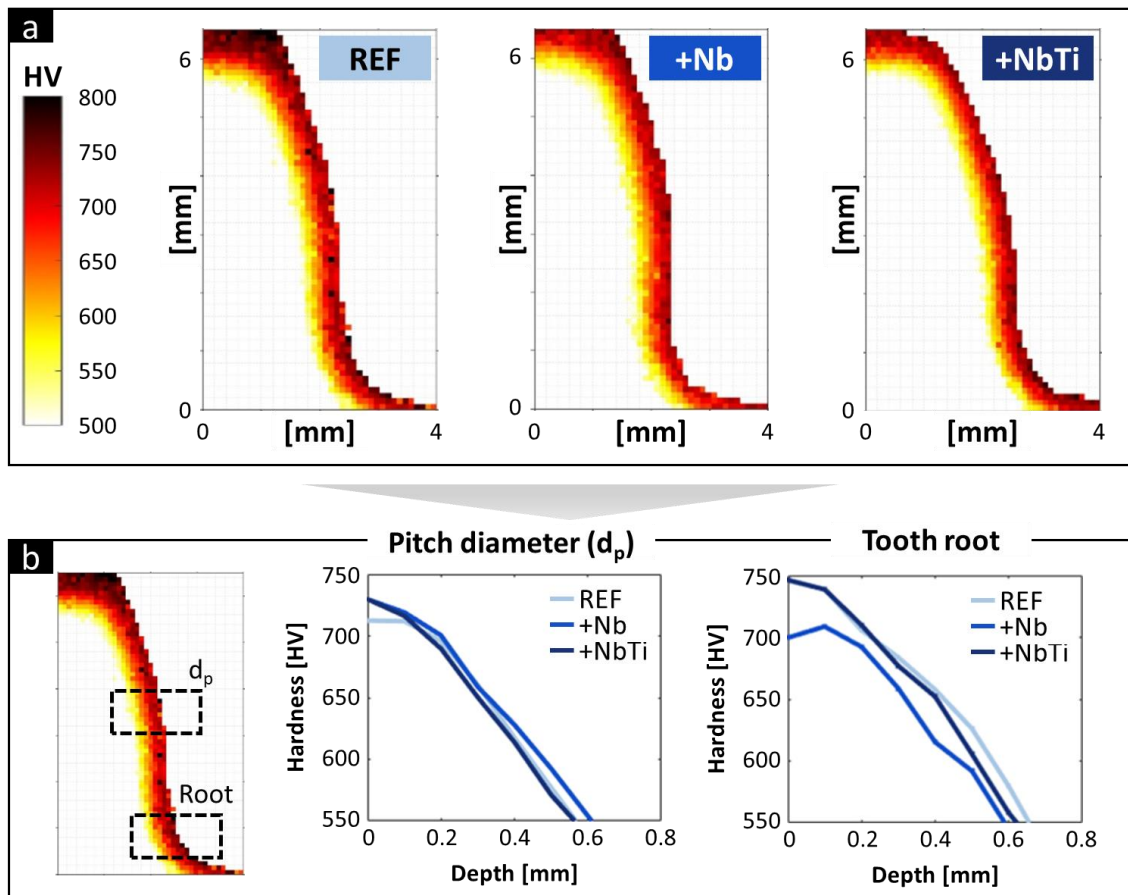


Figure 5.3. Hardness mapping along teeth (a) and hardness profile of carburized layer (b) at the end of the manufacturing chain.

The maps showed that the addition of the microalloying elements did not induce any significant alteration in the carburized layer (Figure 5.3a). Among the apparent changes, a slightly more homogeneous carburized layer is observed for the +NbTi, while in the tip region, the REF showed higher hardness values than microalloyed steels. Nevertheless, this region is not relevant for the gear fatigue lifetime. Regarding to the carburized layer depth, all alloys achieved the desired range.

In the pitch diameter region (Figure 5.3b), microalloyed steels have a surface hardness almost equal, and both proved to be harder than the REF. The +Nb remained superior along the carburized layer depth, while the +NbTi showed a more pronounced gradient. In tooth root region, the +Nb presented an opposite result, lower hardness values along the entire carburized layer. On the surface, the +NbTi and the REF had a similar result, but as in the region of the pitch diameter, again the +NbTi showed a more pronounced hardness gradient.

The results of the hardness maps are not conclusive on the contribution of microalloying elements. According to Gladman (1997), due to the refined grain structure and precipitation dispersion effects, an increase in the hardness values of microalloyed steels was expected, which was not observed, regarding to the carburized layer. In addition, the higher grain boundary density of microalloyed steels and the higher level of irregularity of the crystalline reticulate caused by the precipitate dispersion favor a higher diffusion of carbon, which may lead to additional hardening (SMALLMAN; NGAN, 2014).

Based on the metallurgical effects of the microalloying elements, perceptible alterations in the carburized layer of the alloys were expected. However, the studies in which there is an alteration of carburized layer were conducted by applying microalloyed steels combined to higher carburizing temperatures (THOMPSON; MATLOCK; SPEER, 2007; YANG *et al.* 2013).

Thompson, Matlock, and Speer (2007) investigated the fatigue strength of SAE 8620 steel when added Nb and Ti. During the procedure, the steels were submitted to carburizing at 1050 °C, resulting in a significant variation in grain size. The result of the carburizing shows an apparent increase in the hardness profile along the carburized layer with the increase in Nb content.

The same was observed in Yang *et al.* (2013), using a DIN 20CrMn steel with the addition of Nb and Ti. The carburizing temperature in this study was 1000 °C and also resulted in a hardness increase of the carburized layer on microalloyed steels. This increase occurred particularly in the more superficial layers and then the microalloyed steels had a more pronounced hardness reduction, as it occurred in this study.

In both references, the carburizing temperature was above the temperature used in this study. Along their investigation, Ma *et al.* (2008) performed the carburizing process on Nb-microalloyed steels at a temperature of 930°, similar to the temperature used in this study (920 °C). They observed that the carburized layer was also indifferent to Nb content and the alloy with higher Nb content again had a more pronounced gradient. The results of the mentioned studies are compared to the carburized layer herein obtained in Figure 5.4.

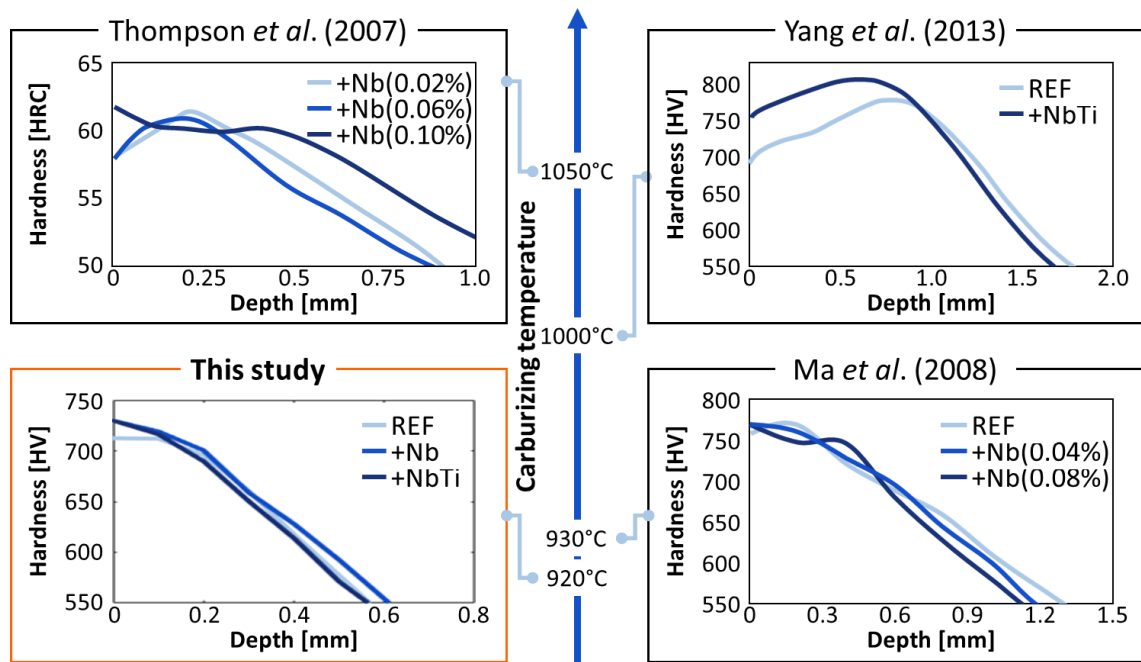


Figure 5.4. Comparison of the hardness profile along the carburized layer at different carburizing temperatures (T_c).

As observed by Bleck *et al.* (2003), it is not possible to detect any significant influence of microalloying elements on the carburized layer. This is only observed at high carburizing temperatures. This may be associated with the pinning effect of precipitates due to the addition of microalloying elements.

In higher temperatures, the inhibition of the grain coarsening in the microalloyed steels compared to the conventional steels is more intensified. As a result, the grain structure of conventional steels becomes excessively coarse, which reduces the material hardness. The precipitates formed with the addition of microalloying elements prevents this from occurring in the microalloyed steels, maintaining a refined grain structure. This leads to the new alloys achieving higher hardness values along the carburized layer, in comparison to the conventional steels. According to Rakhit (2000), such modification in carburizing process may result in cost and time savings, which is economically advantageous for the gear industry.

5.1.2 Dimensional analysis and residual stress state

The comprehension of the gears surface integrity is completed by the analysis of how the new alloys behaved in terms of topography, distortions, and their residual stress state. The

use of the microalloyed steels showed to be beneficial regarding to topography aspects. As shown in Figure 5.5, the addition of microalloying elements was associated with a reduction of surface roughness. According to Liu *et al.* (2019), the lower Rvk values suggest a reduced probability of micropitting. The lower Rpk, related to peaks that are removed at the beginning of the operation, and Rk values allow a better loading distribution during the meshing, reducing the acting contact stresses and, consequently, the failure probability (BRECHER; RENKENS; LÖPENHAUS, 2016).

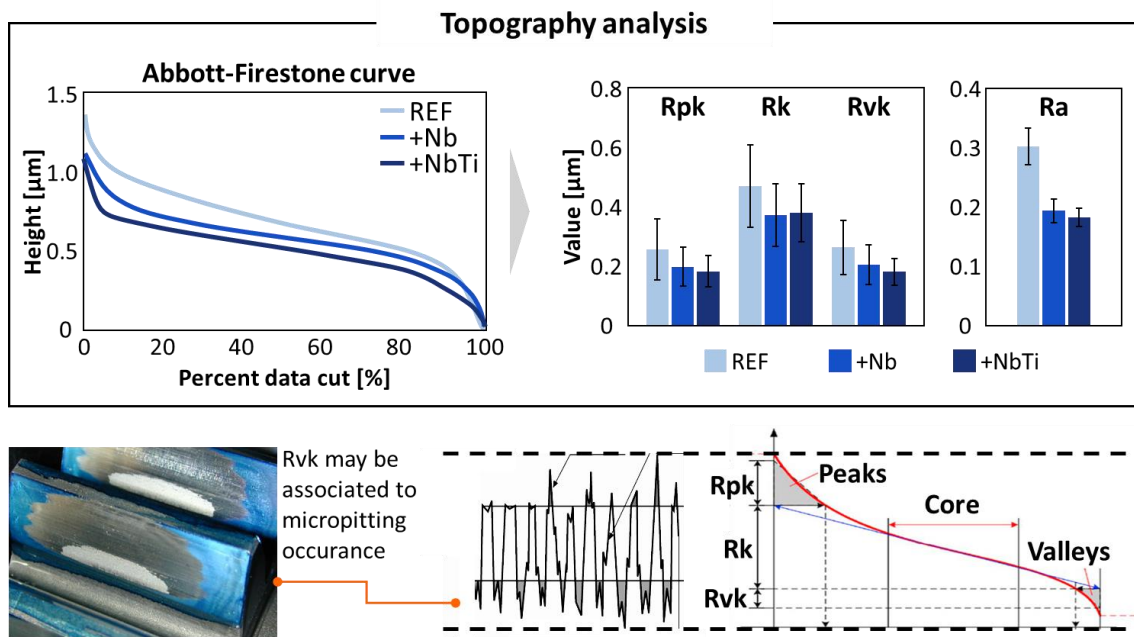


Figure 5.5. Topography analysis of the microalloyed steels (WHITEHOUSE, 1978; AGMA, 2014).

According to Trute, Bleck and Klinkenberg (2007), a homogeneous grain structure leads to more uniform properties. Since the +NbTi microstructure has shown to be more homogeneous, its less rough surface is in agreement with what was expected from its microstructure. In a less pronounced manner, the +Nb also showed better results in comparison with the REF. The results are also in agreement with Zinovieva *et al.* (2013), which observed the reduction of surface roughness with the grain refinement.

Not only topography, but also the distortion level is also a critical factor that may influence contact stress values. High distortion values induce inappropriate meshing, resulting in increased contact stresses and consequently reduced gear fatigue lifetime (ISO, 2007). Additionally, such conditions also increase NVH emission, which is detrimental in many gear applications (BRAUER, 2017). The main distortion parameters among the gears obtained by

the different alloys are compared in Figure 5.6. It is observed that only the +NbTi has tended to reduce the distortion level.

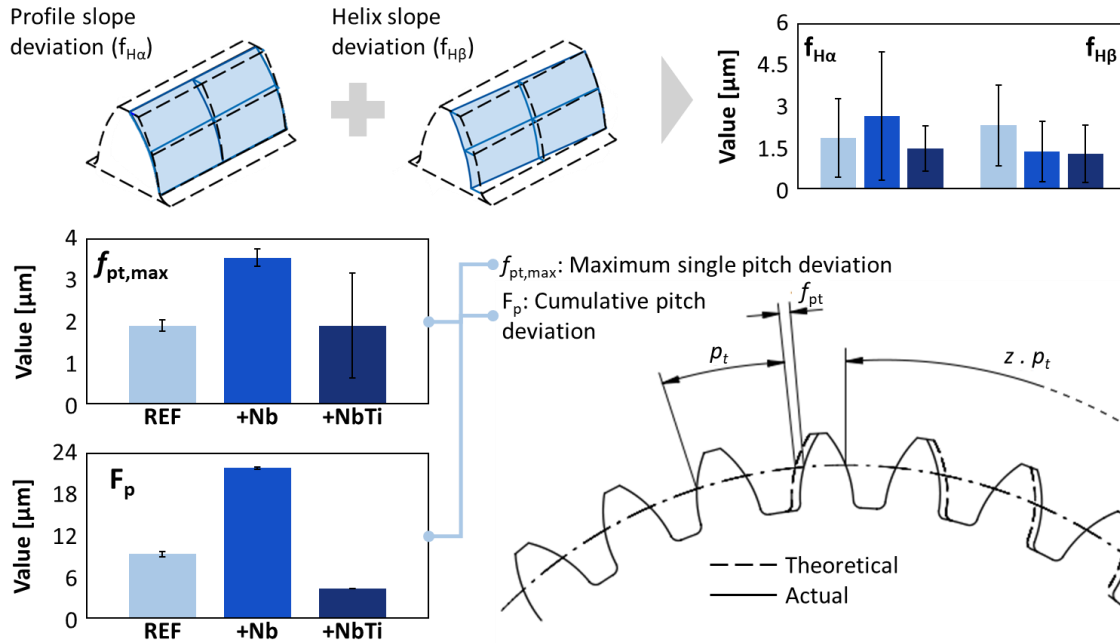


Figure 5.6. Gear distortion level of the microalloyed steels (KLOCKE; BRECHER; BRUMM, 2014; AGMA, 2002).

The result obtained for the +NbTi is in agreement with the results of Tobie, Hippenstiel and Mohrbacher (2017). Such study verified the distortion level of a DIN 25MoCr4 steel with Nb-Ti addition and identified a reduction in the distortion level of approximately 50% when considering microalloyed steels. The results suggest that, considering the conventional parameters, the use of Nb alone as microalloying element was not sufficient to reduce the distortion level.

These dimensional parameters are strongly related to the residual stress state (HUSSON *et al.*, 2012; EPP; HIRSCH, 2012). They should then be investigated together, since the results obtained in one of them may help to explain the behavior in another, thereby providing a more assertive comprehension.

Analogously to the results obtained in the topography and distortion level assessment, the microalloying elements also promoted sensitive alterations in the residual stress state. Figure 5.7 presents the residual stress profile along the depth of each alloy at the end of the manufacturing chain.

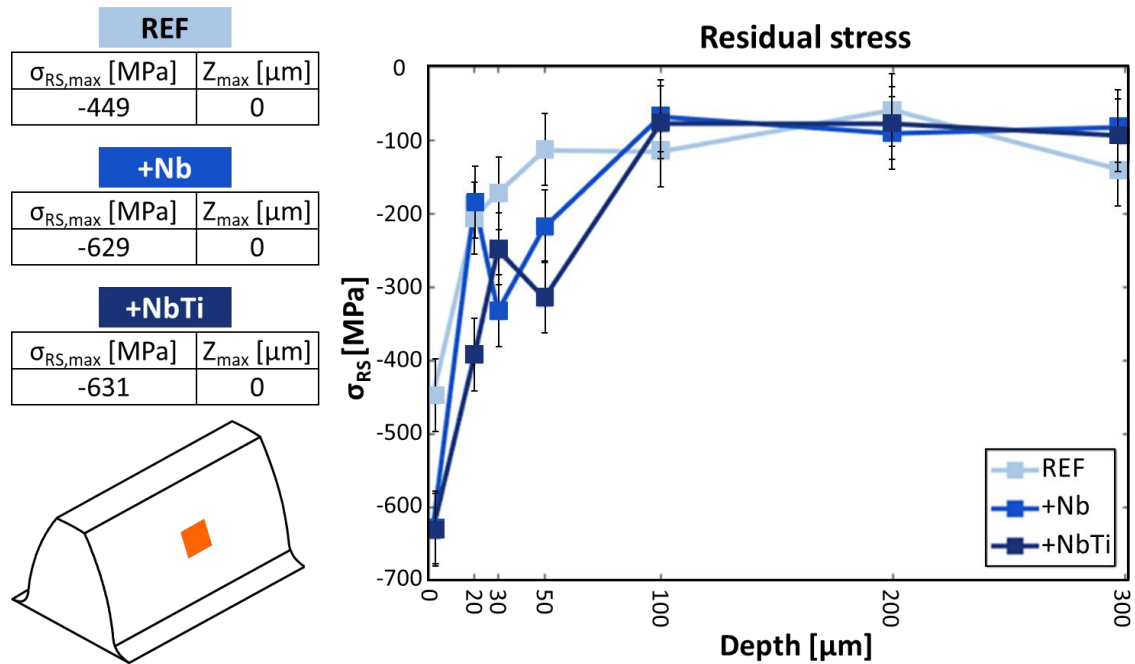


Figure 5.7. Residual stress profile along depth.

The residual stress profile proved to be more compressive when microalloying elements are added. The surface of the microalloyed steels exhibited a compressive residual stress 40% higher than the REF. Only at the depth of 100 μm the residual stress profile of all alloys equalizes and settle at approximately -100 MPa. Among the microalloyed steels, the +NbTi presented a trend of result that are more suitable to fatigue cracks prevention. Differences, however, are not in high magnitude and attempts to distinguish them may be uncertain due to the experimental error of the measurements.

In contrast to the dimensional aspects, the literature is not convergent regarding to the final residual stress state of microalloyed steels. This is because the grain refinement produces opposite effects in some of the processes along the gear manufacturing chain, as described below. The final residual stress profile that microalloyed steels exhibited helps in the partial conclusion that the effects of the grain size is more significant in the processes where this metallurgical characteristic favors compressive residual stresses, considering the entire manufacturing chain.

Nasr (2014) investigated the effect of grain size on the residual stress state after a machining process of four different steels. During the study he used both experimental and numerical analysis by means of the Finite Element Method (FEM), considering the relationship between grain size and mechanical properties by the Hall-Petch relation. Both indicated that

the grain refinement is associated with a more compressive residual stress state. Similarly, Gotoh *et al.* (2010) considered the grinding process to evaluate the influence of the grain size on the residual stress state after this process. His experiments also indicated that a refined grain structure is favorable to induce a more compressive residual stress state.

Between these two processes, a conventional gear manufacturing chain includes a heat treatment stage, consisting of quenching and tempering. In this case, both refinement and homogeneity of the grain size tend to act in an opposite way to obtain a high level of residual stress state. The martensitic transformation occurs uniformly along the refined grains, which may promotes the reduction in both distortion level and surface roughness as previously discussed, but also attenuate the residual stresses associated with the process (YANG; BHADESHIA, 2009; CELADA-CASERO; SIETSMA; SANTOFIMIA, 2019).

Considering the use of microalloyed steels and their martensitic transformation, WU *et al.* (2019) obtained related results. The scope of the study was based on the metallurgical aspects of martensitic formation during quenching. As proposed by the refined grain structure, the alloy with higher content of microalloying elements presented a less compressive residual stress state. The study, however, used alloys with different carbon contents (0.13 and 0.17 wt%, the first being the one with the highest content of microalloying elements), which may affect the comparison between the results in terms of residual stress state.

Considering residual stress, the herein obtained findings suggest that the effect of the grain size is more effective in hobbing and grinding processes, where it is associated with a more compressive residual stress state, than in carburizing, where the effect is opposite. This proposition is only valid when these processes are carried out sequentially, since the final residual stress state is an accumulated influence of each of the intermediate manufacturing processes (REGO, 2016). Although the results of each process are better described in the following sections, this observation requires further exploration and better comprehension of the phenomena involved, which are proposed as forthcoming studies.

High intensities of compressive residual stress is of primary impact on the gear dynamic behavior, however, a homogeneous distribution is also desirable. The evaluation of the residual stress heterogeneity should not be considered as a substitute for the assessment of its intensity, but as a complement (KLOCKE *et al.*, 2016). Even presenting an average compressive residual stress, a region with lower values or even tensile residual stresses is preferred to the nucleation of fatigue cracks (LUKÁŠ, 1996). Thus, a high heterogeneity level may compromise the effort to obtain an average compressive residual stress. As shown in Figure 5.8, the heterogeneity of the residual stress state presented by each of the alloys are then compared.

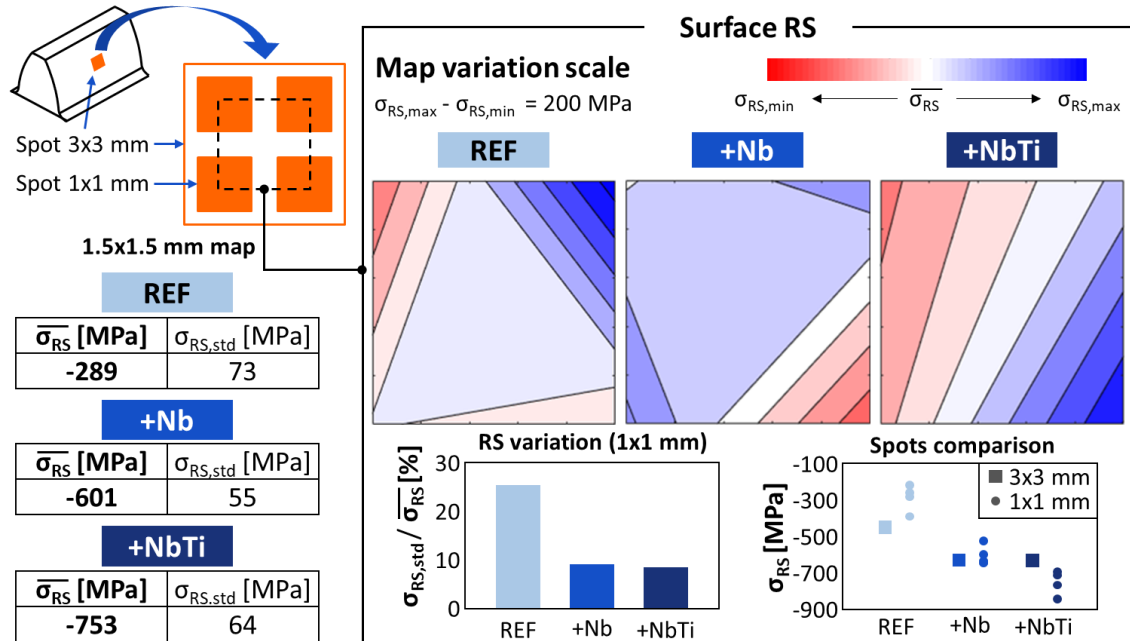


Figure 5.8. Assessment of residual stress heterogeneity on surface.

The maps were constructed by linear interpolation of the values obtained in the 1x1 mm spots and their relative positions. The maps considered a scale of 200 MPa symmetrically distributed over the average value of each alloy. The average values of the measurements are also presented, in addition to the standard deviation of the measurements. Thus, it is possible to understand how much this variation represents, considering the magnitude of the average value. The results of 1x1 mm spots are then compared to 3x3 mm spots.

The effects of the microalloying elements were again observed in terms of homogeneity, enhancing the connection between refined grain structure and properties homogeneity (TRUTE; BLECK; KLINKENBERG, 2007). While the variation among the REF measurements was approximately 25% of the average value, this number was 10% for microalloyed steels. Additionally, the values obtained in the 1x1 mm spots for the REF showed less compressive residual stress than the 3x3 mm spot. It was also possible to distinguish the results of the microalloyed steels in residual stress state, which had not been possible only with the 3x3 mm spots. While the 1x1 mm spot values presented virtually the same value as previously obtained for +Nb, +NbTi presented values of 1x1 mm spot more compressive.

The results of the 1x1 mm spot measurements prove the importance of verifying not only intensity values but also heterogeneity. On a larger scale, the two microalloyed steels showed a result superior to REF, which is already an important result, but both behaved quite

similarly, hindering any distinction between them. Considering more punctual residual stress values, however, the +NbTi showed values in the order of 150 MPa more compressive than the +Nb, suggesting an additional improvement in fatigue lifetime.

5.1.3 Summary

Alloys modified with the addition of microalloying elements have demonstrated to be a class of materials with many potentials not yet fully explored. Few studies have investigated the behavior of these new alloys in the gear manufacturing chain. This section aimed at understanding how the addition of microalloying elements influences the results at the end of the gear manufacturing processes.

The microalloying elements were associated with a more refined grain structure along the processes in which the microstructure remained mostly ferritic/perlitic as expected. After carburizing, the quantification of the grain size was not performed, however the micrographies visually indicate that the martensitic/bainite microstructure also proved to be more refined in the microalloyed steels. On the other hand, it was not possible to accurately identify any difference in the carburized layer among the alloys, when considering the critical regions for gear fatigue failure. According to similar studies, it seems that alterations in the carburized layer, benefiting microalloyed steels, are only detected when the process is performed at higher temperatures than the conventional.

The refined grain structure combined to a higher level of homogeneity presented by +NbTi also promoted a reduction in the distortion level. In topographic aspects, both microalloyed steels produced a less rough surface. The addition of the microalloyed elements also indicated a more compressive residual stress state, although a refined grain structure promotes an attenuation of the residual stresses involved during carburizing, according to literature. The residual stress state of the microalloyed steels was only distinguished on a smaller scale, where +NbTi showed more compressive values than +Nb.

The results show that microalloyed steels may provide gears with more compressive residual stress state and optimized topography. Both characteristics are strongly associated with an increase in fatigue lifetime, which highlights the application of these alloys. Additionally, these observations were made in conventional processes and parameters for gear manufacturing, indicating that the use of these new alloys does not require any modification of manufacturing processes or their parameters. However, the application of microalloyed steels associated with process optimizations, may promote even better results in the final surface

integrity and/or increased productivity, such as raising the carburizing temperature. Such evaluations are discussed in the following section, where each process is individualized.

5.2 Influence of Nb-Ti addition on each manufacturing process

In the second section, associated with the second research question, the manufacturing processes are individualized, and their results are detailed, assessing billet processing, teeth cutting, carburizing and grinding. Thus, it aims to comprehend how the alterations occurred along the manufacturing chain to achieve the final surface integrity. As a result, it may be possible to observe occasional improvements that would lead to an optimized outcome.

5.2.1 Billet processing

The first processes in the conventional gear manufacturing chain herein investigated, which are hot rolling, hot forging, and isothermal annealing, are also applied in the production of several other applications. Since the main well-known benefits of microalloyed steels are associated with high thermal loading processes, the behavior of these new alloys during such processes has been widely studied (FERNANDÉZ *et al.*, 2003; OGAWA *et al.*, 2016; KAYNAR; GÜNDÜZ; TÜRKMEN, 2013). This also means that the findings obtained in this section may be expanded to non-gear applications. This sequence of processes, here referred to as billet processing, anticipates the teeth cutting and is evaluated in terms of grain size. The results of each process are presented and discussed in the same order in which the processes were conducted.

The first condition analyzed is the rolled microstructure. Figure 5.9 presents the microstructures obtained and the results extracted of grain size. Different than expected according to the literature, no difference was identified between microalloyed steels and REF. Instead, the REF revealed a grain structure slightly more homogeneous than the new alloys.

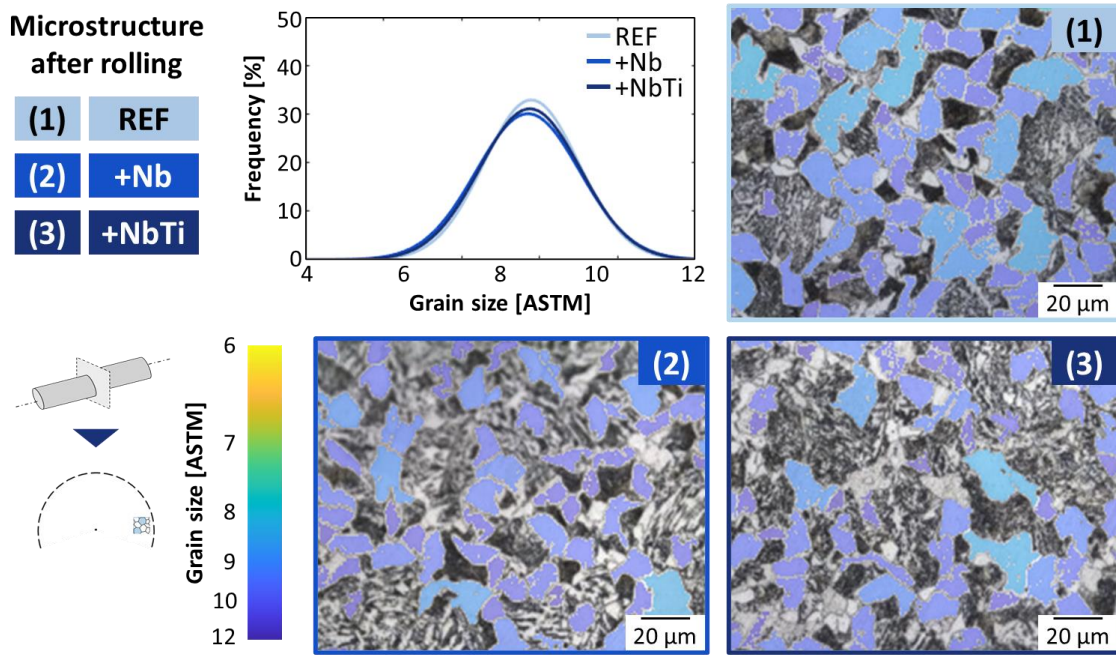


Figure 5.9. Grain size after rolling.

Vervynckt *et al.* (2011) investigated the rolling process in C-Mn steels with the addition of microalloying elements at a temperature of 820 °C. Several combinations were considered, in a range from 0 to 0.16 wt% Nb and 0.01 to 0.08 wt% Ti. Although all alloys used contained some microalloying element content, the study identified a reduction of up to 50% in grain size with the increase in Nb and Ti content.

Similar results were also obtained in Fernández *et al.* (2003), in this case, varying the rolling temperature in the range of 1000 to 1420 °C. Two microalloyed steels, one with Nb and the other with Nb-Ti addition, exhibited a grain size sensitive to the content of microalloyed elements.

The result herein obtained does not accompany the findings of similar studies, however, the similar grain size exhibited by all alloys in the rolled condition favors the assessment of the influence of microalloying elements on the results of the forging process. Since the initial condition is equivalent for all alloys, the results obtained and presented in Figure 5.10 are directly attributed to this process.

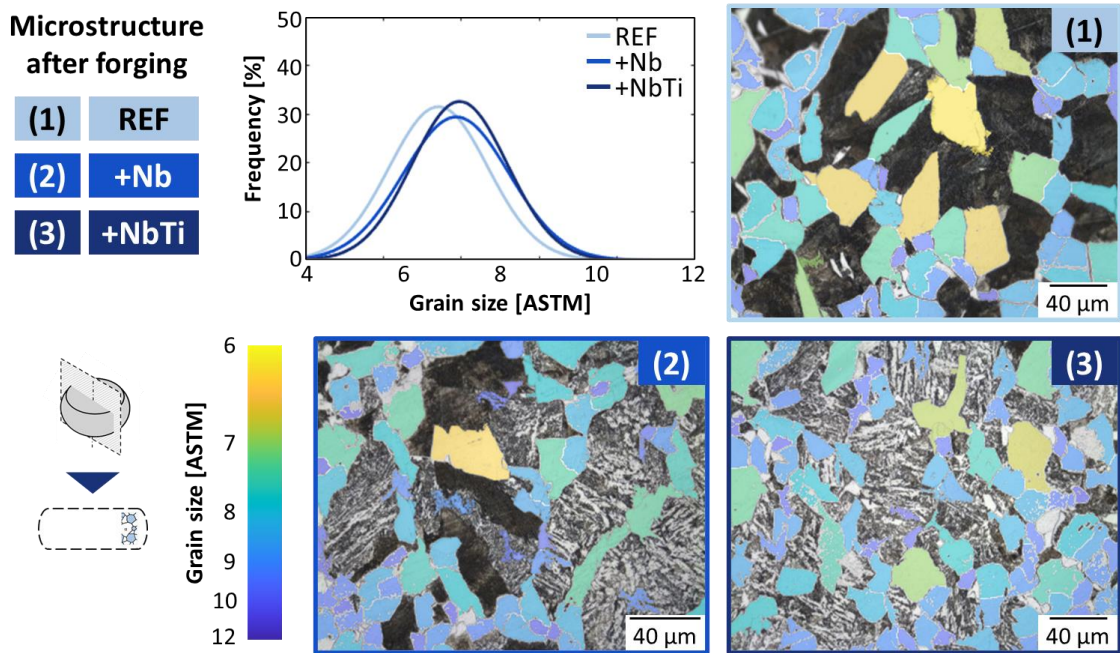


Figure 5.10. Grain size after forging.

In contrast to rolling, it was possible to identify significant alterations in the grain size among the alloys during the forging process. It indicates that the precipitates formed by the addition of the microalloying elements acted preventing the grain coarsening during the high temperatures of the process. All alloys showed an increase in grain size compared to the previous condition, mostly due to the low cooling rate of the box cooling, but this was less pronounced for microalloyed steels. In the comparison between them, there was no significant difference in the grain size. However, the +NbTi sample showed a lower scattering, which means a more homogeneous grain structure. Such findings were expected, as they are in agreement with the literature (MAZZARE; THOMPSON; KRAUSS, 1992; JAHAZI; EGHBALI, 2001; KAYNAR; GÜNDÜZ; TÜRKMEN, 2013).

Kaynar, Gündüz and Türkmen (2013) studied the forging process at a temperature of 1250 °C when using microalloyed steel. Their results found a 33% reduction in grain size when using the microalloying element vanadium. However, the grain size was compared between alloys with different chemical compositions, which may influence the alteration of the grain size.

Mazzare, Thompson and Krauss (1992) investigated the effect of the addition of V and V-Nb on the grain size after the forging. The process was carried out at different temperatures, between 900 and 1200 °C. At all temperatures, microalloyed steels provided a more refined grain structure than the conventional reference alloy. At the lower temperatures, the addition of

Nb minimally altered the grain structure already refined by the V content. At the higher temperatures, similar to the temperature employed in this study, only the V content was not as effective in preventing the grain coarsening, occurring only with the addition of Nb.

Jahazi and Eghbali (2001) compared two microalloyed steels: one with only V content and the other with V and Ti. At a forging temperature of 1200 °C the grain size of the alloys was compared with different cooling rates: box cooling, air cooling and forced air cooling. The Ti addition indicated a significant reduction in the perlite colonies size, with low influence on the ferritic grain size.

Such studies indicate that the reduced grain size presented by microalloyed steels is mostly related to the Nb content, while the Ti major influence is in the perlite colonies size. Since the grain size is quantified considering only the ferritic grains in this study, the findings herein obtained are in good agreement with the literature. Although the Ti addition does not indicate a significant change in the grain size (as it only considers the ferritic grains), the microstructure of the +NbTi had an increase in homogeneity.

The following process is an isothermal annealing, which aims to homogenize the microstructure and mitigate the effects of excessive thermomechanical loading of previous processes. This is the last stage of billet processing and the findings obtained are presented in Figure 5.11.

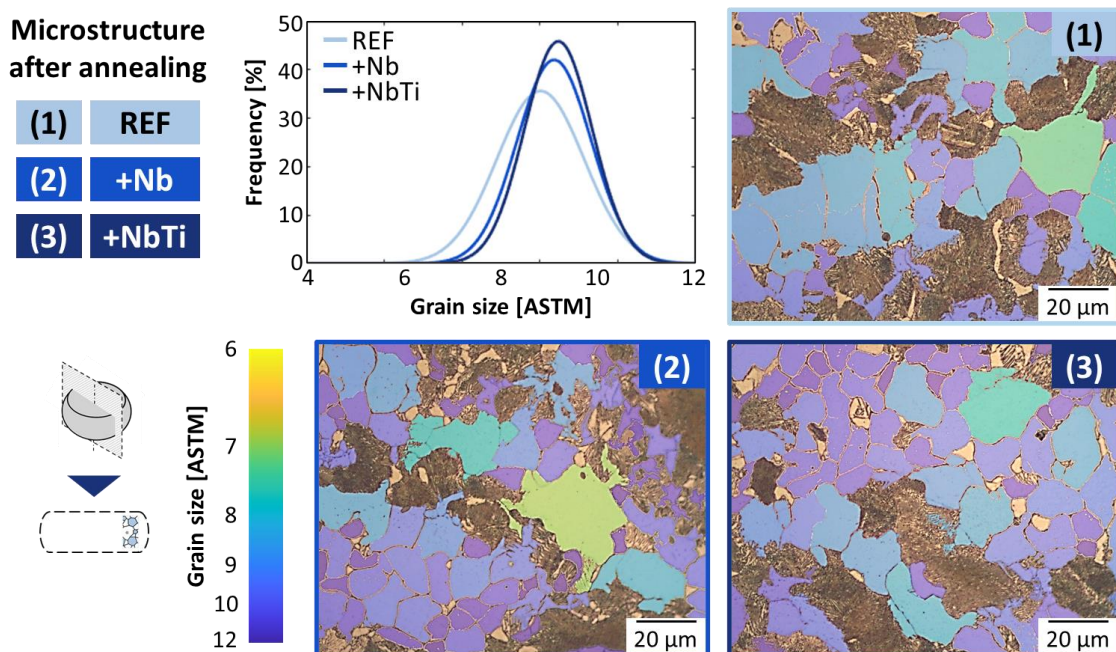


Figure 5.11. Grain size after annealing.

The annealed condition indicates that the microalloying elements acted during the process as expected, avoiding the grain coarsening along the extended time at high temperatures. The findings indicated not only a more refined grain structure in microalloyed steels, but also a distinction between them in terms of homogeneity. The +NbTi again exhibited a lower scattering, which is associated with a more homogeneous grain size distribution. The heterogeneity presented by +Nb, on the other hand, is associated with abnormal grain growth, as indicated in its microstructure in Figure 5.11. Such behavior is undesirable since this heterogeneity may induce reduction of mechanical properties and increase of distortion level (TRUTE; BLECK; KLINKENBERG, 2007).

The application of microalloyed steels in the same process was investigated by Ogawa *et al.* (2016). Two contents of Nb, 0.02 and 0.05 wt% were compared to an alloy without microalloying element after annealing at 750 °C for 3 hours, a time similar to that used in this study. The results indicated that the increase in Nb content reflected in a more refined grain structure.

The results of Kapoor *et al.* (2020) indicated the same effect for Ti addition. At an annealing temperature of 800 °C and time of 2 hours, the grain size of two microalloyed steels was compared, one with only V and the other with V-Ti. It was observed that the addition of Ti avoided the grain coarsening, which did not occur when considering only V-microalloyed steel.

The literature is well established regarding the effects of each microalloying element on the grain size refinement during billet processing, also observed in the processes of this study. However, the results herein presented also indicate that the Ti addition is associated with an improvement in the homogeneity of the grain size. This novel finding leads to greater uniformity in several other parameters and is not fully explored by the literature (TRUTE; BLECK; KLINKENBERG, 2007).

5.2.2 Teeth cutting

After this process sequence, billet is available for teeth cutting, which occurs in this study by the hobbing process. From the teeth cutting, new parameters in addition to the microstructure can be examined. In the case of hobbing, the investigation of the behavior of the microalloyed steels is complemented by the investigation of the topography resultant from the process.

As presented in Figure 5.12, the microstructure has remained quite similar to the previous condition, observed after the annealing process. The microalloyed steels continued

exhibiting a more refined grain structure compared to the REF and the +NbTi still indicated a higher level of homogeneity in terms of grain size.

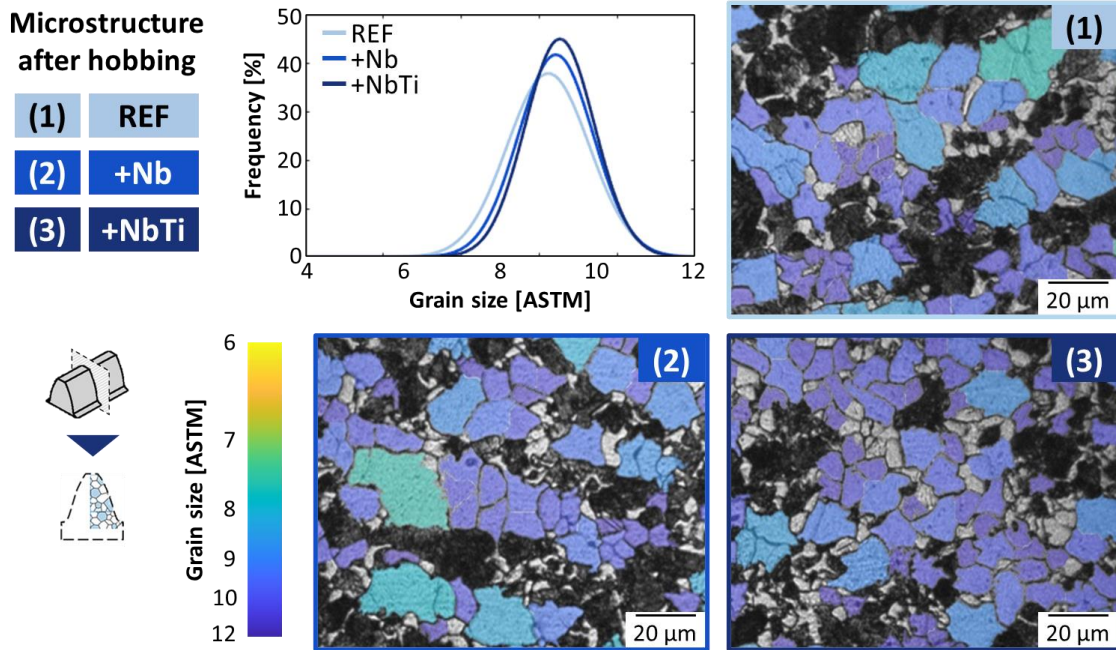


Figure 5.12. Grain size after hobbing.

The insignificant alteration of the teeth cutting in the microstructure of the alloys as it occurred was expected, since hobbing is intended to be a mostly mechanical process. A slight reduction in grain size was observed for all alloys, comparing to the annealed condition. Such reduction was also noted in Pan, Feng and Liang (2017), and occurs due to localized recrystallization along the surface layers.

This difference presented by the alloys in their microstructures led to an apparent difference in topography results, as shown in Figure 5.13. The microalloyed steels showed lower values of surface roughness, both in amplitude parameters, R_a , R_z , and R_q and in functional parameters, R_{vk} , R_k , and R_{pk} . Among the new alloys, the +NbTi stood out in comparison with the +Nb in all parameters, except for R_{pk} and R_{vk} , in which the values of both were very similar.

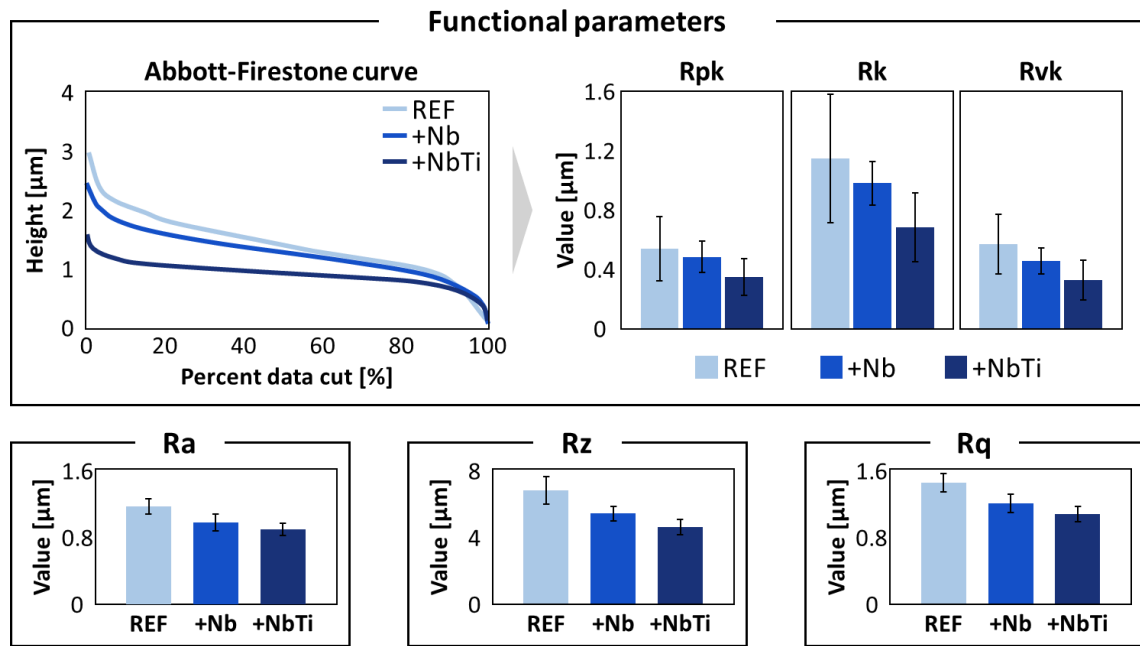


Figure 5.13. Topography analysis after hobbing.

The results obtained are in agreement with Elkaseer *et al.* (2018), which observed that surface roughness is directly influenced by the previous microstructure, with particular emphasis on the grain size. Moreover, the study also highlighted the importance of the homogeneity of the grain structure to obtain better topography results, as it happened with the +NbTi.

The same findings was obtained by Popov *et al.* (2006), who identified a reduction of surface roughness of up to three times only by the grain refinement. According to such study, this effect can be explained by two aspects: chatter vibration attenuation due to simultaneous cutting of a larger number of grains and improvements in the chip formation due to more homogeneous grain structure. Both lead to a better tool-working material interaction and, consequently, reduced surface roughness.

Therefore, the microalloyed steels behaved as expected during the hobbing process. The addition of the microalloying elements did not lead to any undesirable effect on the microstructure, retaining the new alloys with a refined grain structure. Furthermore, it also promoted a reduced surface roughness after the teeth cutting.

5.2.3 Carburizing

After the teeth cutting, the gears are submitted to a heat treatment stage, consisting of quenching and tempering, to attend the mechanical strength requirements (RAKHIT, 2000; DAVIS, 2005). In the case of the conventional gear manufacturing chain investigated in this study, the process used is carburizing. Since the process has a direct influence on the final surface integrity state, part of its results have already been presented in section 5.1, such as the martensitic microstructure and the carburized layer, obtained in this stage.

During the presentation of the carburized layer exhibited by the microalloyed steels, it was observed that the addition of the microalloyed elements was not significant to alter the hardness profile along the carburized layer. Along such discussion, other studies in the literature were compared and it was observed that alterations in the carburized layer are only observed when carburizing occurs at higher temperatures than conventional.

The considerations raised regarding the carburized layer are recalled here with the increment of other parameters to be analyzed together. The carburizing process was also evaluated in terms of topography, distortion level and residual stress state. Therefore, it is possible to better comprehend how the carburizing result is influenced by the addition of microalloying elements.

Although the process is not intended to promote any mechanical loading along the teeth, the topography is significantly altered during carburizing. In addition, there are distortions not observed before the process, which were assessed by means of the gear teeth microgeometry. This occurs mainly due to the relief of residual stresses produced during both the teeth cutting and the carburizing process itself (HUSSON *et al.*, 2012). The new topography values as well as the distortion level resultant from carburizing are presented in Figure 5.14. The figure also shows the roughness values before carburizing, which means as cut, in dashed lines. This allows to evaluate not only the result but also the evolution of the parameters during the process.

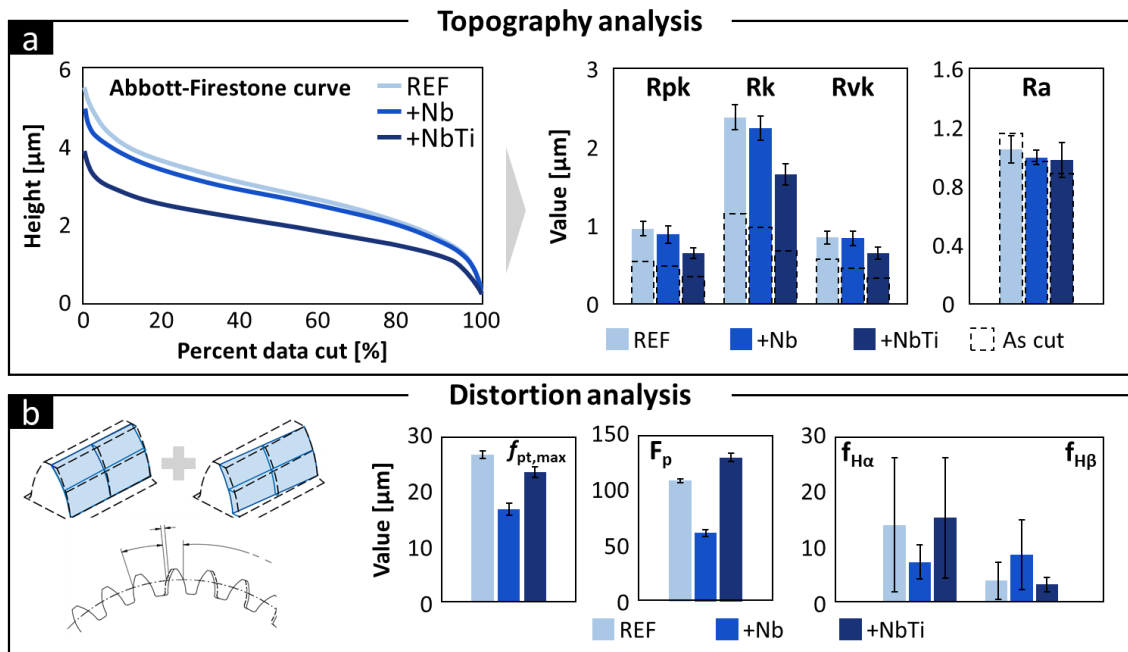


Figure 5.14. Topography (a) and distortion level (b) after carburizing.

It indicates the increase of all functional parameters of surface roughness. The R_a , representing the amplitude parameters, was not significantly altered during the process in the microalloyed steels, while the REF exhibited a slight reduction. The result reinforces the importance of observing the functional parameters, since the comparison only by the amplitude parameter R_a , could lead to the false assumption that the surface roughness after the process was similar for all alloys, which is refuted by the functional parameters.

Brunzel and Fomin (1993) and Kahraman and Sagbas (2010) also identified a reduction of the roughness amplitude parameters after a heat treatment of quenching and tempering in conventional steels, as occurred with the REF. However, such studies do not investigate the functional parameters, which in this study showed an increase for all alloys. Therefore, it can be observed that the addition of microalloying elements does not cause any abnormal behavior during the process, regarding to topography. As a result, the microalloyed steels continued to exhibit the lowest roughness levels, as they were before carburizing.

Figure 5.14b presents the distortion results of the alloys after carburization process. The microalloyed steels behaved in a opposite way. The +NbTi exhibited values close to REF in all investigated distortion parameters. The +Nb tended to present better behavior in terms of distortion, in good agreement with the literature, reducing the value of all parameters except $f_{H\beta}$ (TOBIE; HIPPENSTIEL; MOHRBACHER, 2017).

The effect of the microalloying elements on the result of the carburizing process is lastly investigated by means of the residual stress state. In addition to the mechanical strength enhancement due to the formation of the martensitic microstructure, the process severity induces a residual stress state that directly impacts the gear fatigue lifetime (HAUK, 1997). The results of each alloy are compared according to the residual stress profiles along the depth (Figure 5.15a) and the assessment is then complemented by the residual stress heterogeneity exhibited on the surface (Figure 5.15b).

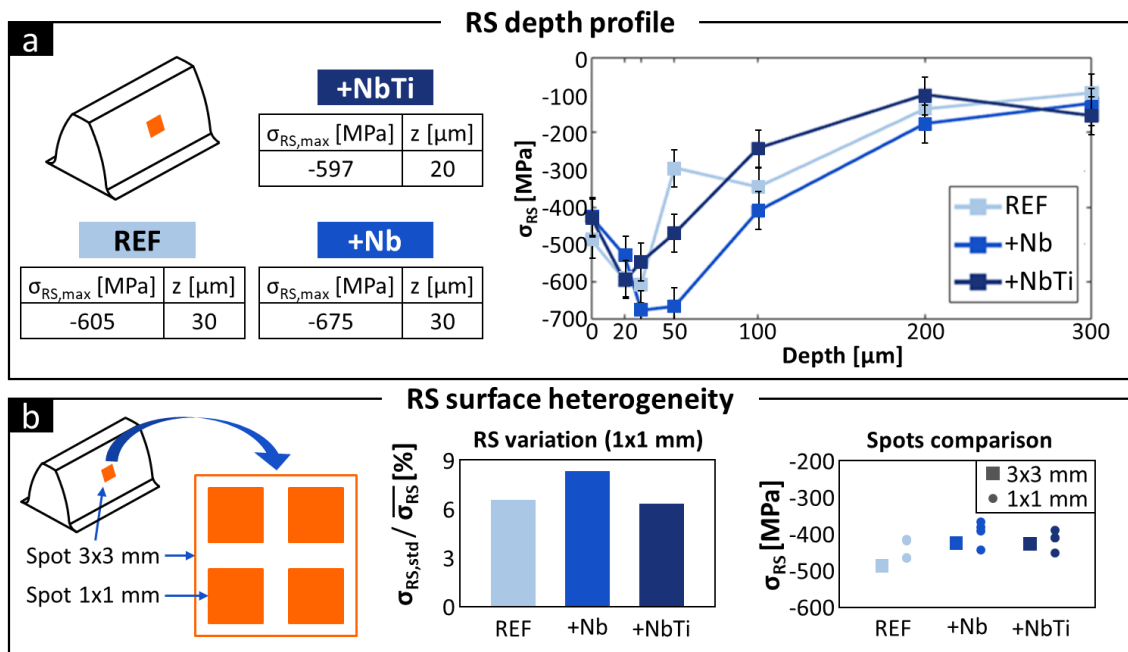


Figure 5.15. RS depth profile (a) and RS surface heterogeneity (b) induced by the carburizing process.

In a first macroscale analysis, the addition of the microalloying elements did not induce any change in the residual stress profile shape (Figure 5.15a). This means that the microalloyed steels also had a compressive profile with a peak between 20 and 30 μm and stabilization at -100 MPa. In comparison with the REF, the +NbTi showed a predominantly less compressive residual stress profile. This reduction during carburizing is in accordance with the findings of Wu *et al.* (2019). This occurs due to the combination of refinement and homogeneity of the grain size presented by the +NbTi. According to Tobie, Hippenstiel and Mohrbacher (2017) the grain size influences the martensitic transformation temperature, and the condition presented by the +NbTi leads the martensitic transformation to occur in a uniform manner along the grains, minimizing the residual stresses associated with the process.

Since the grain refinement exhibited by +Nb is not associated with a high level of homogeneity, the more compressive residual stress profile of the +Nb may be associated with the abnormal grain growth observed after the annealing process. As indicated by Tobie, Hippenstiel and Mohrbacher (2017), the martensitic transformation occurs prematurely in such grains and the deformations caused by the following transformation of the other grains are not well accommodated by the already martensitic regions, intensifying the level of residual stresses of the process. Figure 5.15b shows that the heterogeneous condition of the +Nb, however, was also observed in its residual stress state, which is in agreement with Trute, Bleck and Klinkenberg (2007). The +Nb was the one that exhibited the most heterogeneous surface in terms of residual stress, whereas REF and +NbTi presented a virtually identical value.

High intensities of compressive residual stress, such as the one presented by +Nb, is desired for the gear dynamic behavior, however, its heterogeneous grain structure is also associated with other non-uniform conditions, detrimental to fatigue lifetime (Figure 5.16). A non-uniform grain structure introduces regions of lower mechanical strength, which may be preferential to fatigue crack nucleation (BHADESHIA; HONEYCOMBE, 2017). According to Epp and Hirsch (2012), the higher heterogeneity level may also be associated with an increased distortion level, although this was not observed in this study.

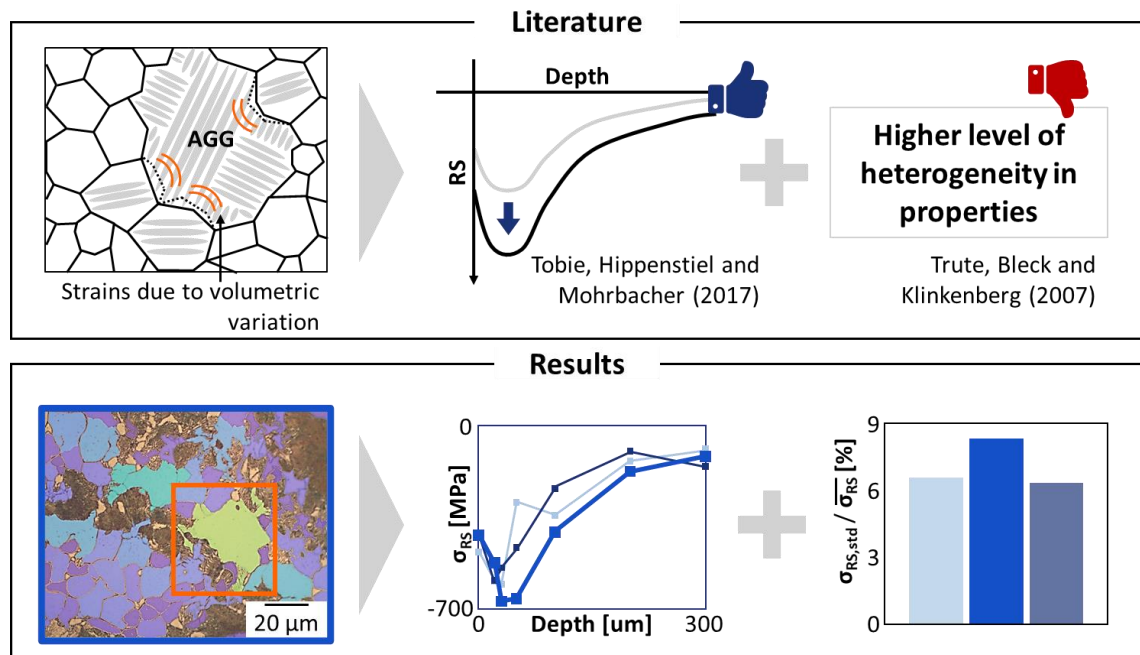


Figure 5.16. The impacts of abnormal grain growth (AGG), as presented by the +Nb, to the homogeneity in properties.

These parameters indicate that the results of the carburizing process are sensitive to the addition of microalloying elements, although the hardness profiles along the carburized layer tend to be similar. The microalloyed steels presented better results in terms of topography, promoting a lower surface roughness. Regarding distortion levels and residual stress state, microalloyed steels diverged, comparing with the REF.

The +Nb showed lower a distortion level, as expected, which did not occur with the +NbTi, in which the process induced a distortion level similar to the REF. The +Nb also presented a more compressive residual stress state, which may be associated with its heterogeneity of the grain structure. The homogeneity of the grain structure presented by the +NbTi is in agreement with the lower intensity of residual stress state.

As briefly introduced in item 5.1, several studies have investigated the increase of the carburizing temperature, allowed by the addition of microalloying elements and consequent prevention of the grain coarsening (MA *et al.*, 2008; YANG *et al.*, 2013; THOMPSON; MATLOCK; SPEER, 2007). Such alteration may be advantageous for the gear industry as it reduces process time and cost (ALOGAB *et al.*, 2007). However, the results obtained in this study show that this alteration should be accompanied by a carefully analysis of the other parameters beyond the carburized layer, ensuring an improvement in the results.

5.2.4 Grinding

The last stage in the conventional gear manufacturing chain considered in this study is the grinding process of the teeth flanks. Since it is the last process, the impacts of the addition of the microalloying elements should be deeply comprehended, as the surface integrity induced by the process is the final condition of the gear.

The process is assessed based on the same parameters observed in the previous condition. Aspects of topography, distortion level and residual stress state are therefore compared among the alloys. In addition to the values obtained after the process, the variation between these values before and after grinding is also evaluated, since the result is a combination of the processes sequence and the effects of the microalloying elements (REGO, 2016).

Since the grinding process is the last process in the gear manufacturing chain, its result is the same presented in section 5.1. Therefore, here it is evaluated the contribution of the process in obtaining the final surface integrity state from the carburized condition. Figure 5.17

shows how the process altered the topography of the alloys in terms of surface roughness and distortion level.

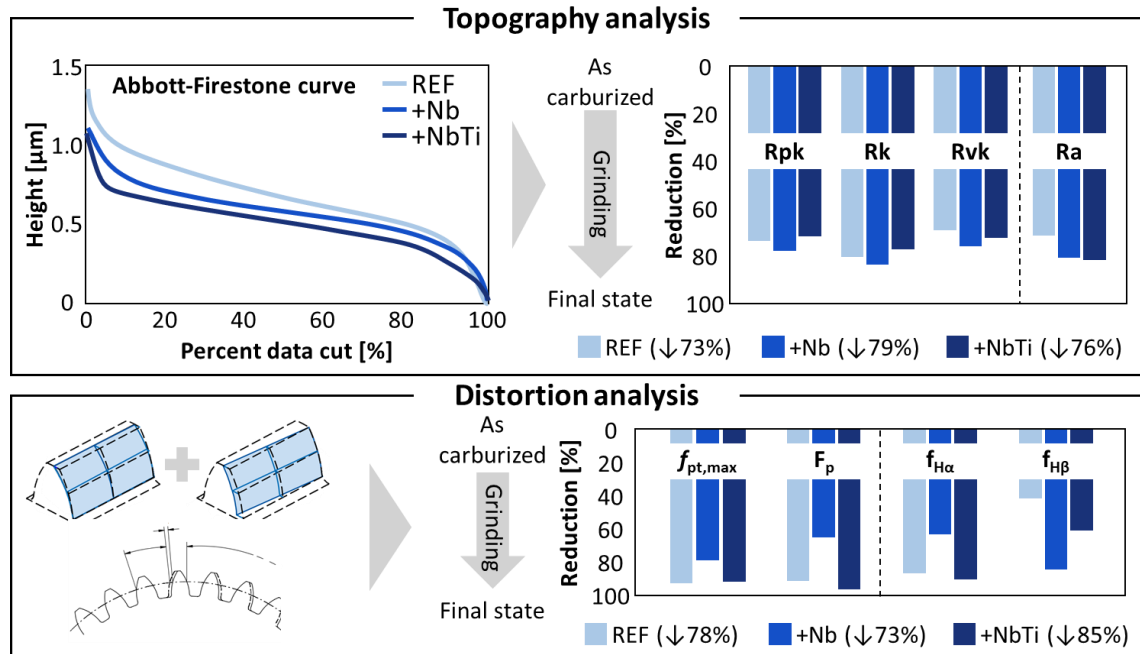


Figure 5.17. Topography (a) and distortion level (b) after grinding.

The findings indicate that the addition of the microalloying elements has a beneficial effect on the results of the grinding process. The process achieved a greater reduction of roughness in the microalloyed steels (Figure 5.17a). This occurred both in the functional parameters, where the microalloyed steels already had lower values, and in the amplitude parameters, where the alloys had almost equal values, indicating that this effect is due to the different alloys rather than the previous condition.

The increased performance presented by the grinding process when considering microalloyed steels, combined with the previous condition of lower roughness, provides an optimized surface in terms of topography. Such findings are in agreement with Zinovieva *et al.* (2013). They investigated the effect of the grain size on surface roughness after mechanical loading and observed that a refined grain structure is associated with lower levels of surface roughness.

Figure 5.17b shows that the reduction in the distortion level during the grinding process in the +NbTi was also more pronounced in comparison with the REF. The +Nb did not behave in the same way, presenting a lower reduction in the distortion level. Although the literature indicates reduced distortion levels associated with the use of microalloyed steels, these studies

do not fully examine the connection between this parameter and abnormal grain growth (TOBIE; HIPPENSTIEL; MOHRBACHER, 2017). This non-uniformity presented by the +Nb may be associated with its more heterogeneous grain structure, according to Trute, Bleck and Klinkenberg (2007).

The impacts of the grinding on the surface integrity of the alloys are then evaluated considering the residual stress state. During the process, a material surface layer, named stock, is removed and with the disturbance of the equilibrium state, the residual stress state is altered (LEMASTER *et al.* 2009). The process parameters should then be well established since the grinding can annulate the compressive stresses obtained in the carburizing and, consequently, adversely affect the fatigue lifetime (LEMASTER *et al.* 2009; DING *et al.*, 2017)

The designed stock depth for the gears in this study is 80 μm . Since the peaks of maximum compressive residual stress after carburizing were situated between 20 and 30 μm , the regions of maximum compressive residual stress in the carburized condition are completely removed, as presented in Figure 5.18. It also shows the residual stress profiles after grinding and its heterogeneity assessment.

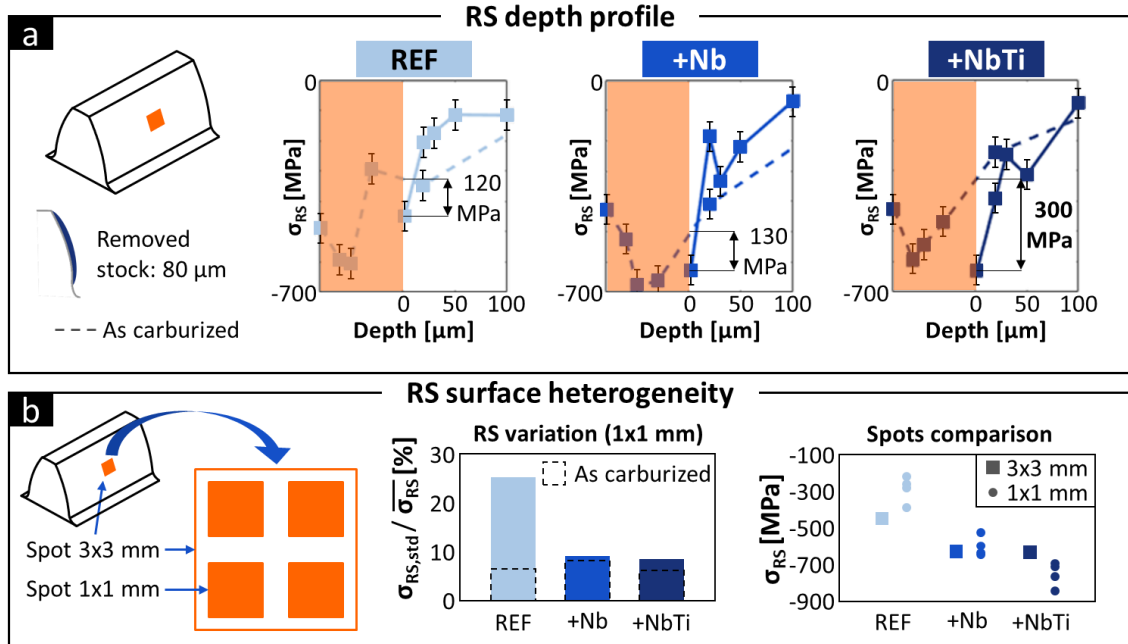


Figure 5.18. RS depth profile (a) and RS surface heterogeneity (b) induced by the grinding process.

In all alloys, the grinding process acted as expected, introducing compressive residual stresses in the surface layers after grinding. The intensity of this additional compressive residual

stresses varied for each alloy. The REF showed the lowest increment of surface residual stresses and the resultant profile becomes less compressive than the carburized condition at 20 μm . The +Nb exhibited a larger increment, but also had its new profile less compressive at the same depth. On the other hand, the +NbTi proved to be the most sensitive to the grinding process. It presented the highest increase in surface residual stress, and its new profile became more compressive along the first 100 μm (Figure 5.18a).

These results indicate that the use of microalloyed steels is associated with the input of compressive residual stresses during the grinding process. By studying the results of this process on a Nb-microalloyed steel, Chakraborty, Chattopadhyay and Chakrabarti (2003) found similar results to this study. They concluded that the increase in the residual stress state occurs due to the precipitate dispersion, which offers greater resistance to material removal and, consequently, there is an increase in the associated residual stresses.

The results are also in agreement with Gotoh *et al.* (2010), which investigated the effects of grain size on the residual stress state induced by grinding. His experiments indicated that a refined grain structure favors the development of compressive residual stresses. This can be explained by the fact that the grain boundaries act as a barrier to the dislocation movement (BHADESHIA; HONEYCOMBE, 2017). As a result, the deformations of the process mechanical loadings are not well distributed, increasing the magnitude of the process-induced residual stresses.

Figure 5.18b presents the results of the heterogeneity level of the surface residual stress of each alloy. The REF had a large increase in residual stress heterogeneity, around three times compared to the carburized condition. This is in agreement with LeMaster *et al.* (2009), who investigated the influence of grinding on the residual stress state and also identified the increase in residual stress heterogeneity associated with the process. The findings herein obtained indicates that the addition of microalloying elements tends to be beneficial in preventing such situation to occur. Therefore, in addition to an increase in the residual stress state caused by the grinding process, the microalloyed steels also ensure an increased homogeneity in terms of residual stress state.

The results of the grinding process have shown to be highly influenced by the addition of the microalloying elements. Figure 5.19 summarizes the aspects observed in carburized condition, comparing to the REF, and the contribution of the grinding to achieve the final surface integrity.

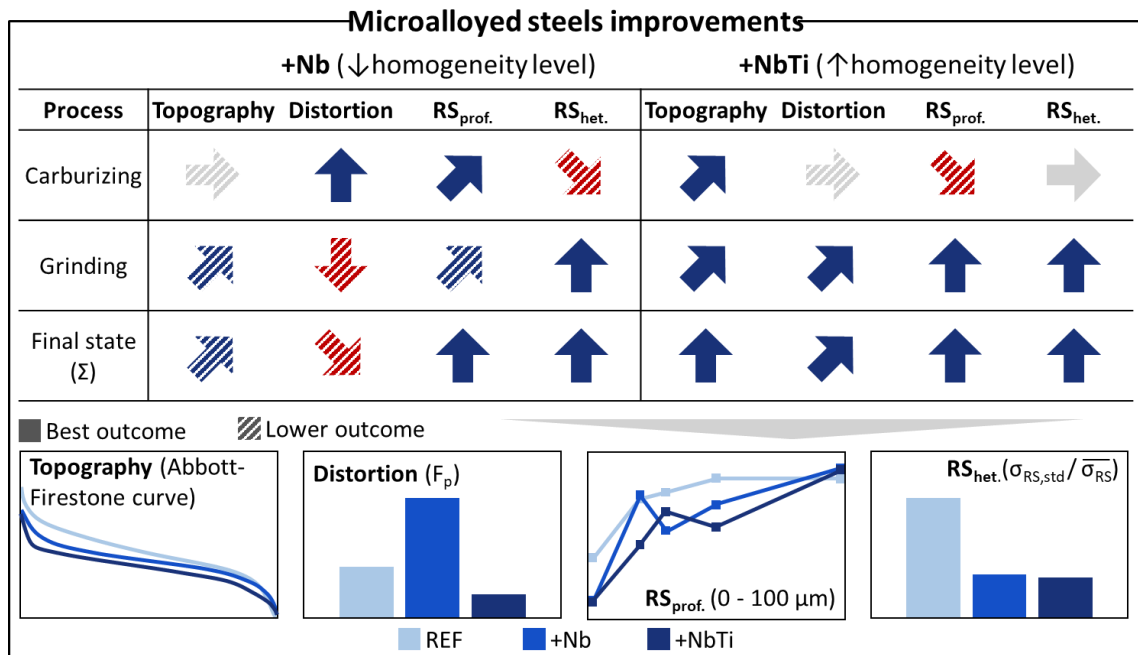


Figure 5.19. The improvements of the microalloyed steels and the contribution of the grinding process.

The new alloys offer several benefits to the process, as demonstrated in the results herein presented. However, as previously stated, not only the process deserves attention but the initial condition as well, since a fraction of the process outcome is a reflection of the previous condition (REGO, 2016). The adequate design of each process ensures the best homogeneity level of the grain structure, which proved to maximize the benefits of the microalloyed steels.

5.2.5 Summary

The billet processing, which means the sequence of the rolling, forging, and annealing, was investigated concerning the microstructure evolution in terms of grain size. As expected, it was identified a refined grain structure in the microalloyed steels after the forging and annealing processes. The rolled condition did not indicate significant variation in the grain size of the alloys. An improvement in the homogeneity of the grain structure was also observed, when both Nb and Ti were considered as microalloying elements. However, the conventional parameters considered in this study resulted in abnormal grain growth in the +Nb microstructure.

The billet in the annealed condition is submitted to the hobbing process, in which the teeth cutting occurs. The microstructure identified a low impact due to the loading of this

process. The process was also evaluated regarding the topography along the teeth. The addition of the microalloying elements was associated with a lower surface roughness after the hobbing process.

The behavior of the microalloyed steels during the following process, which was carburizing, was based on the examination of topography parameters, distortion level and residual stress state. These observations also complement the discussion of section 5.1 on the carburized layer and the process temperature. Compared to the previous condition, surface roughness increased proportionally for all alloys. For the distortion level, microalloyed steels presented different outcomes. The +Nb revealed a reduction in the distortion level, as expected, while +NbTi had a result similar to the REF.

As indicated by the literature, a refined and homogeneous grain structure reduces the residual stress state presented after the carburizing process, as occurred for the +NbTi. On the other hand, the +Nb presented a more compressive residual stress profile, which may be associated with its heterogeneous grain structure. This condition also led to a higher residual stress heterogeneity in this microalloyed steel.

Finally, the grinding process was also investigated by observing the same parameters employed in the carburized condition. In addition to already exhibiting lower surface roughness, the process also provided a greater reduction of surface roughness in microalloyed steels, increasing the difference between the new alloys and the REF. In terms of distortion level, the greatest reduction was observed for the +NbTi, while the +Nb showed a similar behavior to the REF. It may also be associated with the high heterogeneity of the grain structure.

The residual stress state resultant from the grinding process was highly influenced by the addition of the microalloying elements. The microalloyed steels showed a higher tendency to compressive residual stresses during the process. The same result was observed in other studies and may be associated with the precipitate dispersion and grain refinement. In addition, microalloying elements also acted by avoiding a significant increase in residual stress heterogeneity, as observed in the REF.

6 Conclusions and outlook

Microalloyed steels are a class of materials that can offer better outcomes when employed in manufacturing processes with high thermal or thermomechanical loading. Microalloying elements contribute to the achievement of a refined grain structure and it is associated with an increase in mechanical strength and toughness at the same time. These new alloys also present an additional hardening by precipitate dispersion.

Although many studies have investigated these alloys, few studies consider its utilization in the gear manufacturing chain, which consists of a complex sequence of processes combining thermal and/or mechanical loadings. The addition of microalloying elements in the conventional steels currently used in gear applications may provide several economic advantages in different aspects. The potential gain of mechanical properties may lead to optimized dynamic behavior, as well as enable a new gear design, such as downsizing. These new alloys may also offer productivity improvements during gear manufacturing by reducing processes time.

The study herein presented was conducted to investigate how a conventional gear steel microalloyed with Nb and Ti behave along a conventional gear manufacturing chain. Not only the final outcome, but also the evolution of surface integrity, considering the interaction in-between the manufacturing processes were evaluated. Thus, it was sought to understand what are the main benefits that these new alloys offer to the gear industry.

For this purpose, *ITA Geometry* was conceived as the gear specimen. It consists of a geometry that intends to represent gears typically used in automotive sector. Its conception allows, therefore, to correlate it with both ICE and electric vehicle gears, considering the current trends. Although some results can be extrapolated to other gear and even non-gear applications, this study considered the automotive sector, which represents the largest share of gears, as the focus of the investigation.

The research was structured in two sections. The first section aimed at understanding the final surface integrity state obtained when using microalloyed steels. Thus, it was possible to identify the overall benefits of the gears manufactured with the new alloys. Then, the results of each process were evaluated individually. The most sensitive processes to the addition of microalloying elements were pointed out, as well as the interaction in-between the processes when considering microalloyed steels.

The addition of the microalloying elements has promoted a refined grain structure along nearly the entire manufacturing chain, as expected. The rolled condition was the only one in which no significant changes in the grain size were identified. The combined addition of Nb and Ti proved to favor greater homogeneity in the grain structure, while the single addition of Nb indicated abnormal grain growth. Both the refinement and the homogeneity level of the grain structure were correlated to other alterations presented by the microalloyed steels.

The application of microalloyed steels also promoted a significant improvement in the gear topography, in terms of surface roughness reduction. This condition indicates a better loading distribution during the operation and, consequently, an improvement in fatigue lifetime. Regarding the distortion level, the homogeneity of the grain structure has proved to play an important role. To achieve a reduced distortion level at the end of the manufacturing chain, the processes have to be carefully designed to ensure that the grain structure remains homogeneous.

The effect of microalloying elements on the residual stress state is opposite in some of the manufacturing processes, however, a more compressive residual stress state at the end of the manufacturing chain proved to be one more of its contributions. In addition, the new alloys also demonstrated a high improvement in residual stress homogeneity. It is then suggested that this residual stress state will also lead to an improved fatigue lifetime.

The carburized layer was not significantly altered, both in depth and hardness. From this result and similar studies, it can be observed that this alteration occurs when the application of the new alloys is accompanied by an increase in the carburizing temperature. In this case, the difference in the grain size is emphasized and, consequently, the microalloyed steels present an enhanced hardness profile along the carburized layer.

The alterations observed along the gear manufacturing chain by the new alloys were induced not only by the grain refinement and precipitate dispersion, but also by the homogeneity level of the grain structure. Part of the results of Nb-microalloyed steel was hindered by its heterogeneous grain structure, compared to NbTi-microalloyed steel. The manufacturing process that highlighted this situation was the annealing. Therefore, this process should be carefully designed to avoid abnormal grain growth, especially when considering the single Nb addition.

The carburizing process has also demonstrated high sensitivity to the application of the new alloys. The above-mentioned homogeneity level of the grain structure also had a great impact on the results of this process. The increase in the carburizing temperature, allowed by the addition of the microalloying elements, is beneficial in terms of productivity as it reduces

both time and cost of the process. However, several factors in addition the carburized layer should be considered to achieve an optimized outcome.

Although the thermal loading is not as high as the carburizing or annealing, the grinding outcomes were greatly influenced by the addition of the microalloying elements. Additionally to its improvements in topography and distortion aspects, the residual stresses induced by the grinding showed to be more compressive for the new alloys due to the refined grain structure and precipitate dispersion.

The novel findings herein obtained confirm the high potential of the microalloyed steels in the gear manufacturing chain. The results showed that the addition of the microalloying elements not only provides a refined grain structure but also offers an improved surface integrity, considering the main influencers of fatigue lifetime. The final surface integrity state obtained can also lead to a reduction in NVH emission. Both situations place the microalloyed steels in a prominent position in automotive applications, with particular relevance to the electric vehicle trends. This study also assessed the manufacturing processes individually, contributing to the identification of those more sensitive to the addition of microalloying elements.

This study focused on the gear manufacturing chain. The results achieved offer further research on the comprehension of how the benefits presented by microalloyed steels influence the dynamic behavior of gears manufactured with the new alloys. By fatigue tests, it is possible to observe not only how the final surface integrity state is reflected in fatigue lifetime improvement, but also to understand how the microalloying elements themselves directly affect the fatigue stages.

These benefits were obtained considering conventional processes and parameters of the gear manufacturing chain. Better outcomes may be achieved by considering the alteration of some parameters oriented to the application of the micro alloyed steels. For this purpose, further studies are necessary to enhance the knowledge of the effects of the microalloying elements on the most sensitive processes. Therefore, it is possible to fully understand to which extent microalloyed steels can be applied to the gear industry.

References

- ALBAN, L. E. **Systematic analysis of gear failures**. 3. ed. Materials Park: ASM International, 1985. 232 p.
- ALBAN, L. E. Failure of Gears. In: BECKER, W. T.; SHIPLEY, R. J. **ASM Handbook: Failure Analysis and Prevention**, Materials Park: ASM International, v. 11, p. 2558-2603, 2002.
- ALOGAB, K. A. et al. The Influence of Niobium Microalloying on Austenite Grain Coarsening Behavior of Ti-modified SAE 8620 Steel. **ISIJ international**, v. 47, n. 2, p. 307-316, Feb. 2007.
- AMERICAN GEAR MANUFACTURERS ASSOCIATION (AGMA). **ANSI/AGMA 2015-1-A01: Accuracy Classification System - Tangential Measurements for Cylindrical Gears**. Alexandria: AGMA, 2002.
- AMERICAN GEAR MANUFACTURERS ASSOCIATION (AGMA). **ANSI/AGMA 2001-D04: Fundamental Rating Factors and Calculation Methods for Involute Spur and Helical Gear Teeth**. Alexandria: AGMA, 2004.
- AMERICAN GEAR MANUFACTURERS ASSOCIATION (AGMA). **ANSI/AGMA 2004-C08: Gear Materials and Heat Treatment Manual**. Alexandria: AGMA, 2008.
- AMERICAN GEAR MANUFACTURERS ASSOCIATION (AGMA). **ANSI/AGMA 1012-G05: Gear Nomenclature, Definition of Terms with Symbols**. Alexandria: AGMA, 2011.
- AMERICAN GEAR MANUFACTURERS ASSOCIATION (AGMA). **ANSI/AGMA 1010-F14: Appearance of Gear Teeth - Terminology of Wear and Failure**. Alexandria: AGMA, 2014.
- AMERICAN SOCIETY FOR TESTING AND MATERIALS (ASTM). **ASTM E112-13: Standard Test Methods for Determining Average Grain Size**. West Conshohocken: ASTM International, 2013.
- AN, X. et al. Suppression of Austenite Grain Coarsening by Using Nb–Ti Microalloying in High Temperature Carburizing of a Gear Steel. **Advanced Engineering Materials**, v. 21, n. 1900132, p. 1-10, Jun 2019.
- ANDERSON, T. **Fracture Mechanics: Fundamentals and Applications**. 3. ed. Boca Raton: Taylor & Francis, 2005.
- BAKER, T. N. Microalloyed steels. **Ironmaking & Steelmaking**, v. 43, n. 4, p. 264-307, Mar. 2016.
- BAKER, T. N. Titanium microalloyed steels. **Ironmaking & Steelmaking**, v. 46, n. 1, p. 1-55, Nov. 2019.
- BELSAK, A.; FLASKER, J. Method for detecting fatigue crack in gears. **Theoretical and Applied Fracture Mechanics**, v. 46, n. 2, p. 105-113, Oct. 2006.

BERGSETH, E.; SJÖBERG, S.; BJÖRKLUND, S. Influence of real surface topography on the contact area ratio in differently manufactured spur gears. **Tribology International**, v. 56, p. 72-80, Dec. 2012.

BHADESHIA, H. K. D. H. Material Factors. In: TOTTEN, G. E.; HOWES, M.; INOUE, T. **Handbook of residual stress and deformation of steel**, Materials Park: ASM International, p. 3-10, 2002.

BHADESHIA, H. K. D. H.; HONEYCOMBE, R. W. K. **Steels: Microstructure and Properties**. 4. ed. Oxford: Elsevier Science Ltd., 2017. 488 p.

BLECK, W. et al. New developments for microalloyed heat treating steels. **Materials Science Forum**, v. 426-432, n. 2, p. 1201-1206, Aug. 2003.

BOUCHARD, P. J.; WHITERS, P. J. Identification of Weld Residual Stress Length Scales for Fracture Assessment. In: GDOUTOS, E. E. **Fracture of Nano and Engineering Materials and Structures**, Alexandroupolis: Springer, p. 1327-1328, 2006.

BRAUER, S. **High speed electric vehicle Transmission**. 2017. 84 f. Dissertation (Master of Science in Mechanical Engineering) - Karlstads Universitet: Karlstads, 2017.

BRECHER, C.; RENKENS, D.; LÖPENHAUS, C. Method for Calculating Normal Pressure Distribution of High Resolution and Large Contact Area. **Journal of Tribology**, v. 138, n. 011402, p. 1-9, Jan. 2016.

BRUNZEL, Y. M.; FOMIN, I. M. Effect of heat treatment on the surface roughness of a steel after turning on a lathe and the form of the shavings obtained. **Metal science and heat treatment**, v. 35, n. 3-4, p. 175-176, Mar. 1993.

CELADA-CASERO, C.; SIETSMA, J.; SANTOFIMIA, M. J. The role of the austenite grain size in the martensitic transformation in low carbon steels. **Materials and Design**, v. 167, n. 107625, p. 1-10, Apr. 2019.

CHAKRABORTY, K.; CHATTOPADHYAY, A. B.; CHAKRABARTI, A. K. A study on the grindability of niobium microalloyed. **Journal of Materials Processing Technology**, v. 141, n. 3, p. 404-410, Nov. 2003.

CLARKE, K. D. Austenite Formation and Microstructural Control in Low-Alloy Steels. In: HASHIMI, S. **Comprehensive Materials Processing**, v. 12, n. 10, p. 345-361, May. 2014.

COMSTOCK, G. F. Titanium and its effects on steel. **Journal of Industrial and Engineering Chemistry**, v. 7, n. 2, p. 87-94, Nov. 1915.

CULLITY, B. D. **Elements of X-Ray Diffraction**. Reading: Addison-Wesley Publishing Company, 1956. 514 p.

DAVIS, J. R. High-Strength Low-Alloy Steels. **Alloying: Understanding the Basics**, Materials Park: ASM International, p. 193-202, Dec. 2001.

DAVIS, J. R. **Gear Materials, Properties, and Manufacture**. Materials Park: ASM International, 2005. 339 p.

DEARDO, A. J. Niobium in modern steels. **International Materials Reviews**, v. 48, n. 6, p. 371-402, Nov. 2003.

DEUTSCHES INSTITUT FÜR NORMUNG (DIN). **DIN 3961**: Accuracy of cylindrical gears: general bases. Berlin: DIN, 1978.

DEUTSCHES INSTITUT FÜR NORMUNG (DIN). **DIN EN 10084**: Case hardening steels - Technical delivery conditions. Berlin: DIN, 2008.

DING, W. et al. Review on grinding-induced residual stresses in metallic materials. **The International Journal of Advanced Manufacturing Technology**, v. 88, n. 9, p. 2939-2968, Feb. 2017.

DING, Y.; RIEGER, N. F. Spalling formation mechanism for gears. **Wear**, v. 254, n. 12, p. 1307-1317, Nov. 2003.

DUDLEY, D. W. Fatigue and Life Prediction of Gears. In: ASM HANDBOOK COMITEE. **ASM Handbook: Fatigue and Fracture**, Materials Park, v. 19, n. 3, p. 345-354, 1996.

EITEL, E. **Comparing rack-and-pinion sets to other options**, New York: Machine Design, 2003. Available at: <<https://www.machinedesign.com/mechanical-motion-systems/linear-motion/article/21829948/comparing-rackandpinion-sets-to-other-options>>. Accessed on: 09 May. 2020.

EL-BITAR, T. et al. Effect of cooling rate after controlled forging on properties of low carbon multi-microalloyed steels. **Materials Science and Engineering A**, v. 534, p. 514-520, Feb. 2012.

ELKASEER, A. M. et al. Material microstructure effects in micro-endmilling of Cu99.9E. **Proceedings of the Institution of Mechanical Engineers, Part B: Journal of Engineering Manufacture**, v. 232, n. 7, p. 1143-1155, May 2018.

EPP, J.; HIRSCH, T. Characterisation of the carrier of distortion potential “residual stresses” in the collaborative research centre “distortion engineering”. **Materialwissenschaft und Werkstofftechnik**, v. 43, n. 1-2, p. 112-119, Jan. 2012.

FAID, S. A highly efficient two speed transmission for electric vehicles. In: 28th International Electric Vehicle Symposium and Exhibition, 2015, Goyang. **Proceedings [...]**, Goyang: EVS28, 2015. 1-22.

FEDERAÇÃO NACIONAL DA DISTRIBUIÇÃO DE VEÍCULOS (FENABRAVE). **Informativos - Emplacamentos**. São Paulo: Fenabrave, 2019. 46 p.

FERNANDÉZ, A. I. et al. Dynamic recrystallization behavior covering a wide austenite grain size range in Nb and Nb-Ti microalloyed steels. **Materials Science and Engineering A**, v. 361, n. 1-2, p. 367-376, Nov. 2003.

FRANULOVIC, M. et al. Numerical modeling of life prediction of gears. **Procedia Engineering**, v. 10, p. 562-567, Jan. 2011.

GLADMAN, T. **The physical metallurgy of microalloyed steels**. London: Institute of Materials, 1997. 363 p.

GONZALEZ, C. **What's the Difference Between Spur, Helical, Bevel, and Worm Gears?**, New York: Machine Design, 2015. Available at: <<https://www.machinedesign.com/learning-resources/whats-the-difference-between/article/21832142/whats-the-difference-between-spur-helical-bevel-and-worm-gears>>. Accessed on: 09 May. 2020.

GOTOH, M. et al. Influence of Steel Grain Size on Residual Stress in Grinding Processing. **Materials Science Forum**, v. 638-642, p. 2389-2394, Jan. 2010.

GRIFFITHS, B. J. **Manufacturing Surface Technology: Surface Integrity and Functional Performance**. London: Penton Press, 2001. 253 p.

GROSCH, J. Microstructure and properties of gas carburized steels. In: HASHMI, S. **Comprehensive Materials Processing**, Oxford: Elsevier Science Ltd., v. 12, n. 12, p. 379-411, 2014.

GUTERRES, N. F. D. S.; RUSNALDY; WIDODO, A. Gear distortion analysis due to heat treatment process. In: International Conference on Engineering, Science and Nanotechnology, 2016, Solo. **Proceedings [...]**, Melville: AIP Publishing, 2017. p. 1-7.

HARADA, Y.; MORI, K.; MAKI, S. Lining of metal surface with hard-metal foil using shot peening. In: WAGNER, L. **Shot Peening**, Weinheim, p. 200-207, 2003.

HAUK, V. **Structural and Residual Stress Analysis by Nondestructive Methods**. Amsterdam: Elsevier Science Ltd., 1997. 640 p.

HUSSON, R. et al. Evaluation of process causes and influences of residual stress on gear distortion. **CIRP Annals - Manufacturing Technology**, v. 61, n. 1, p. 551-554, 2012.

INOUE, T. Metallo-Thermo-Mechanical Coupling in Quenching. In: HASHMI, S. **Comprehensive Materials Processing**, Oxford: Elsevier Science Ltd., v. 12, n. 6, p. 177-251, 2014.

INTERNATIONAL ORGANIZATION FOR STANDARDIZATION (ISO). **ISO 13565-2: 1996: Geometrical Product Specifications (GPS) - Surface texture: Profile method; Surfaces having stratified functional properties - Part 2: Height characterization using the linear material ratio curve**. Geneve: ISO, 1996.

INTERNATIONAL ORGANIZATION FOR STANDARDIZATION (ISO). **ISO 6336-1: 2007: Calculation of load capacity of spur and helical gears - Part 1: Basic principles, introduction and general influence factors**. Geneve: ISO, 2007.

INTERNATIONAL ORGANIZATION FOR STANDARDIZATION (ISO). **ISO 6336-2: 2007: Calculation of load capacity of spur and helical gears - Part 2: Calculation of surface durability (pitting)**. Geneve: ISO, 2007.

INTERNATIONAL ORGANIZATION FOR STANDARDIZATION (ISO). **ISO 6336-3: 2007: Calculation of load capacity of spur and helical gears - Part 3: Calculation of tooth bending strength**. Geneve: ISO, 2007.

INTERNATIONAL ORGANIZATION FOR STANDARDIZATION (ISO). **ISO 6336-5: 2007: Calculation of load capacity of spur and helical gears - Part 5: Strength and quality of materials**. Geneve: ISO, 2007.

INTERNATIONAL ORGANIZATION FOR STANDARIZATION (ISO). **ISO 6507-1**: 2018: Metallic materials - Vickers hardness test - Part 1: Test method. Geneve: ISO, 2018.

JAHAZI, M.; EGHBALI, B. The influence of hot forging conditions on the microstructure and mechanical properties of two microalloyed steels. **Journal of Materials Processing Technology**, v. 113, n. 1-3, p. 594-598, Jun. 2001.

JÖNSSON, S. Assessment of the Fe-Ti-C system, calculation of the Fe-Ti-N system, and prediction of the solubility limit of Ti (C, N) in liquid Fe. **Metallurgical and Materials Transactions B**, v. 29, n. 2, p. 371-384, Apr. 1998.

KAHRAMAN, F.; SAGBAS, A. An investigation of the effect of heat treatment on surface roughness in machining by using statistical analysis. **Iranian Journal of Science and Technology Transaction B: Engineering**, v. 34, n. 5, p. 591-595, Sep. 2010.

KAPOOR, I. et al. Correlative analysis of interaction between recrystallization and precipitation during sub-critical annealing of cold-rolled low-carbon V and Ti-V bearing microalloyed steels. **Materials Science and Engineering: A**, v. 785, n. 139381, p. 1-16, May. 2020.

KARPUSCHEWSKI, B.; KNOCHE, H. J.; HIPKE, M. Gear finishing by abrasive processes. **CIRP Annals - Manufacturing Technology**, v. 57, n. 2, p. 621-640, Dec. 2008.

KAYNAR, A.; GÜNDÜZ, S.; TÜRKMEN, M. Investigation on the behaviour of medium carbon and vanadium. **Materials and Design**, v. 51, p. 819-825, Oct. 2013.

KIRK, D. Shot peening. **Aircraft Engineering and Aerospace Technology**, v. 71, n. 4, p. 349-361, Aug. 1999.

KLOCKE, F. **Manufacturing Processes 2**: Grinding, Honing, Lapping. Berlin: Springer, 2009. 433 p.

KLOCKE, F. et al. Assessing the heterogeneity of residual stress for complementing the fatigue performance comprehension. **The Journal of Strain Analysis for Engineering Design**, v. 51, n. 5, p. 347-357, Mar. 2016.

KLOCKE, F.; BRECHER, C.; BRUMM, M. **Zahnrad- und Getriebetechnik**. Aachen: Apprimus Wissenschaftsverlag, 2014. 328 p.

KLOCKE, F.; BRINKSMEIER, E.; WEINERT, K. Capability profile of hard cutting and grinding processes. **CIRP Annals - Manufacturing Technology**, v. 54, n. 2, p. 22-45, Jan. 2005.

LAMBERT, R. D.; AYLOTT, C. J.; SHAW, B. A. Evaluation of bending fatigue strength in automotive gear steel subjected to shot peening techniques. **Procedia Structural Integrity**, v. 13, p. 1855-1860, Dec. 2018.

LAN, L. Y. et al. Dynamic and Static Recrystallization Behavior of Low Carbon High Niobium Microalloyed Steel. **Journal of Iron and Steel Research, International**, v. 18, n. 1, p. 55-60, Jan. 2011.

LECHNER, G.; NAUNHEIMER, H. **Automotive Transmissions: Fundamentals, Selection, Design and Application**. New York: Springer, 1999. 448 p.

LEMASTER, R. et al. Grinding Induced Changes in Residual Stresses of Carburized Gears. **Gear Technology**, v. 26, n. 3, p. 42-49, Mar. 2009.

LIEB, J. W. Leonardo da Vinci - Natural philosopher and engineer. **Journal of the Franklin Institute**, v. 192, n. 1, p. 47-68, Jul. 1921.

LITVIN, F. L. **Development of Gear Technology and Theory of Gearing**. Cleveland: NASA, 1997. 124 p.

LIU, H. et al. A Review on Micropitting Studies of Steel Gears. **Coatings**, v. 9, n. 1, p. 1-42, Jan. 2019.

LIU, W. J.; JONAS, J. J. Calculation of the $Ti(CyN_{1-y})-Ti_4C_2S_2-MnS$ -austenite equilibrium in Ti-bearing steels. **Metallurgical Transactions A**, v. 20, p. 1361-1374, Aug. 1989.

LÖHE, D.; LANG, K. H.; VÖHRINGER, O. Residual Stresses and Fatigue Behavior. In: TOTTEN, G. E.; HOWES, M.; INOUE, T. **Handbook of Residual Stress Deformation of Steel**, Materials Park: ASM International, p. 27-53, 2002.

LU, J. Prestress engineering of structural material: A global design approach to the residual stress problem. In: TOTTEN, G. E.; HOWES, M.; INOUE, T. **Handbook of residual stress and steel deformation**, Materials Park: ASM International, p. 11-26, 2002.

LUKÁŠ, P. Fatigue Crack Nucleation and Microstructure. In: ASM Handbook Committee. **ASM Handbook: Fatigue and Fracture**, Materials Park: ASM International, v. 19, p. 96-109, 1996.

MA, L. et al. Influence of niobium microalloying on rotating bending fatigue properties of case carburized steels. **Materials Science and Engineering A**, v. 498, n. 1-2, p. 258-265, Dec. 2008.

MAZZARE, P. T.; THOMPSON, S. W.; KRAUSS, G. Microalloying and austenite grain size control: implications for direct-cooled forgings. In: International Conference on Processing, Microstructure and Properties of Microalloyed and Other Modern High Strength Low Alloy Steels, 1991, Pittsburgh. **Proceedings [...]**, Warrendale: Iron and Steel Society, 1992. 1-34.

MAZZO, N. **Engrenagens Cilíndricas: Da Concepção à Fabricação**. 2. ed. São Paulo: Blucher, 2013. 838 p.

MCPHERSON, D. R.; RAO, S. B. Mechanical Testing of Gears. In: KUHN H.; MEDLIN D. **ASM Handbook: Mechanical Testing and Evaluation**, Materials Park: ASM International, v. 8, p. 861-872, 2000.

MEDINA, S. F. et al. Influence of Ti and N Contents on Austenite Grain Control and Precipitate Size in Structural Steels. **ISI International**, v. 39, n. 9, p. 930-936, Sep. 1999.

MILETI, M. et al. Design of a Hyper-High-Speed Powertrain for EV to Achieve Maximum Ranges. In: Euroforum Deutschland GmbH (eds) CTI SYMPOSIUM, 2018, Berlin. **Proceedings [...]**, Berlin: Springer, 2020. 265-273.

MORRISON, W. B. Overview of microalloying in steel. In: Vanitec Symposium, 2000, Guilin. **Proceedings [...]**, Westerham Kent: Vanitec Limited, 2000. p. 25-35.

NASR, M. N. A. Predicting the Effects of Grain Size on Machining-induced Residual Stresses in Steels. **Advanced Materials Research**, v. 996, p. 634-639, Aug. 2014.

NAVAS, V. G. et al. Residual stresses and structural changes generated at different steps of the manufacturing of gears: Effect of banded structures. **Materials Science and Engineering: A**, v. 528, n. 15, p. 5146-5157, Jun. 2011.

NIKOLAOS, T.; ARISTOMENIS, A. CAD-Based Calculation of Cutting Force Components in Gear Hobbing. **Journal of Manufacturing Science and Engineering**, v. 134, n. 3, p. 1-8, Jun. 2012.

NOYAN, I. C.; COHEN, J. B. **Residual stress: Measurement by diffraction and interpretation**. New York: Springer, 1987. 276 p.

OGAWA, T. et al. Role of Nb on microstructural evolution during intercritical annealing in low-carbon steels. **ISIJ International**, v. 56, n. 12, p. 2290-2297, Dec. 2016.

OLEA, C. A. W. **Caracterização por microscopia eletrônica de varredura do aço SAE1141 microligado ao Nb**. 2002. 106 f. Dissertation (Master of Science in Material Science) - Universidade Federal do Rio Grande do Sul: Porto Alegre, 2002.

OUYANG, T. et al. A model to predict tribo-dynamic performance of a spur gear pair. **Tribology International**, v. 116, p. 449-459, Dec. 2017.

PADILHA, A. F.; SICILIANO JR, F. **Encruamento, Recristalização, Crescimento de grão e Textura**. 3. ed. São Paulo: ABM, 2005. 232 p.

PAN, Z.; FENG, Y.; Y., L. S. Material microstructure affected machining: a review. **Manufacturing Rev.**, v. 4, n. 5, p. 1-12, May. 2017.

PEREIRA JR., R. F. Nióbio. In: NEVES, C. A. R.; LIMA, T. M. **Sumário Mineral 2014**, Brasília: DNPM, v. 34, p. 94-95, 2014.

PICKERING, F. B. Overview of titanium in microalloyed steels. In: Titanium technology in microalloyed steels, 1995, Sheffield. **Proceedings [...]**, Sheffield: Institute of Materials, 1997. p. 10-43.

POORHAYDARI, K.; PATCHETT, B. M.; IVEY, D. G. Correlation Between Microstructure and Yield Strength in Low-Carbon High-Strength Microalloyed Steels. In: International Pipeline Conference, 2006, Calgary. **Proceedings [...]**, New York: ASME, 2006. 29-40.

POPOV, K. B. et al. Micromilling: material microstructure effects. **Proceedings of the Institution of Mechanical Engineers, Part B: Journal of Engineering Manufacture**, v. 220, n. 11, p. 1807-1813, Nov. 2006.

PRICE, D. J. S. On the Origin of Clockwork, Perpetual Motion Devices, and the Compass. **U.S. National Museum Bulletin 218: Contributions from the Museum of History and Technology**, n. 6, p. 81-112, 1959.

RAKHIT, A. K. **Heat Treatment of Gears: A Practical Guide for Engineers**. Materials Park: ASM International, 2000. 209 p.

REGO, R. R. **Influência do uso de distribuição bimodal de classes de granalha no processo de shot peening sobre o perfil de tensões residuais de engrenagens**. 2011. 184 f. Dissertation (Master in Industrial Management and Technology) - Faculdade de Tecnologia SENAI-CIMATEC: Salvador, 2011.

REGO, R. R. **Residual stress interaction in-between processes of gears manufacturing chain**. 2016. 193 f. Thesis (Doctor of Science in Materials and Manufacturing Processes) - Instituto Tecnológico de Aeronáutica: São José dos Campos, 2016.

REICHERT, U. et al. High Speed Electric Drive with a Three-Speed Gearbox. In: CAR TRAINING INSTITUTE. **CTI Mag: The Automotive TM, HEV & EV Drives**, Dusseldorf: CTI, 2016. 25-27.

RÉTI, T. Residual stresses in carburized, carbonitrided, and case-hardened components. In: TOTTEN, G. E.; HOWES, M.; INOUE, T. **Handbook of residual stress and deformation of steel**, Materials Park: ASM International, p. 189-208, 2002.

ROBATTO, L. B. **Residual stresses heterogeneity assessment of high performance powder metallurgy gears**. 2016. 100 f. Dissertation (Master of Science in Materials and Manufacturing Processes) - Instituto Tecnológico de Aeronáutica: São José dos Campos, 2017.

SCHULHAUSER, F. R. et al. **Drive technology - Gears**. Wiesbaden: Capitalmind, 2016. 8 p.

SELLARS, C. M.; WHITEMAN, J. A. Recrystallization and grain growth in hot rolling. **Metal Science**, v. 13, n. 3-4, p. 187-194, Mar. 1979.

SILVEIRA, A. C. F. et al. Influence of Hot Forging Parameters on a Low Carbon Continuous Cooling Bainitic Steel Microstructure. **Metals**, v. 10, n. 5, p. 601, May. 2020.

SMALLMAN, R. E.; NGAN, A. H. W. **Modern Physical Metallurgy**. Oxford: Elsevier Science Ltd., 2014. 697 p.

TAKAHASHI, A.; IINO, M. Improvement of yield strength-transition temperature balance by microstructural refinement. **ISIJ international**, v. 36, n. 3, p. 341-346, Mar. 1996.

TEZEL, T.; TOPAL, E. S.; KOVAN, V. Failure analysis of 3D-printed steel gears. **Engineering Failure Analysis**, v. 110, n. 104411, p. 1-12, Mar. 2020.

THOMPSON, R. E.; MATLOCK, D. K.; SPEER, J. G. The Fatigue Performance of High Temperature Vacuum Carburized Nb Modified 8620 Steel. **SAE Transactions**, v. 116, n. 5, p. 392-407, Apr. 2007.

TOBIE, T.; HIPPENSTIEL, F.; MOHRBACHER, H. Optimizing gear performance by alloy modification of carburizing steels. **Metals**, v. 7, n. 10, p. 415, Oct. 2017.

TRUTE, S.; BLECK, W.; KLINKENBERG, C. Advanced material and processing for the high temperature carburising of microalloyed case hardening steels. **Materials Science Forum**, v. 539-543, p. 4470-4475, Mar. 2007.

VERVYNCKT, S. et al. Recrystallization-precipitation interaction during austenite hot deformation of a Nb microalloyed steel. **Materials Science and Engineering A**, v. 528, n. 16-17, p. 5519-5528, Jun. 2011.

WANG, Z.; GONG, B. Residual Stress in the Forming of Materials. In: TOTTEN, G. E.; HOWES, M.; INOUE, T. **Handbook of residual stress and steel deformation.**, Materials Park: ASM International, p. 149-149, 2002.

WARNER, J. **A Look at Belt, Chain and Gear Drive Technology**, Chicago: Power Transmission Engineering, 2017. Available at: <<https://www.powertransmission.com/blog/a-look-at-belt-chain-and-gear-drive-technology/>>. Accessed on: 09 May. 2020.

WHITEHOUSE, D. J. Surfaces - A Link between Manufacture and Function. **Proceedings of the Institution of Mechanical Engineers**, v. 192, n. 1, p. 179-188, Jun. 1978.

WISE, J. P.; MATLOCK, D. K. Bending Fatigue of Carburized Steels: A Statistical Analysis of Process and Microstructural Parameters. **SAE Transactions**, v. 109, n. 5, p. 182-191, Mar. 2000.

WU, B. B. et al. Toughening of martensite matrix in high strength low alloy steel: Regulation of variant pairs. **Materials Science and Engineering: A**, v. 759, p. 430-436, Ju. 2019.

WULPI, D. J. **Understanding How Components Fail**. 3. ed. Materials Park: ASM International, 2013. 310 p.

XU, H. et al. Prediction of mechanical efficiency of parallel-axis gear pairs. **Journal of Mechanical Design**, v. 129, n. 1, p. 58-68, Jan. 2007.

YANG, H. S.; BADHESHIA, H. K. D. K. Austenite grain size and the martensite-start temperature. **Scripta Materialia**, v. 60, n. 7, p. 493-495, Apr. 2009.

YANG, Y. H. et al. Microstructure and Mechanical Properties of Gear Steels After High Temperature Carburization. **Journal of Iron and Steel Research, International**, v. 20, n. 12, p. 140-145, Dec. 2013.

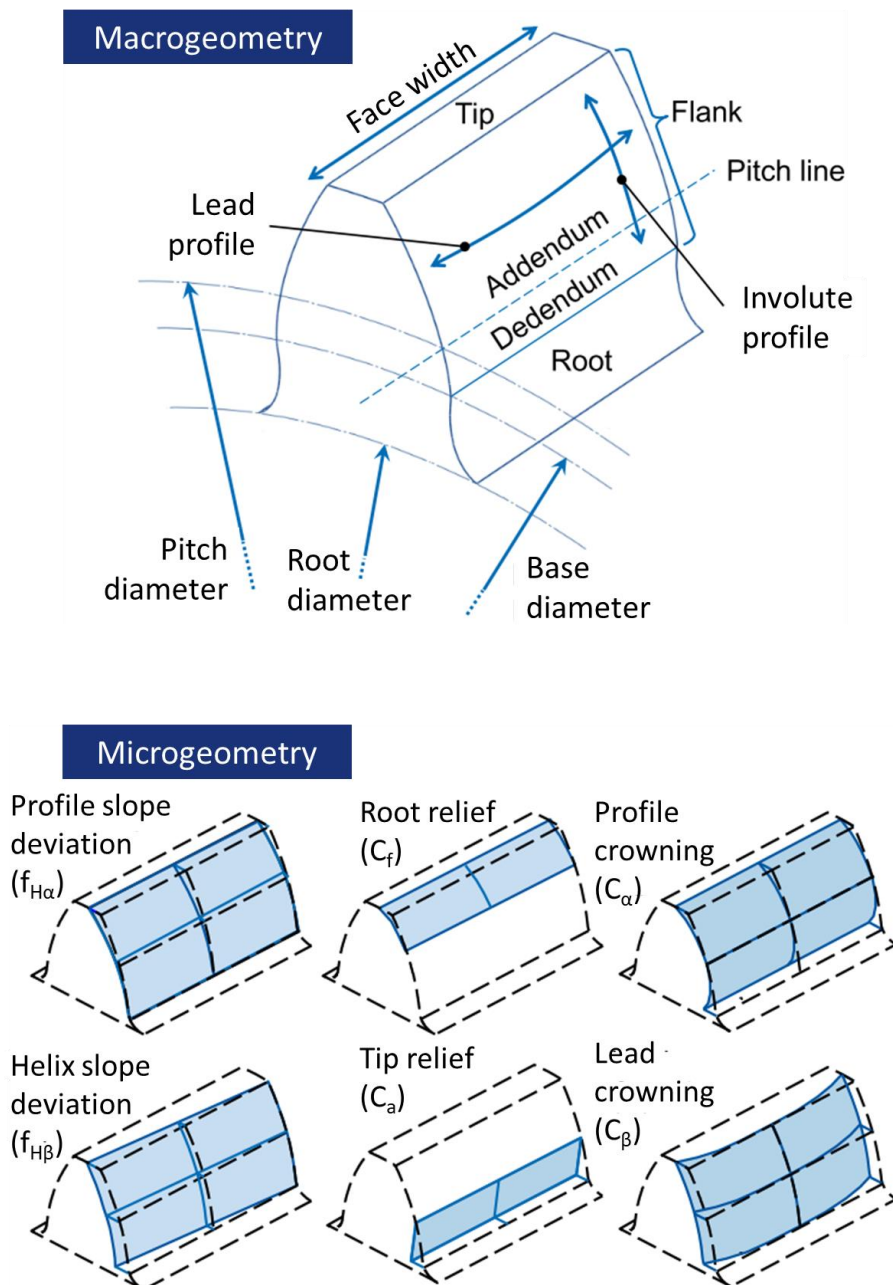
ZHAO, P. et al. The potential significance of microalloying with niobium in governing very high cycle fatigue behavior of bainite/martensite multiphase steels. **Materials Science and Engineering A**, v. 650, p. 438-444, Jan. 2016.

ZHOONGYAO, S. et al. Effects of B and Ti on the toughness of HSLA Steel weld metals. **Chinese Journal of Materials Sciences & Technology**, v. 8, n. 4, p. 294-298, Jul. 1992.

ZINOVIEVA, O. S. et al. Effects of modified surface layer and grain size on surface. In: XLI International Summer School-Conference APM, 2013, Saint Petersburg. **Proceedings [...]**, Saint Petersburg: IPME, 2013.

Appendix A – Terminology

A.1 Gear nomenclature for macro and microgeometry



(DIN, 1978; AGMA, 2011; MAZZO, 2013; KLOCKE; BRECHER; BRUMM, 2014; REGO, 2016)

Appendix B – Material specifications

B.1 Conventional gear steels

Steel grade	Chemical composition [wt%]									Region
		C	Si	Mn	P	S	Cr	Mo	Ni	
16MnCr5	min.	0.14	-	1.00	-	-	0.80	-	-	Western Europe
	max.	0.19	0.40	1.30	0.025	0.035	1.10	-	-	
20MnCr5	min.	0.17	-	1.10	-	-	1.00	-	-	
	max.	0.22	0.40	1.40	0.025	0.035	1.30	-	-	
18CrNiMo7-6	min.	0.15	-	0.50	-	-	1.50	0.25	1.40	
	max.	0.21	0.40	0.90	0.025	0.035	1.80	0.35	1.70	
SAE 8620	min.	0.18	0.15	0.70	-	-	0.40	0.15	0.40	North America
	max.	0.23	0.35	0.90	0.030	0.040	0.60	0.25	0.70	
SAE 9310	min.	0.08	0.15	0.45	-	-	1.00	0.08	3.00	
	max.	0.13	0.35	0.65	0.025	0.040	1.40	0.15	3.50	
20CrMnTi	min.	0.17	0.17	0.80	-	-	1.00	-	-	China
	max.	0.23	0.37	1.10	0.035	0.035	1.30	0.15	0.30	
20CrMnMo	min.	0.17	0.17	0.90	-	-	1.10	0.20	-	
	max.	0.23	0.37	1.20	0.025	0.035	1.40	0.30	0.30	
SCM420	min.	0.18	0.15	0.60	-	-	0.90	0.15	-	Japan
	max.	0.23	0.35	0.85	0.030	0.030	1.20	0.30	-	

(DAVIS, 2005; DIN, 2008)

FOLHA DE REGISTRO DO DOCUMENTO			
1. CLASSIFICAÇÃO/TIPO DM	2. DATA 03 de agosto de 2020	3. REGISTRO Nº DCTA/ITA/DM-041/2020	4. Nº DE PÁGINAS 113
5. TÍTULO E SUBTÍTULO: Surface integrity evolution of Nb-Ti microalloyed steels along the gear manufacturing chain			
6. AUTOR(ES): Angelo Alves Carvalho			
7. INSTITUIÇÃO(ÕES)/ÓRGÃO(S) INTERNO(S)/DIVISÃO(ÕES): Instituto Tecnológico de Aeronáutica - ITA			
8. PALAVRAS-CHAVE SUGERIDAS PELO AUTOR: 1. Gear. 2. Surface integrity. 3. Microalloyed steel.			
9. PALAVRAS-CHAVE RESULTANTES DE INDEXAÇÃO: Engrenagens; Tratamento de superfícies; Aços; Fabricação; Engenharia mecânica.			
10. APRESENTAÇÃO: <div style="text-align: right;">X Nacional Internacional</div> ITA, São José dos Campos. Curso de Mestrado. Programa de Pós-Graduação em Engenharia Aeronáutica e Mecânica. Área de Materiais, Manufatura e Automação. Orientador: Prof. Dr. Ronnie Rodrigo Rego; coorientador: Prof. Dr. Tiago Cristofer Aguzzoli Colombo. Defesa em 27/07/2020. Publicada em 2020.			
11. RESUMO: The increasing demand for high performance gears promotes the study of application of new materials, such as microalloyed steels that appear as an alternative with economic potential to some of the steels currently used in gears. Gear manufacturing chain involves a sequence of processes with thermal and/or mechanical loading that alters the equilibrium state of the material. The influence of each process can be identified even at the end of the chain, which requires an understanding of each individualized process. In this scenario, the study herein presented has the objective of characterizing the surface integrity evolution of niobium and titanium microalloyed steels along a conventional gear manufacturing chain. The addition of microalloying elements in steels usually applied for gears is evaluated both holistically considering the entire manufacturing chain and individually for each manufacturing process. Investigations are conducted to understand how processes impact the surface integrity of microalloyed steels in terms of grain size, residual stress state, topography, and distortion level. The results herein obtained show that the addition of microalloying elements induces a microstructure with refined grain structure after the processes with thermal loading. The combined addition of niobium and titanium also indicated an increase in grain size homogeneity. The benefits of the new alloys are observed in the residual stress state and in the topography, in which they present higher levels of compressive residual stress combined with a surface with reduced roughness. The results also indicate a reduction in the distortion levels associated with homogeneous grain structure, such as that obtained with the combined addition of Nb and Ti. Finally, a potential process improvement is raised, the increase of the carburizing temperature may lead to the achievement of the required carburized layer with cost and process time savings. The results of this study showed that the gear manufacturing chain is sensitive to the addition of microalloying elements, so that the new alloys showed modified surface integrity. Among the manufacturing processes, those which presented the highest modification in their results were isothermal annealing, carburizing, and grinding. Therefore, microalloyed steels represent a class of materials that can be employed in the gear manufacturing chain and offer an optimized surface integrity state.			
12. GRAU DE SIGILO: <div style="text-align: center;">(X) OSTENSIVO () RESERVADO () SECRETO</div>			